

**UNIVERSITÀ  
DEGLI STUDI  
DI PADOVA**

**Università degli Studi di Padova**

Dipartimento di Scienze Chimiche  
SCUOLA DI DOTTORATO DI RICERCA IN: SCIENZE  
MOLECOLARI  
INDIRIZZO: SCIENZE CHIMICHE  
CICLO XXVII

**Innovative antimicrobial textiles based on natural  
fibers**

**functionalized with peptaibiotics**

**Direttore della Scuola:** Ch.mo Prof. Antonino Polimeno

**Supervisore:** Dott.ssa Cristina Peggion

**Dottorando:** Andrea Orlandin



## **Aknowledgement**

1. FT-IR Analysis: Dott. Renato Schiesari, University of Padova
2. EPR analysis: Prof. Antonio Toffoletti, University of Padova
2. Antimicrobial test:  
Dott.ssa Simona Oancea, University «Lucian Blaga» , Sibiu (RO)  
Dott.ssa Getta Hilma, University «Lucian Blaga» , Sibiu (RO)
3. XPS Analysis:  
Dott. Paolo Dolcet, University of Padova  
Dott.ssa Silvia Gross, University of Padova
4. Financial support: Cariparo foundation





## *Index*

<i>Abstract</i> .....	<i>i</i>
<i>Riassunto</i> .....	<i>ii</i>
<i>Abbreviation</i> .....	<i>iii</i>
<b>1.Introduction</b> .....	<b>1</b>
<b>1.1Bacteria</b> .....	<b>3</b>
<b>1.2. Antimicrobial textiles</b> .....	<b>15</b>
<b>1.3. Peptides as antimicrobial agents</b> .....	<b>23</b>
<b>1.4 Why use cotton?</b> .....	<b>37</b>
<i>Aim of the work</i> .....	<b>43</b>
<b>Reference</b> .....	<b>45</b>
<b>2. Results and Disscussion</b> .....	<b>51</b>
<b>2.1 Peptide Synthesis</b> .....	<b>51</b>
<b>2.2. Textile functionalization</b> .....	<b>69</b>
<b>2.3. Biological activity</b> .....	<b>111</b>
<b>2.4 Conclusions</b> .....	<b>115</b>
<b>Reference</b> .....	<b>119</b>
<b>3. Experimental part</b> .....	<b>123</b>



## **Abstract**

The need to develop new materials for a variety of applications is greatly promoting academic and industrial research. In this thesis work antimicrobial textiles were prepared.

To contribute to this topic, we started a research program that heavily relies on our expertise in the field of antibacterial peptides. Among the many polymeric materials available, cellulose fibers are particularly attractive, being naturally occurring, and easy to functionalize. Peptides and dendrimers were immobilized, as antimicrobial agent, onto cotton fabrics. Preparation of immobilized peptide-cotton materials was obtained using different innovative synthetic methods.

Characterization analysis by FT-IR, XPS, UV-Vis, TGA and EPR was also performed for qualitative and quantitative determination of cotton functionalization. Moreover, enzymatic degradation was carried out allowing the application of NMR spectroscopy in solution.

Antimicrobial activity of samples were tested against *Staphylococcus aureus* (Gram positive bacteria) and *Escherichia coli* (Gram negative bacteria). Promising results were obtained against the Gram positive strain, while only few samples show good activity against Gram negative bacteria.





## **Riassunto**

La necessità di sviluppare nuovi materiali per una varietà di applicazioni sta interessando fortemente la ricerca accademica e industriale. In questo lavoro di tesi sono stati preparati dei tessuti antimicrobici.

Per contribuire a questo argomento, abbiamo avviato un programma di ricerca che si basa sulla nostra esperienza nel campo dei peptidi antibatterici. Peptidi e dendrimeri sono stati immobilizzati, come agenti antimicrobici, su tessuti.

Tra i molti materiali polimerici disponibili, le fibre di cellulosa sono particolarmente attraenti, essendo esse presenti in natura e facile da funzionalizzare.

Caratterizzazioni FT-IR, XPS, UV-Vis, TGA e EPR sono state effettuate per la determinazione qualitativa e quantitativa della funzionalizzazione del cotone. Inoltre, la degradazione enzimatica ha consentito l'applicazione della spettroscopia  $^1\text{H-NMR}$  in soluzione.

L'attività antimicrobica dei campioni è stata testata contro lo *Staphylococcus aureus* (batterio Gram-positivo) e l'*Escherichia coli* (batterio Gram-negativo). Risultati promettenti sono stati ottenuti contro i batteri Gram-positivi, mentre solo pochi campioni hanno mostrato una buona attività contro i batteri Gram-negativi.



## Abbreviation

**Aib** =  $\alpha$ -aminoisobutyric acid

**Ala** = L-Alanine

**D-Ala** = D-Alanine

**AgNp** = silver nanoparticle

**AMP** = Antimicrobial peptide

**Arg** = L-Arginine

**Boc** = tert-butoxycarbonyl

**CD** = Circular Dichroism

**COSY** = Correlation spectroscopy

**DCM** = Dichloromethane

**DIPEA** = N,N- Diisopropylethylamine

**DMF** = Dimethylformamide

**DMSO** = Dimethyl sulphoxide

**EP** = Petroleum ether

**EPR** = electron paramagnetic resonance

**ESI** = electrospray ionization

**Fmoc** = 9-fluorenylmethoxycarbonyl

**FT-IR** = Fourier transformed infrared spectroscopy

**Gln** = Glutamine

**Gly** = Glycine

**HATU** = O-(azabenzotriazol-1-yl)-1,1,3,3-tetramethyluronium hexafluoro phosphate

**Hepes** = acido 2-[4-(2-idrossietil)-1-piperazino]etansolfonico

**His** = L-Histidine

**HOAt** = 1-hydroxy-7-aza-1,2,3-benzotriazole

**HOBt** = 1-hydroxy-1,2,3-benzotriazole



**HPLC** = High performance liquid chromatography

**Hyp** = Hydroxyproline

**Leu** = Leucine

**Lys** = L-Lysine

**MeOH** = methanol

**NMR** = Nuclear magnetic resonance

**NOESY** = Nuclear overhauser effect

**Ott** = Ottanoyl

**Pal** = Palmitoyl

**Phe** = L-Phenylalanine

**SPPS** = Solid phase peptide synthesis

**TEM** = Transmission electron microscopy

**TEMPO-OH** = 4-hydroxy-2,2,6,6-tetramethyl-1-oxy-piperidine

**TFA** = Trifluoro acetic acid

**TGA** = thermogravimetric analysis

**TOCSY** = Total correlation spectroscopy

**Trp** = triptophan

**Trt** = triphenyl methyl

**Triton X-100** = polietilenglicole terzocetilfeniletere

**UV-Vis** = Ultraviolet-Visible Absorption spectroscopy

**Val** = L-Valine

**XPS** = X-ray photoelectron spectroscopy

# **1. Introduction**

In the last century an authentic “war” against a variety of microorganisms responsible of infectious diseases was started. Chemotherapeutic treatment of infection diseases was introduced in 1910 by Paul Ehrlich which used organoarsenical compounds. In the following decades the study regarding this field rapidly increased through the work of Fleming, Domagk, Waksman and their many co-workers [1,2]. The discovery of antibiotics, natural products produced by microorganisms to fight against bacteria, allowed to prevent bacteria proliferation and thus to cure infection diseases. This discovery changed the medical practice and saved countless millions of human lives. In 1940 penicillin and streptomycin were the first antibiotics used in the treatment of bacterial diseases known as pneumonia and tuberculosis, respectively.

In the 1950s-60s the study about the antibiotic-producing organisms discovered several bioactive molecules with antimicrobial activity: tetracycline, quinolone and aminoglycoside families.

From the 1970s the trend changed as the number of new bactericide molecules rapidly discovered decreased, and the idea that all the principal families of antibiotics had been already discovered took place. In fact in this period the Surgeons General of the US said that “it is time to close the book on infectious diseases, declare the war against pestilence won, and to shift national resources to such chronic disease problems as cancer and heart disease” [3]. Looking at the actual situation about infection diseases it is clear that the war against bacteria is not finished.

Bacteria in fact demonstrate the ability to evolve and develop mechanisms of resistance against the common antibiotics such as penicillin and streptomycin. Drug-resistant bacterial diseases arise both in communities and hospital were the use of antibiotics is intensive and constant.

So in recent years new classes of bioactive molecules against bacteria were studied, one of these are antimicrobial peptides (AMP), a class of natural products usually synthesized by multicellular organisms as natural defense against bacteria. These biomolecules usually interact with the outer membrane of bacteria and do not need

to be transported inside the cell, differently to what happens for penicillin and other antibiotics [4].

However, the rate of developing resistance to the common drug is higher in comparison with the development of new antibiotics agents.

In order to reduce the development of infection diseases it is important to prevent bacteria proliferation. The idea to produce materials able to inhibit bacterial growth is currently an actual field for scientists. Many studies are directed towards the development of protective and safe textiles that are of fundamental importance for health care workers and for immuno-compromised or debilitated people who need to be protected from infections

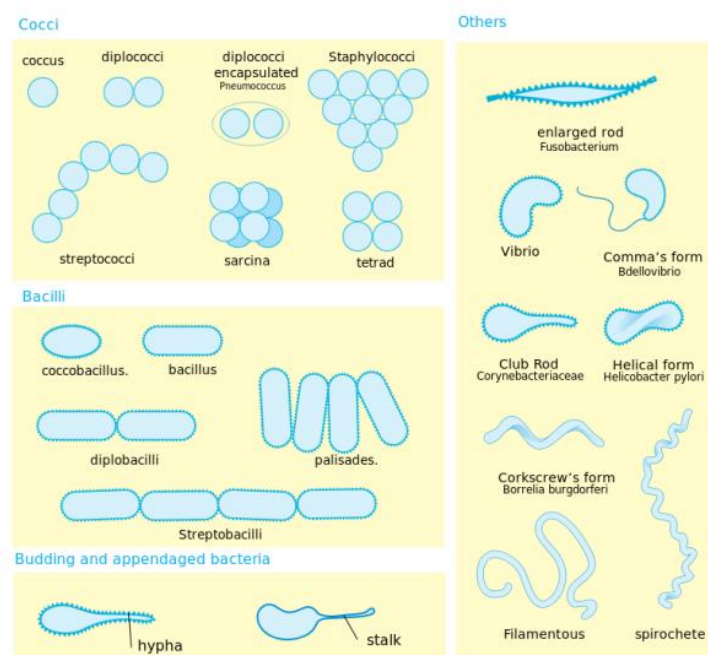
Recently a great effort has been done to use textiles, both natural (es. wool and cotton) and synthetic (es. polyesters and polyamide), as scaffolds for adsorption of antimicrobial agents [5]. Textiles treated with biocides are already available on the market. Usually the antimicrobial agents are metallic and metal oxide nanoparticle (usually silver or copper oxide), triclosan and quaternary ammonium salts. In these products the bioactive agent is only adsorbed on the surface of the textile and could be removed by washing and abrasion. Free bioactive agent could be dangerous for human health or for the environment. For these reasons the possibility to prepare bioactive textiles where the antimicrobial agent is covalently linked becomes of fundamental importance. The work described in this thesis develops in this framework.

As antimicrobial agents we focused on antimicrobial peptides (AMP). The main advantage of using amino acids and peptides comes from their presence in Nature. The antimicrobial peptides may be considered low molecular weight proteins having a broad antimicrobial spectrum against bacteria, viruses and fungi. These peptides are generally cationic and therefore able to interact with the negatively charged phospholipid membranes [3]. They are usually relatively short (from 10 to 20 amino acids), helical and amphipathic [6]. These features make them soluble in an aqueous environment, but also related to the environment of the lipid membranes. Many AMPs are used by complex organisms as a defense against microbial attacks.

In this work as the textile we focused on cotton because it is the most common worldwide used natural fiber, it is cheap and its chemical structure based on cellulose, allowed a good functionalization. We exploited the free hydroxyl groups of cellulose to covalently anchor the peptides. Being the antimicrobial agent not only adsorbed the textile surface, it should be more durable and environmentally safe during all the life of the textile itself..

## 1.1 Bacteria

Bacteria represent the simplest organisms living on earth today and constitute a large domain of prokaryotic microorganisms... Bacteria were the first forms of life to appear on Earth, and are present in several of its habitats. In fact bacteria were found in soil, water, acidic hot springs, radioactive waste and the deep portions of Earth's crust. Bacteria also live in symbiotic and parasitic relationships with plants and animals. Typically a few micrometers in length, bacteria show different shapes. Most bacterial species are either spherical, called cocci (sing. coccus, from Greek κόκκος, grain, seed), or rod-shaped, called bacilli (sing. bacillus, from Latin baculus, stick). Some bacteria, called vibrio, are shaped like slightly curved rods or comma-shaped; others can be spiral-shaped, called spirilla, or tightly coiled, called spirochaetes.

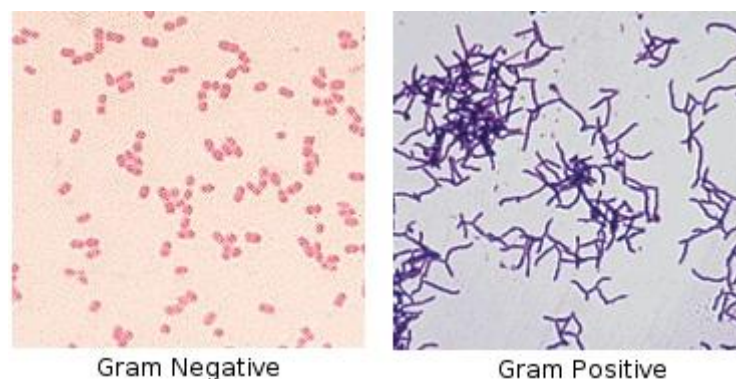


**Figure 1.** Bacteria classification by their shapes.

Many bacterial species exist simply as single cells, others associate themselves in characteristic patterns: Neisseria form diploids (pairs), Streptococcus form chains, and Staphylococcus group together in "bunch of grapes" clusters. Bacteria can also be elongated to form filaments, for example the Actinobacteria. Filamentous bacteria are often surrounded by a sheath that contains many individual cells. Certain types, such as species of the genus Nocardia, even form complex, branched filaments, similar in appearance to fungal mycelia.

### **Gram classification**

Among all the different classification systems, the Gram stain has withstood the test of time. Discovered by H.C. Gram in 1884, it remains an important and useful technique up to now. It allows a large proportion of clinically important bacteria to be classified as either Gram positive or Gram negative, based on their morphology and differential staining properties. Slides are sequentially stained with crystal violet, iodine, then destained with alcohol and counter-stained with safranin. Gram positive bacteria stain blue-purple and Gram negative bacteria stain red. The difference between the two groups is believed to be due to the larger peptidoglycan (cell wall) present in Gram positives. As a result, the iodine and crystal violet precipitate in the thickened cell wall and are not eluted by alcohol in contrast with the Gram negatives where the crystal violet is readily eluted from the bacteria. As a result bacteria can be distinguished based on their morphology and staining properties.

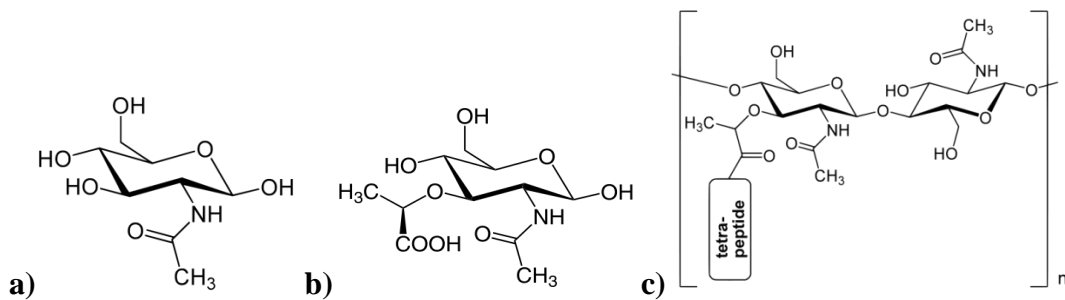


**Figure 2.** Result obtained after Gram colorimetric test for Gram negative and Gram positive bacteria, respectively.

Some bacteria, for instance mycobacteria that causes tuberculosis, are not reliably stained due to the large lipid content of peptidoglycan. Alternative staining techniques (Kinyoun or acid fast stain) are therefore used.

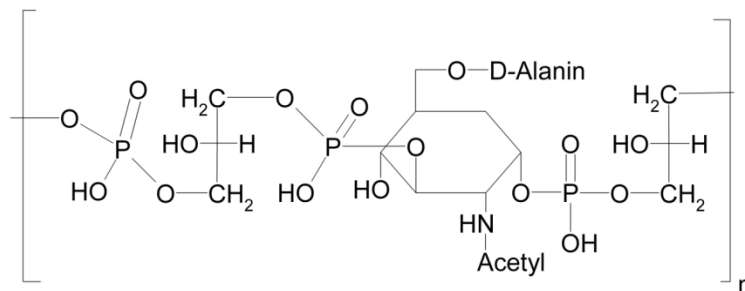
### Gram positive bacteria

The membrane of Gram positive bacteria is composed by an outer part of peptidoglycan, a linear polysaccharide formed by units of N-acetylglucosamine and N-acetylmuramic acid and these chains are cross linked by short peptides (4 or 5 residues) anchored to carboxylic moiety of N-acetylmuramic acid. The nature of the cross linking peptide differs from different bacteria in the same Gram positive class. [7].



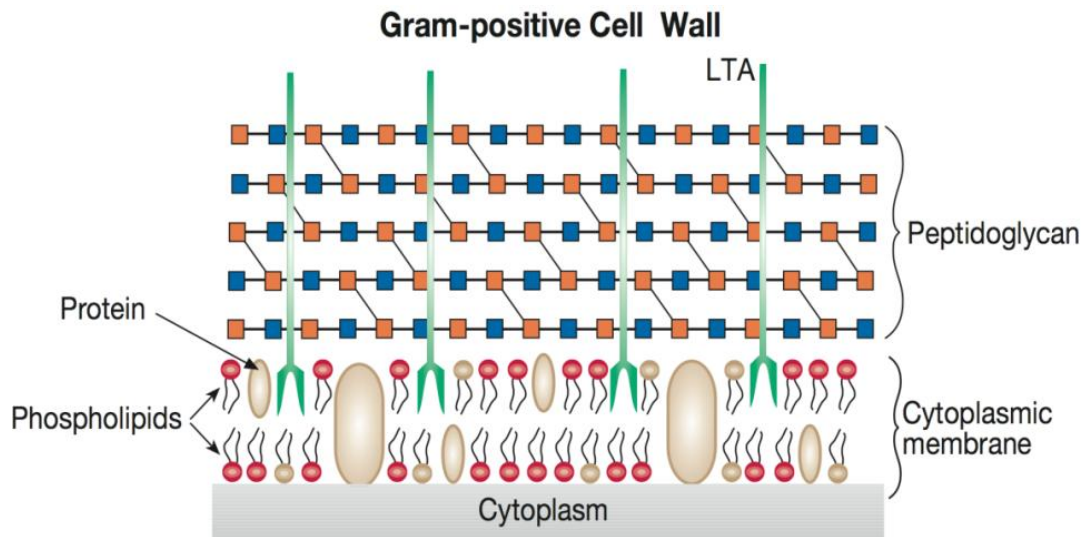
**Figure 3.** Chemical structures of N-acetylglucosamine (a), N-acetylmuramic acid (b), and disaccharide unit (c).

In Gram positive bacteria the peptidoglycan layer is also crossed by teichoic acid which linked lipids of the inner membrane layer forming lipoteichoic acids. These structures, absent in Gram negative bacteria, confer more strength at the outer cell wall.



**Figure 4.** Basic chemical structure of teichoic acid.

The structure of Gram positive bacterial membrane is show below. In different Gram positive bacteria the peptidoglycan layer differs for the peptidic component while glucidic part remains usually the same [8].

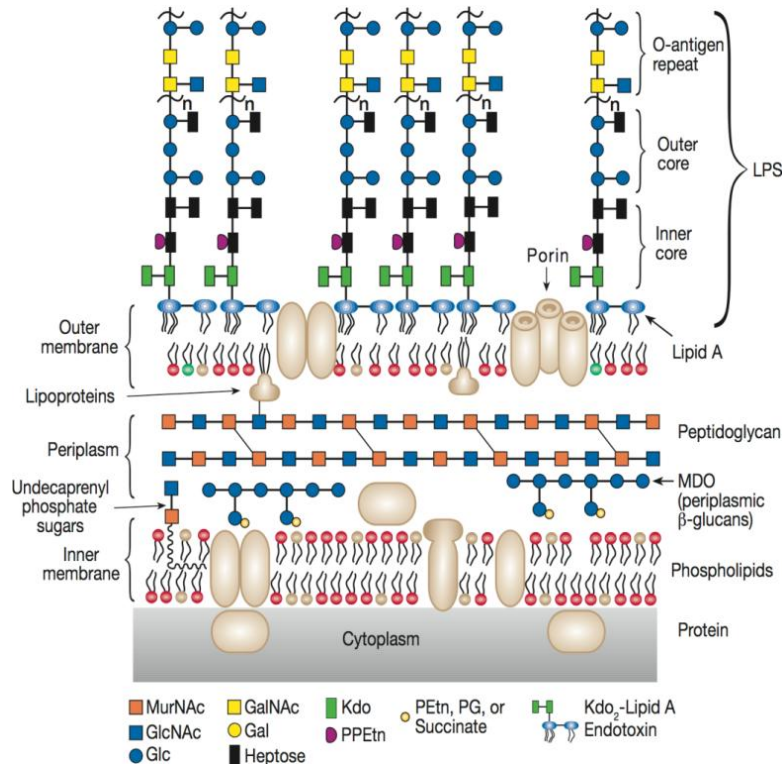


**Figure 5.** Schematic representation of the cell wall of Gram-positive bacteria. The blue and orange squares are N-acetylglucosamine and N-acetylmuramic acid, respectively. The black lines cross between the squares represent peptides. The green lines represent vertical lipoteichoic acids (LTA).

Examples of Gram positive bacteria are *Staphylococcus MRSA* and *Streptococcus*.

## Gram negative bacteria

Gram negative bacteria possess a more complex and lipid cell wall. Usually, these membranes are composed mainly by three components: the outer membrane, the periplasm and the inner membrane (fig. 6) [8].



**Figure 6.** Schematic representation of the cell wall of Gram negative bacteria. The periplasm, in addition to peptidoglycan, contains  $\beta$ -glucans known as oligosaccharides derived from membrane (MDO). LPS = lipopolysaccharide; Glc = glucose, Gal = galactose; heptose = *l*-glycero-*D*-mannoepstosio; Kdo = 3-deoxy-*D*-manno-ottulosonic acid; PPEtn = pyrophosphoethanolamine.

Gram negative bacterial membranes are characterized by the presence of a lipoprotein called *purine* that passes through the membrane by transmembrane channel formation. This ability is due to the presence in the inner channel of residues with charged lateral chains. For this reason *purine* allows the transition of ions through the membrane. In opposition, the external part of *purine* is characterized by the presence of hydrophobic residues which interact with the phospholipid layer.

*Purines* penetrate up to the limit of the outer layer of the cell wall. Below the maximum limit of penetration of *purines* there is a layer of peptidoglycan, which follows a periplasmic space, and a cytoplasmic membrane, rich in phospholipids and proteins. In this membrane there are also the receptors for  $\beta$ -lactams (penicillin binding protein), while the proteins that hydrolyze them, the  $\beta$ -lactamases, are



located in the *periplasm* layer [9]. Examples of Gram negative bacteria are *Escherichia Coli* and *Salmonella*.

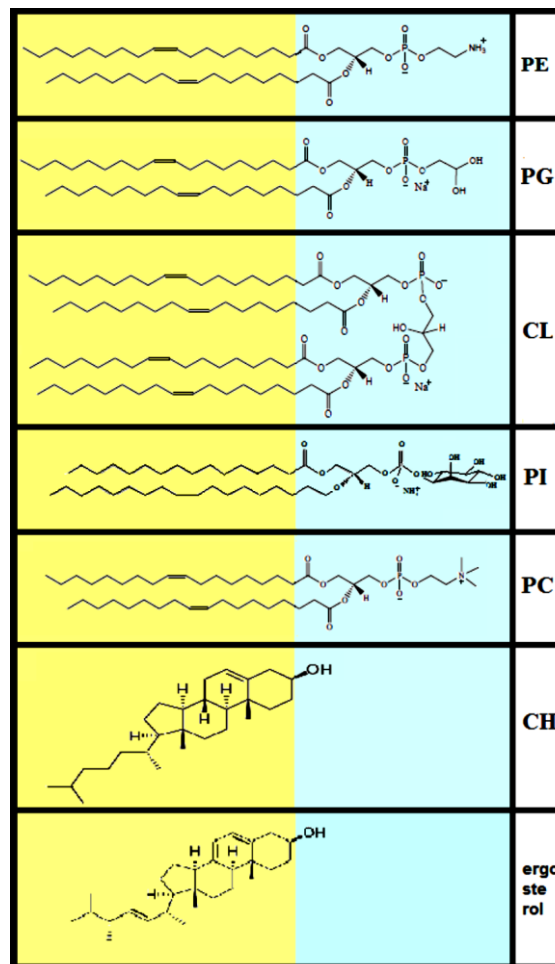
### Phospholipid in Gram positive and Gram negative bacteria

Inside the Gram differentiation of bacteria the two class of microorganism are also differentiated by the structure of the phospholipid components in the membranes.

Bacterial membranes are composed mainly by negative charged constituents

(i.e. PG, phosphatidylglycerol) and zwitterionic phospholipids (i.e. PE, phosphatidylethanolamine).

Lipids as sterols (i.e. CH, cholesterol) are rarely present in bacterial membranes, while they are mostly situated in eukaryotic membranes conferring them a better stability.



**Figure 7.** Common phospholipids and sterols present in bacterial, fungal or mammalian cell membranes. In yellow the hydrophobic moiety is shown and in blue the hydrophilic moiety. PE phosphatidylethanolamine; PG, phosphatidylglycerol; CL, cardiolipin; PI, phosphatidylinositol; PC, phosphocholine; CH, cholesterol.

Generally, Gram positive bacteria are composed mainly by negatively charged phospholipids while Gram negative membranes contain mainly phosphatidylethanolamine (PE) molecules. However bacterial membranes, both Gram positive and Gram negative, contain a minimum of 15% in negatively charged phospholipids. For this reason, bacterial membranes have a negative character [10].

### **Bacteria drug-resistance and infection diseases: a worldwide problem**

Infections remain a leading cause of morbidity and mortality, claiming an estimated 14 million lives in 2011 [11]. Due to the globalization the risk of infection diseases is increased very rapidly respect to the last 50th years thanks to the displacement of the population, poverty and war. Moreover the intense use of antibiotics in hospital and in alimentary industries induce the arise of drug-resistant form of bacteria, both Gram positive and Gram negative. Today drug resistance is common among all the major class of antibiotics. Infections developed by drug resistant bacteria are dangerous because the possible treatments for this disease are strongly reduced. Below the drug resistant situation in Europe and United States evaluated for drug resistant *Staphylococcus aureus* is reported.

### **Bacteria resistance to common antibiotics**

In order to appreciate the mechanisms of resistance developed by bacteria against common antibiotics, it is important to understand how antimicrobial agents act. Antimicrobial agents act selectively on vital microbial functions with minimal effects or without affecting host functions.

Different antimicrobial agents act in different ways. The understanding of the mechanisms that regulate the antibacterial action as well as the chemical nature of the antimicrobial agents is crucial to elucidate the mechanisms of resistance.

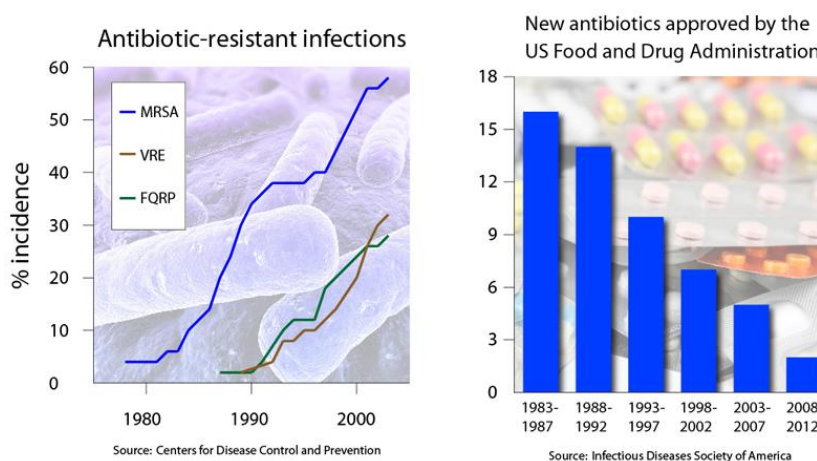
Broadly, antimicrobial agents may be described as either bacteriostatic or bactericidal. Bacteriostatic antimicrobial agents only inhibit the growth or multiplication of the bacteria giving the immune system of the host time to clear them from the system. Complete elimination of the bacteria in this case is dependent on the competence of the immune system. Bactericidal agents kill the bacteria and therefore, with or without a competent immune system of the host, the bacteria die.

The mechanism of action of antimicrobial agents can be categorized further based on the structure of the bacteria or the function that is affected by the agents.

**Table 1** Example of antibiotics and their mode of action against bacteria

Group of antimicrobial agents	Effect on bacteria	Mode of action
<b>Penicillins</b>	Bactericidal	Inhibition of cell wall synthesis
<b>Cephalosporins</b>	Bactericidal	Inhibition of cell wall synthesis
<b>Polypeptide antibiotics</b>	Bactericidal	Inhibition of cell wall synthesis
<b>Quinolones</b>	Bactericidal	Inhibits DNA synthesis
<b>Rifamycins</b>	Bactericidal	Inhibition of RNA transcription
<b>Aminoglycosides</b>	Bactericidal	Inhibition of protein synthesis
<b>Tetracyclines</b>	Bacteriostatic	Inhibition of protein synthesis
<b>Sulfonamides</b>	Bacteriostatic	Competitive inhibition

Prior to the 1990s the problem of antimicrobial resistance was never taken so much in consideration for the management of infectious diseases. Microorganisms were increasingly becoming resistant to ensure their survival against the arsenal of antimicrobial agents to which they were being bombarded. They achieved this through different means primarily based on the chemical structure of the antimicrobial agent and the mechanisms through which the agents acted. Moreover, in the last 20 years the attention of pharmaceutical industries strongly reduced studies relative to antibiotics for focusing on other chronic diseases like cancer and heart diseases (fig. 8).


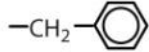
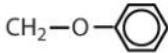
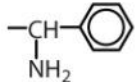
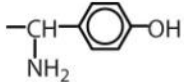
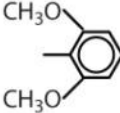


**Figure 8.** Incidence of drug resistant bacteria infections vs time (left); Number of new antibiotics approved by US Food and Drug Administration in the last thirty years.

In addition, several commercially available antibiotics are characterized by the same active group. Some penicillin-like antibiotics which act by the action of  $\beta$ -lactam ring are reported in table 2. The  $\beta$ -lactam ring is important for the activity of

these antibiotics as it inactivates a set of transpeptidases crucial for the synthesis of bacteria.

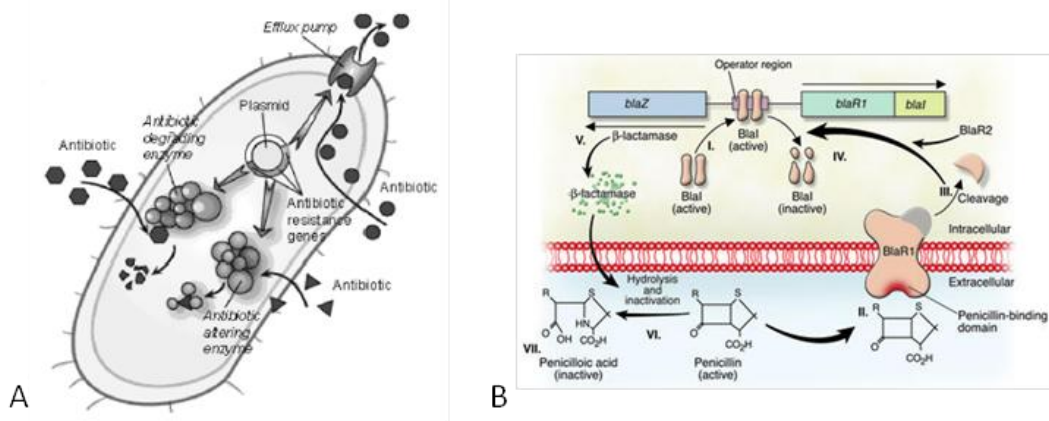
**Table 2** Example of  $\beta$ -lactam ring based antibiotics

Penicillin Structure	R Group	Drug Name
		penicillin G
		penicillin V
		ampicillin
		amoxicillin
		methicillin

The abuse of these antibiotics, both in humans and animals, has induced the development of resistance by bacteria.

The resistance mainly takes place in the following ways:

- development of enzymes able to inactivate the active component of the antibiotics, especially for extracellular antibiotics;
- recognition of antibiotic agents inside the cell bacteria and successive removal by efflux pumps; modification of membrane potential, limiting the electrostatic interaction between anionic charged membrane and cationic antibiotics. [12]

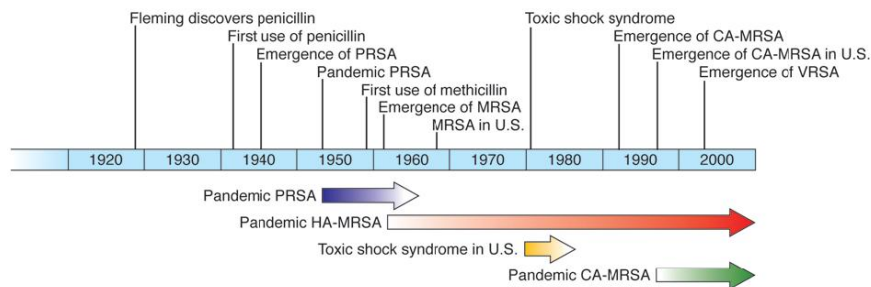


**Figure 9.** A) Illustration of how some antimicrobial agents are rendered ineffective (from [www.chembio.uoguelph.ca](http://www.chembio.uoguelph.ca)); B) Mechanisms of resistance developed by *S. aureus* against  $\beta$ -lactam ring antibiotics.

The resistance mechanisms therefore depends on the specific pathways that are inhibited by the drugs.

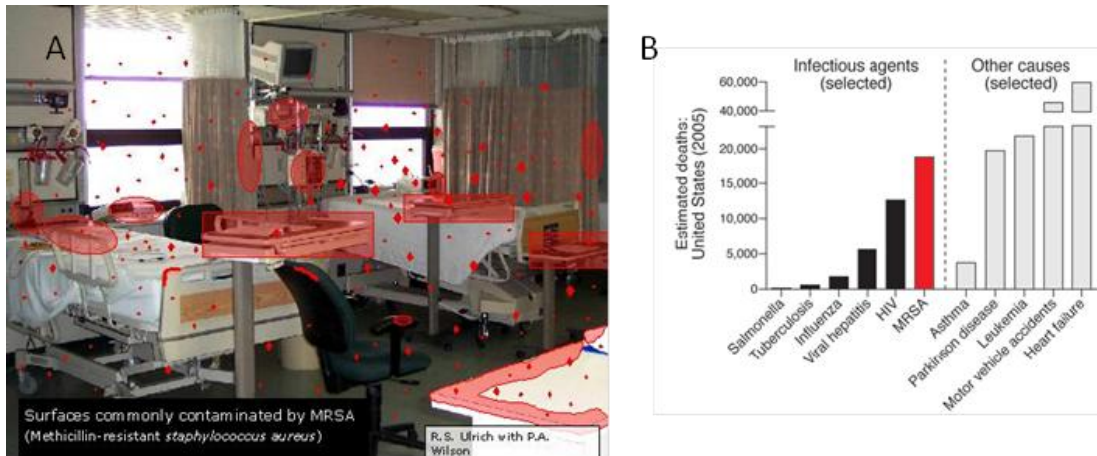
**An example of drug-resistant bacteria: *Staphylococcus aureus*.**

*Staphylococcus aureus* (*S. aureus*) is a Gram positive bacteria able to live in dryness and in high salt concentration. It is the leading cause of bacterial infections involving the bloodstream, lower respiratory tract, and skin and soft tissue in many developed countries, including the United States [13]. Initially (c.a. 1940) *S. aureus* was strongly sensitive to penicillin but in few years it was able to develop resistance against it, becoming pandemic in 1950's -1960's. Several analogues of penicillin were studied, till introduction of methicillin in 1959 induced a decrease in *S. aureus* growth and infection [14]. As for penicillin, *S. aureus* was able to develop resistance against methicillin in few years (MRSA, Methicillin Resistant *Staphylococcus Aureus*).



**Figure 10.** Timeline between the introduction of new antibiotics and the develop of resistance of *S. aureus*.

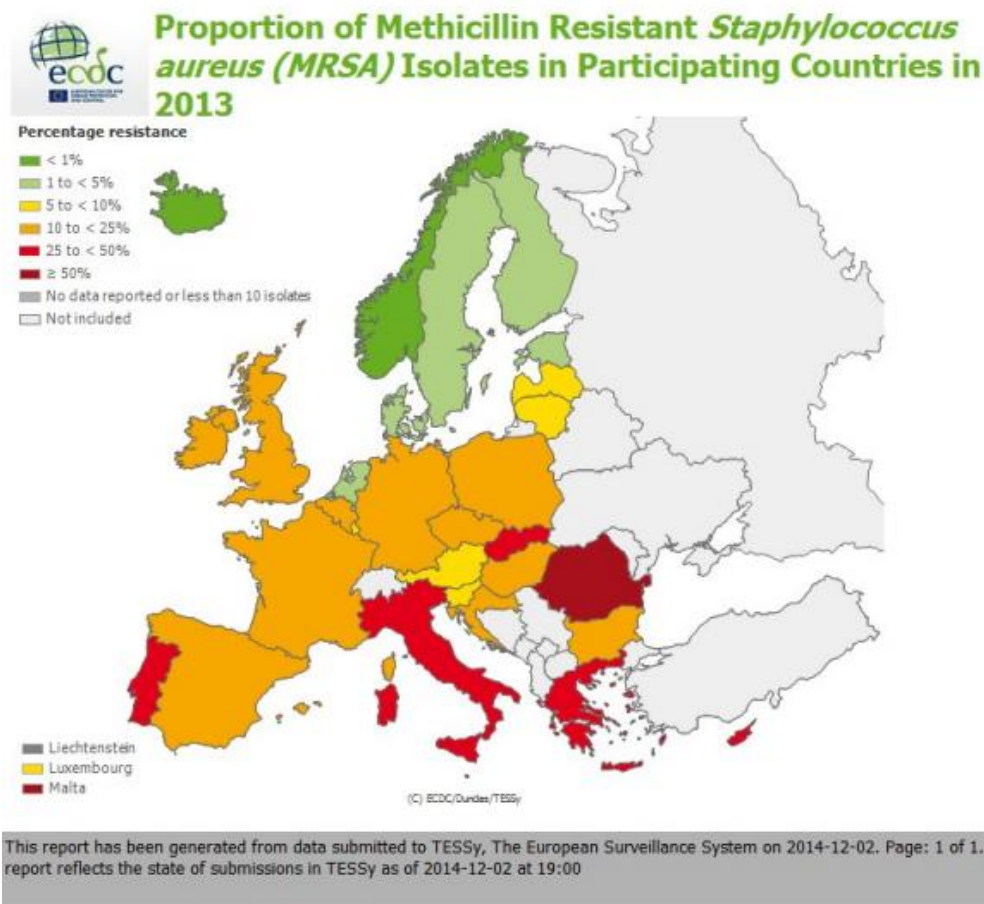
MRSA, to date, represents one of the most dangerous pathogens present world-wide in hospitals. Recent studies show that the mortality related to MRSA infection is over the 20%. In U.S. the number of death for MRSA infections surpass the sum of the death for HIV, homicides and hepatitis.



**Figure 11.** A) Incidence of MRSA in a hospital room. B) Incidence of infection estimated in US in 2005.

MRSA finds in hospital a favorable location for its growth (fig. 11).

Europe presents the same problem related to drug resistant bacteria (DR-bacteria), mainly MRSA. The map, presented below, shows the results obtained by ECDC (European Centre of Diseases Control) regarding the identification of MRSA in hospital.



**Figure 12.** European incidence of MRSA, from [http://www.ecdc.europa.eu/en/healthtopics/antimicrobial\\_resistance/database/Pages/map\\_reports.aspx](http://www.ecdc.europa.eu/en/healthtopics/antimicrobial_resistance/database/Pages/map_reports.aspx)

In 2007 in EU there were over 4 million of nosocomial and hospital-acquired infections, and, about half million of them are induced by drug resistant bacteria, in some countries the amount of DR-bacteria is around the 25%. Infections related to *S. Aureus* cause direct problems, but also they indirectly represent a societal overall cost related to the cure of patients. Recent estimations indicate that DR bacteria represent a large cost in human lives (around 25000 die/year) and in money. This cost is evaluated around 35 billion dollars/years for U.S. and for EU around 1.5 billion of euros/years [15], so that the necessity to fight against bacteria is becoming impellent.

In this field we insert our work that has as the final aim the preparation of textiles with antimicrobial properties. The new material have particular interest for medical and health-care and wherever an aseptic environment is required.

## **1.2 Antimicrobial textiles**

All textiles represent an environment for microbes. Cotton and wool fabrics are particularly favorable to microbial life because they retain oxygen, water, and nutrients. Like in a house, microbial contamination of surfaces is a common problem in hospitals. Textile fabrics can promote bacterial proliferation and consequently induce cross-infections.

Textiles are largely used in medical and healthcare applications. Irrespective of their applications medical textiles, both internal (surgical threads) and external (gauzes, bandages, surgical masks, gowns and apparel, nappies, tampons, and so on), need to be characterized by bioactive properties, especially antimicrobial. To reduce the transmission of pathogens within a curative environment, hospital protective clothing and materials have to ensure adequate protection against microorganisms and biological fluids. [16]. Therefore, decreasing the growth of microorganisms on textiles is becoming important, especially for the medical textile industry.

The fact that textile materials are one of the main vehicles for infections and the necessity to enhance the quality of life of people that work in a risky context (medical staff, patients, and visitors) has stimulated intensive research and development of antimicrobial textiles.

Functional textiles include durable or permanent finished garments, textiles with self-cleaning properties, and also textiles with antimicrobial finishing. Recently nanotechnology has been applied by industry to obtain hi-tech textiles which have attracted the interest of the global market. Over \$106.9 billion in technical textiles were sold in 2005 [17]. It was estimated that the global economy saw a \$20.4 billion increase in the sales of hi-tech textiles in 2006 alone [17]. We live in a society of ease and functionality and scientific research prospers from this trend.



## **Antimicrobial finishing**

The term 'antimicrobial' refers to a broad range of technologies that provide varying degrees of protection for textile materials against microorganisms [18]. A lot of antimicrobial agents differ for chemical nature, mode of action, impact on people and environment, durability, costs..

Ideal antimicrobial finishing needs the effective inhibition against a broad spectrum of bacterial and fungal species, non-toxicity to the consumer and to the environment, durability, avert from irritations and allergies, applicability with no adverse effects on the mechanical properties of the textile.

## **Modes of antimicrobial action**

In literature different way for classify antimicrobial agents are reported based on their chemistry [16, 19], mechanism of action and washing-resistance [20]. From these works, antimicrobial substances can be divided into biocides and biostatics, controlled-release (adsorbed) and covalently linked, synthetic and natural, and by the resistance to washing. Biocides cause the death of microorganisms and biostatics inhibit microbial growth. In general, antimicrobial agents have a biocidal or biostatic effect on microbial growth rates.

There are several commercially available antimicrobial products which use metal salt and nanoparticles, triclosan (TCS), polyhexamethylen biguanid (PHMB) and quaternary ammonium compounds as biocides.

Generally, the antimicrobial action is done by limiting cell reproduction and making cell life impossible by damages to cell walls or cell permeability, denaturation of proteins and inhibition of enzymes. Polycationic antimicrobial agents target the cytoplasmic membranes of microorganisms [21].

Antimicrobial agents can act in two distinct ways:

(i) **by contact**: the antimicrobial agent remains permanently on the fibers and inhibits microbes;

(ii) **by diffusion**: the antimicrobial agent is adsorbed on the fibers and it is slowly released into the environment (controlled-release mechanism).

In class (i) antimicrobial agents are chemically bound to the textile fibers forming a barrier against microorganisms and limiting the diffusion of those microorganisms that interact with the fibers. The principal advantage of these agents is that they do not spread from the textile to the surroundings, so the probability of microorganisms to develop resistance is small. Moreover they are more durable to laundering than products with adsorbed antimicrobials.

Chemical bond between fibers and antimicrobials agents is related to the their functional group. Generally, chemical bond formations need the use of auxiliary chemicals and cross-linking agents, such as epibromohydrin (EBH), and this may be a disadvantage for the effect of biocompatibility in medical applications.

The second class of chemical action is the *controlled-release* mechanism. Antimicrobial agents spread onto the fiber surface or in the surrounding environment. They are not chemically bonded to the textile surface but adsorbed into the fibers, so the 'reservoir' of agent is limited. In fact the concentration of active agents decreases gradually, therefore after some time the minimal inhibition concentration (MIC) required to be active cannot be obtained. Releasing of this kind of agents can also be dangerous for health and environment.

### **Common Antimicrobial textiles**

The antimicrobial effect is obtained through the application of specific chemical products during the finishing stage, or through the incorporation of these substances into fibers during the spinning process.

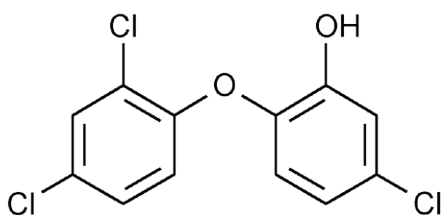
Actually the antimicrobial agents used for textiles include metal and metal salts such as silver, metal oxides such as CuO and ZnO, quaternary ammonium compound (QAC), halogenated phenols such as triclosan and metal organic complexes like Zn pyrithione (ZnPT). Among them, the most used are QAC, phenol derivatives, organometal compound and silver in its different forms (salt and nanoparticles).

The antimicrobial agent mentioned so far are not covalently linked to the textile but usually adsorbed on its surface. In this condition the biocide could be removed by washing and/or abrasion and eventually end up in aquatic environment. Recent studies have reveal that a large amount of Ag, nano Ag and triclosan are removed by washing textiles. Respectively 85-99% of Ag [22], >95% for AgCl and nano-Ag [22]

and 90-96% for triclosan. Washing is not the only way to remove the antimicrobial agent; another mechanism that induces the loss of the biocide is degradation. For example triclosan is degradable under aerobic condition [23].

### ***Triclosan***

Triclosan (2,4,4-hydrophenyl trichloro (II) ether) (TCS), a member of the antiseptic and disinfectant family, is a halogen containing a derivative of phenol active against Gram negative and Gram positive bacteria.



**Figure 13.** *Chemical structure of Triclosan.*

This compound, thanks to the presence of the acaricide benzyl benzoate, also offers protection against mites, arthropods belonging to the subclass Acari, and is used in acaricide for the treatment of scabies. TCS has found widespread use in a variety of consumer products including toothpastes, deodorants, soaps, polymers and fibers [24].

Toxicity studies were performed for different type of organism from bacteria to human passing through fishes, birds and plants. TCS toxicity on these organisms is correlated to chronic effects due to its bioaccumulation. Moreover the sensitivity of some species (microorganisms and aquatic plants) showed that ecosystems can be disturbed by TCS presence [25]. Due to TCS large presence in aquatic environment and in different terrestrial and aquatic animals and plants the exposure of humans to this compound is very easy. Very few works on chronic toxicity are available. However some studies of the last decades on mice have shown the development of hypothermia and depressant effects on the nervous system [26], while other works cleared that TCS can cause endocrine disruption [25], reduce sperm production [27] and that can bind thyroid hormone receptor [28]. Cytotoxic study in vitro of gingival human cells showed that TCS could induce cell death by impairment of plasma

membrane and by apoptosis [29]. Moreover Prins in 2008 confirm that endocrine disruption could induce prostate cancer [30].

TCS also can be degraded developing toxic by-products. These by-products could be divided in five classes:

- 1) Chlorinated diphenyl ethers (tetraclosan and pentaclosan). Chlorination of TCS give as products 4,5-dichloro-2-(2,4-dichlorophenoxy)phenol, 5,6-dichloro-2-(2,4-dichlorophenoxy)phenol (two isomers of tetraclosan) and 4,5,6-trichloro-2-(2,4-dichlorophenoxy)phenol (pentaclosan). Tetraclosan and pentaclosan were detected as precursor of stable by-products (2,4-dichlorophenol and 2,4,6-trichlorophenol), precursor of polychlorodibenzo-*p*-dioxins [31], the second class of TCS by-products.
- 2) The third class corresponds to chlorinated hydroxylated, hydroxyquinone and quinone triclosan. These compounds were found unstable in wastewater and irradiated with sunlight give polichlorophenols [31].
- 3) The fourth class is chlorophenols derivatives and chloroform, well known compound with high toxicity for human and environment.
- 4) The last class is due to biodegradation of TCS with the formation of methyl TCS that is more hydrophilic than TCS and showed higher toxicity than the precursor [31].

TCS such as the antimicrobial presented at point a) showed very dangerous consequences for ecosystem and for human.

### ***Metallic salts and metal nanoparticles***

Metal salts and metal nanoparticles have the capability to be very toxic against microorganisms. Usually, their action is done through the bind of intracellular proteins and their consequent [32].

The metal that is mostly used for textiles is silver, but also other metals such as copper, zinc and cobalt, have attracted attention as effective antimicrobial agents. Silver is largely used in many fields because it shows strong biocidal effects on many pathogenic bacteria. Silver has a MIC value of 0.05– 0.1 mg/l against *Escherichia Coli*. In synthetic fibers, silver particles can be incorporated into the polymer before

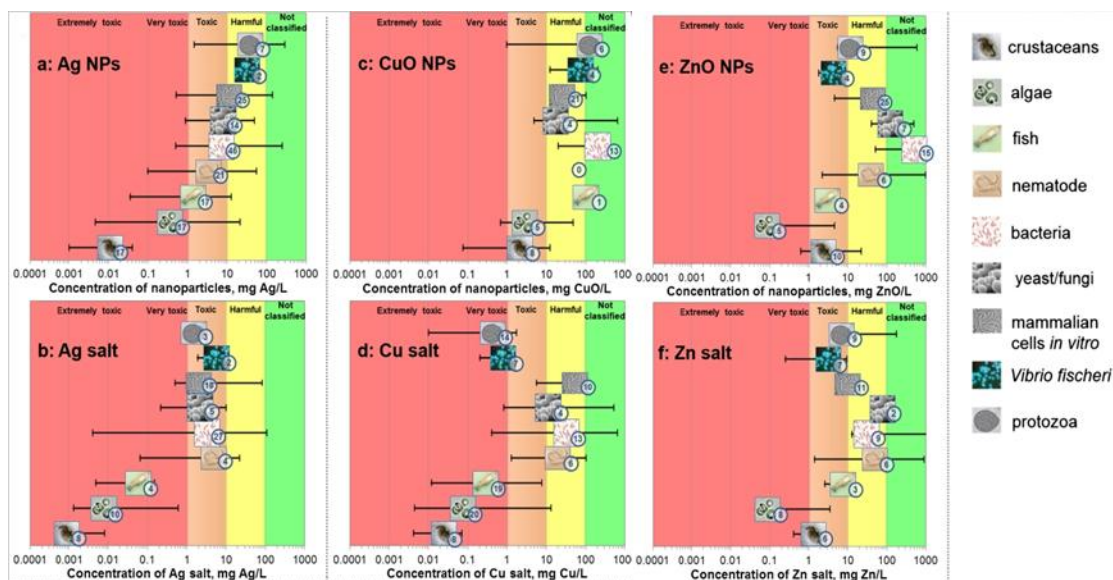
extrusion or before nanofiber formation using electro spinning. Metals can be applied to natural fiber only at the finishing stage and with the application of different strategies. For example metal ions ( $\text{Ag}^+$  and  $\text{Cu}^{2+}$ ) are adsorbed on cotton fiber pretreated with succinic acid anhydride, that act as ligand for and to provide very effective antibacterial activity.

Nano-sized metals and metal oxides, mainly silver (Ag), zinc oxide (ZnO) and copper II oxide (CuO) represent another class of biocides agents.

Unfortunately, Ag nanoparticles (NPs) exhibited the highest toxicity for crustaceans and algae, with a MIC of 0,01 mg/L and 0,36 mg/L respectively. Ag NPs should be classified as very toxic for aquatic organism [33]. Moreover the MIC of AgNPs for bacteria is in the range of 0,1-20 mg/L and for eukaryotic cells *in vitro* in the range of 10-100 mg/L. A similar behavior was observed for Ag ions. Moreover, one of the most known and well documented negative concerns of Ag is the human disease called *Argiria*.

Similarly to Ag NPs, CuO nanoparticles display high toxicity level to crustaceans and algae in the range of 2-3 mg/L. Considering that the bacterial MIC is around 250 mg/L is obviously that CuO NPs are more toxic to aquatic species than to bacteria. So the use of this metal oxide should be re-considered for antimicrobial purpose. Moreover Cu ions are more toxic than the metal oxide nanoparticles except for mammalian cell.

ZnO NPs present also a very elevated toxicity. ZnO NPs have a MIC in the range 0.08-3 mg/L for aquatic species, while the MIC for bacteria is around 620 mg/L. So ZnO NPs, similarly to CuO, present a high toxicity for aquatic species while are less toxic for bacteria.[34].

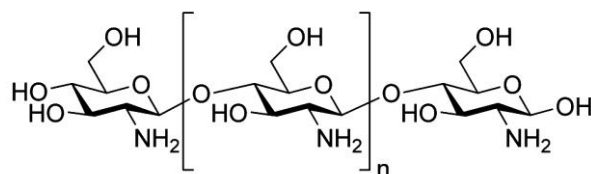


**Figure 14.** Comparison between the MIC for bacteria and for aquatic species of different metal salts and metal nanoparticles.

In conclusion, from the discussion above it is clear that the use of metal salts, metal nanoparticles and metal oxide nanoparticles as antimicrobial agents in textile industry is more dangerous for the environment than useful as antimicrobial treatment.

### Chitosan

Chitosan [poly-(1-4)-d-glucosamine] is a cationic polysaccharide obtained by alkaline deacetylation of chitin, the principal component in crustaceans exoskeleton.



**Figure 15.** Chemical structure of chitosan polymer.

Due to their many properties, such as water binding capability, fat binding capability, bioactivity, biodegradability, nontoxicity and biocompatibility, chitosan and its modified analogs have found many applications in medicine, cosmetics, agriculture, biochemical separation systems, biomaterials and drug controlled release systems. Chitosan is obtained from the shells of crabs, shrimps and other crustaceans. It is a nontoxic, biodegradable and biocompatible natural polymer, and has long been used

as a biopolymer and natural material in the pharmaceutical, medical, papermaking and food processing industries. Because of its polycationic nature, chitosan possesses good antibacterial properties against various bacteria and fungi through ionic interaction at a cell surface, which eventually kills the cell. Previous studies have shown that its antimicrobial activity is strongly related to molecular weight, degree of deacetylation, temperature, pH and cations in solution [35]. In addition, antimicrobial textiles based on chitosan show low durability to washing processes and so the loss in time of the antimicrobial agent.

### ***Quaternary ammonium***

Quaternary ammonium compounds seem attractive because their target is primarily the microbial membrane and they accumulate in the cell driven by the membrane potential. To maximize efficiency, quaternary ammonium compound is used as monomeric link in the polymeric leash and polyhexamethylen biguanid (PHMB) is usually selected as the carrying polymer. Tiller et al. showed that the surfaces of commercial polymers treated with N-alkylated poly-vinylpyrrolidone (PVP) groups were lethal on contact to both Gram positive and Gram negative bacteria, and it was also shown that N-alkyl chain of six carbon units in length was the most effective.

Shao et al. showed that a novel quaternary ammonium salt, which contains both perfluoroalkyl group and diallyl groups, should be a suitable finishing agent for providing the fabrics with barriers against microorganisms, water, oil, soil and blood. However this antimicrobial agent, as the others previously shown, is toxic for aquatic species such as crustaceans, algae and fishes [36].

### **1.3 Peptides as antimicrobial agents**

Antimicrobial peptides (AMPs) are oligopeptides with a varying number (from five to over a hundred) of residues. AMPs have a broad spectrum of targeted organisms from viruses to bacteria. AMPs can be classified as anionic AMPs [37], cationic AMPs [38], host defense peptides [39], and  $\alpha$ -helical antimicrobial peptides [40].

AMPs were discovered in 1939 by Dubos when he extracted a bioactive agent from a soil *Bacillus* strain. This extract was demonstrated to protect mice from pneumococci infection.

In the following year, Hotchkiss and Dubos [41] fractionated this extract and identified an AMP called gramicidin. Gramicidin was found effective for the treatment of wounds and ulcers [42]. In 1941, another AMP, tyrocidine, was discovered and found to be effective against both Gram negative and Gram positive bacteria [43]. In the same year, another AMP called purothionin and active against some fungi and bacteria was isolated from a plant, *Triticumaestivum* [44]. .

The first reported animal-originated AMP is defensin, that was isolated from rabbit leukocytes in 1956. In the following years, several AMPs were discovered from different sources: epithelia and cow milk were both described. It was also demonstrated that human leukocytes contain AMPs in their lysosomes.

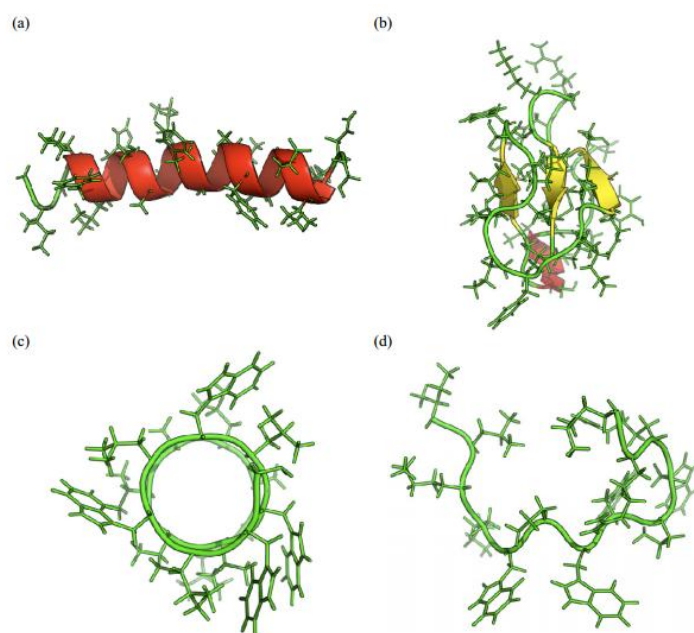
In total, more than 5,000 AMPs have been discovered or synthesized up to date. Natural AMPs were found in both prokaryotes (e.g., bacteria) and eukaryotes (e.g., protozoan, fungi, plants, insects, and animals) [45]. In animals, AMPs are mostly found in the tissues and organs that are exposed to airborne pathogens and are part of the innate immune defense against viruses, bacteria, and fungi. Thus, AMPs play an important role in stopping most infections before they cause any symptoms. For example, frog skin is the source of more than 300 different AMPs [46].

Most AMPs are produced by specific cells at all times, while the production of some AMPs is inducible. Some studies [28] showed how epithelial cells from different tissues of mice increased rate of mRNA transcription for defensin production after infection with *Pseudomonas aeruginosa*.

Most AMPs reported to date can be characterized by the types of secondary structure adopted:  $\beta$ -sheet,  $\alpha$ -helix, extended, and loop. Among these structural groups,  $\alpha$ -helix



and  $\beta$ -sheet structures are more common [47] and to date the  $\alpha$ -helical peptides are the most studied AMPs.



**Figure 16.** Examples of the secondary conformations adopted by AMPs (a,  $\alpha$ -helix; b,  $\beta$  sheet; c, loop; d, random coil)

Many peptides adopt their active structure only when they interact with the membranes of target cells. For example, *indolicin* shows globular and amphipathic conformation in aqueous solutions while it is wedge-shaped in lipid bilayer mimicking environments [48]. This AMP also changes its conformation during interaction with DNA evidenced with decreased fluorescence intensity and a slight shift in the wavelength of maximum emission.

Unlike antibiotics, which target specific cellular activities (e.g. synthesis of DNA, protein, or cell wall), AMPs target the lipopolysaccharide layer of cell membrane, which is ubiquitous in microorganisms. Moreover the presence of high level of cholesterol and low anionic charge puts eukaryotic cells out of the target range of many AMPs [49].

AMPs are made by amino acids, so it is relatively easy to modify their structure and immobilize them on surfaces [50]. AMPs can be directly prepared by chemical synthesis or by using recombinant expression systems [48].

These artificial sources of AMPs allow modifying existing AMPs and designing new synthetic AMPs. Such modifications have the potential to change the targets of

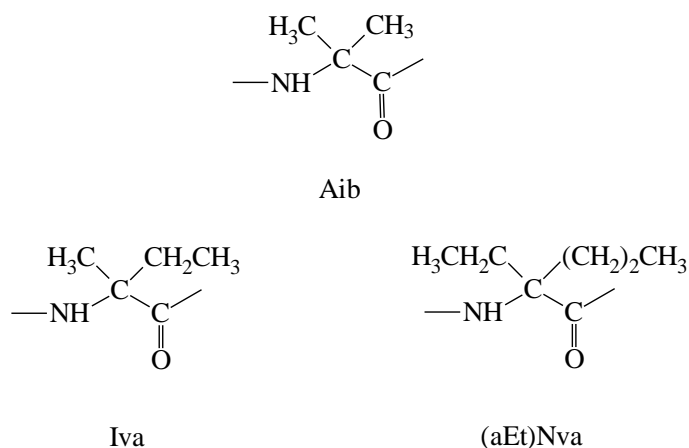
AMPs and improve the stability of AMPs against enzymatic degradation caused by proteases [51].

Particularly, in this work three types of AMPs were considered as peptides for the preparation of antimicrobial textiles:

- Peptaibols.
- Synthetic peptides based on FA-YXXY pattern (Y = cationic residue; X = hydrophobic residue) and short peptides rich in Arg and Trp residues.
- Peptide dendrimers.

## Peptaibols

Peptaibols belong to the class of ionophores channel former. Their name is related to the fact that they are linear compounds of peptidic nature composed from five to twenty amino acids [52]. They usually are constituted by one or more  $\alpha$ -aminoisobutyric acid (Aib), the simplest  $C^\alpha$ -tetrasubstituted amino acid, and bear a C-terminal 1,2-aminoalcohol. The N-terminus is generally blocked by an acyl group, typically by the acetyl group. Some peptaibols contain, in addition to Aib, two other  $C^\alpha$ -tetrasubstituted amino acids: Isovaline (Iva) and  $\alpha$ -ethylnorvalin [( $\alpha$ Et) Nva] [53]. Iva is usually present as D enantiomer, but some sequences contain L-Iva.



**Figure 17.** Chemical structure of Aib, Iva and ( $\alpha$ Et)Nva residues respectively.

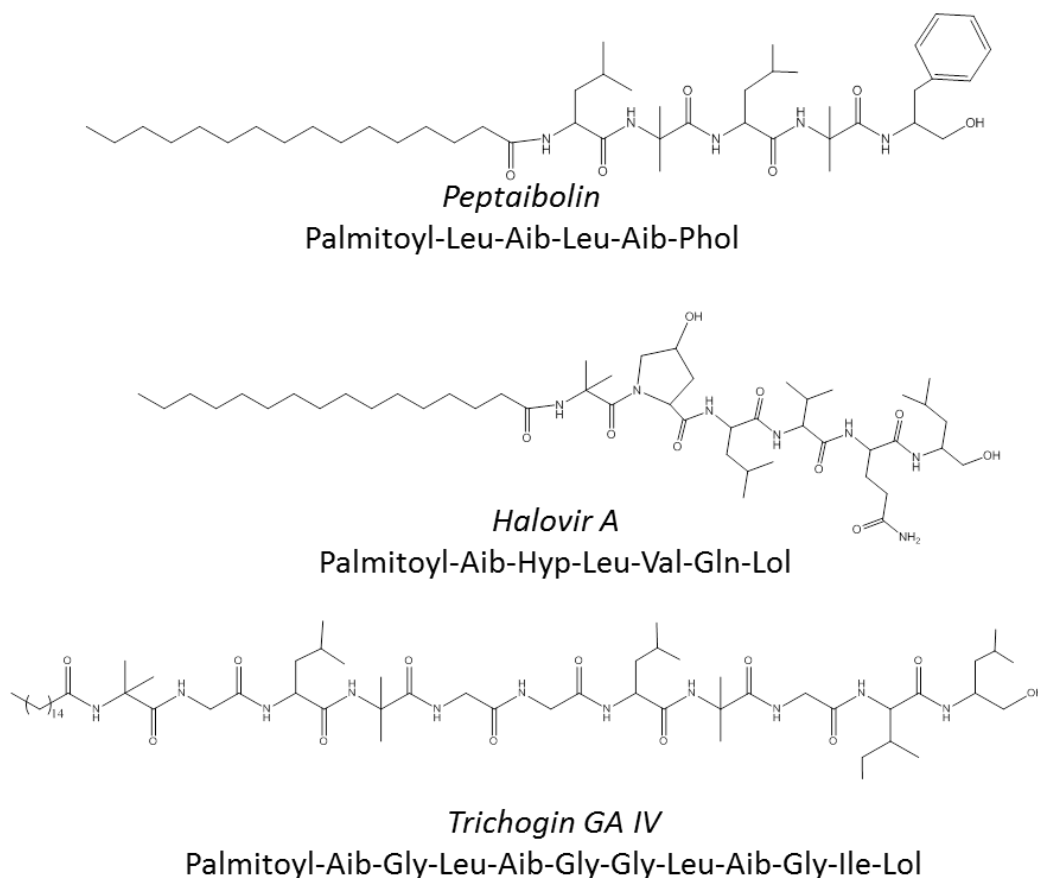
Peptaibols occur naturally as a mixture of several components (at least twelve in the case of alamethicin) as a consequence of the non-ribosomal synthesis of these

compounds [54]. The peptides found in such mixtures often differ in the substitution of a single amino acid residue, complicating the separation of the different analogues. However, the HPLC has been particularly useful for this purpose. Moreover, the presence of Aib and of the blocking groups at N- and C-termini has made it difficult to determine the primary structure of peptaibols. In this sense, it is decisive the employment of mass spectrometry and  $^1\text{H}$  and  $^{13}\text{C}$  NMR spectrometry [55].

The antibiotic activity of peptaibols is accomplished by modulating the permeability of biological membranes: they may therefore have hemolytic and cytotoxic activity, [56] can uncouple oxidative phosphorylation and increase the permeability of liposomes [57]. Some peptides, as alamethicin, can also create channels of voltage-dependent self-assembling a variable number of molecules, (4 to 12) [54-56]. Alamethicin and peptides related to it may in fact serve as a model [57] for understanding more complex systems, involving channels formed by proteins in cell membranes. Over the last few years some peptides with antimicrobial activity have been identified. They are Trichogin GAIV [58], Trichonigin KB KB II, LP237-F7, [59] LP237-F8 [60,61] and LP237-F5 [62], Trichodecine I and II, [63]), which present at the N-terminus a long linear acyl chain. These compounds are therefore referred to as lipopeptaibols. [64] Lipopeptaibols possess other properties that distinguish them from N-acetylated peptaibols, such as the limited chain length (up to eleven residues) and the low acid Aib.

A particular case of peptaibols is represented by Peptaibolin, introducing an acetyl group at the N-terminus, similarly to longer peptaibols, but consists of only five residues including the C-terminal aminoalcohol. This compound manifests antimicrobial activity, although moderate, against Gram positive bacteria and yeasts. [63]

From this class we selected Peptaibolin [64], Halovir A [65] and Trichogin GA IV [58] analogues to be used as antimicrobial agents in cotton textile. All the peptides prepared have a fatty acid linked to the N-terminus.



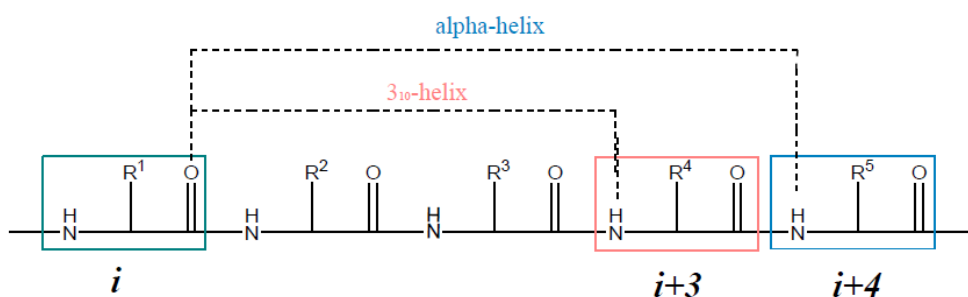
**Figure 18.** Chemical structure of the lipopeptaibols used in this work.

### **Conformation of Aibcontaining peptides**

The C<sup>α</sup>-tetrasubstitued amino acid  $\alpha$ -aminoisobutyric acid (Aib) was commonly encountered in vivo in microbial peptides (such as peptaibols). The stability of this class of peptides is due to the presence of many Aib residues which favor the helical conformation and the resistance to proteolytic enzymes [66]. For these reasons Aib is widely used to design promising antimicrobial peptides [67].

Secondary structures of proteins depend on the values of the torsional angles  $\varphi$  and  $\psi$  of the peptidic backbone (figure 19). Classical secondary structures are helices,  $\beta$ -sheets and  $\beta$ -turns. Because Aib residue is an  $\alpha$ - and  $3_{10}$ -helix and  $\beta$ -turn inductor, these conformations will be briefly described in this paragraph.

The number of residues per turn of a  $3_{10}$ -helix is 3,24 and the pitch is 6 Å. This helix is characterized by hydrogen bonds between the CO moiety of a  $i$  residue and the NH moiety of the  $i+3$  residue.

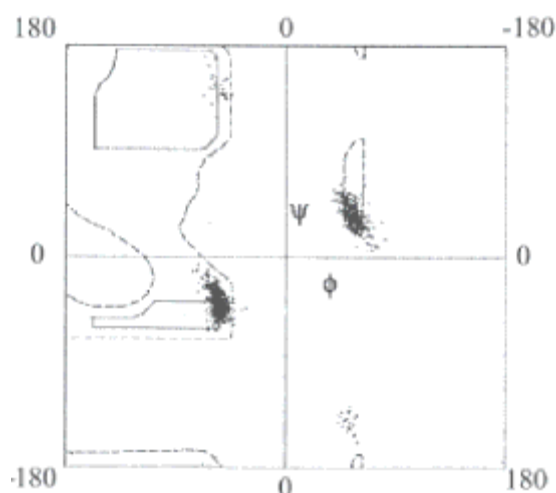


**Figure 19.** Data of canonical  $\alpha$ -helix and  $3_{10}$ -helix

The resulting macrocycle is composed by 10 atoms. Hydrogen bonds of  $3_{10}$ -helices are distorted and dipoles are tilted by  $30^\circ$  compared to the axis of the helix.

The presence of two substituents on C $\alpha$  causes a restriction in possible torsional angles  $\varphi$  and  $\psi$ , compared with common amino acids, due to the Thorpe-Ingold (or gem-dialkyl) effect of quaternary carbon atoms [68].

According to the Ramachandran plot (figure 20) the two major allowed conformations are gathered in the zone of right- or left-handed  $\alpha$ - and  $3_{10}$ -helices.



**Figure 20.** The  $(\varphi, \psi)$  energy map for the Aib residue.

Usually peptides containing Aib residues have an  $\alpha$ -helical,  $3_{10}$ -helical or mixed  $\alpha/3_{10}$ -helical conformation, depending on length, environment, size of side chains and distribution of residues. Aib rich peptides fold in a  $3_{10}$ -helix conformation if they are shorter than 9 residues; longer peptides can fold into a mix of a  $3_{10}$ - and  $\alpha/3_{10}$ -helix. However  $\alpha$ -helical conformation is not favored below 7-8 residues [69]. Because of the achiral nature of Aib left- and right- handed helices are isoenergetic, thus equiprobable. Chiral residues of the chain determine the conformation of the

helix: D residues favor left handed helices, while L amino acids favor right handed helices [70].

## Synthetic peptides

### *FA-YXXY peptides*

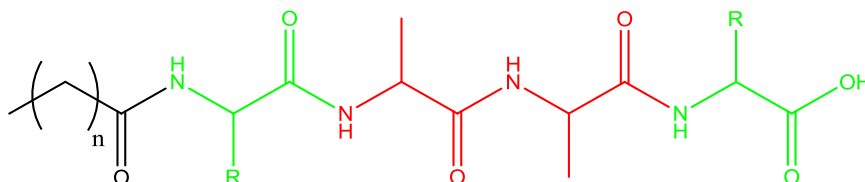
In 2006, Shai's group, knowing that the conjugation of long aliphatic chains to the N-terminus of natural and non-natural AMP endowed them with selective antimicrobial activity [71], synthesized ultrashort peptides, with the essential constituent elements of AMP, obtaining potent antimicrobial activity against a high variety of microorganisms.

The most effective lipopeptides consist of four amino acids with L and D conformation, connected to an aliphatic carboxylic acid of variable length. The peptide sequence is Lys-XX-Lys (where X is Leu, Ala, Gly, Lys, or Glu). The best fatty acid tested results to be the *palmitic* acid, composed by 16 saturated carbon atoms.

**Table 3.** Short lipopeptide prepared and tested by Shai's group [71]

C16-Lys-Leu-D-Leu-Lys	C12- Lys-Ala-D-Ala-Lys
C14- Lys-Leu-D-Leu-Lys	C16- Lys-Gly-Gly-Lys
C12- Lys-Leu-D-Leu-Lys	C16- Lys-D-Lys-Lys-Lys
C16-Lys-Ala-D-Ala-Lys	C16- Lys-D-Lys-Glu-Lys
C14- Lys-Ala-D-Ala-Lys	C16-Gly-Ile-Gly-Lys

The general structure of peptides introduced by Shai and used in this thesis work is reported in figure 21.



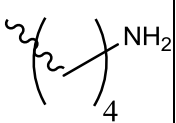
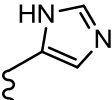
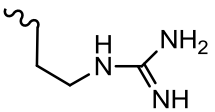
**Figure 21.** General structure of synthetic peptides with pattern FA-YXXY.

Main features of the peptides are:

- A long aliphatic chain linked to N-terminus in black in figure 21. This feature is typical of natural short hydrophobic peptides and promotes the insertion of the peptide into the lipid membrane.
- Two cationic residues (green in figure 21), at positions 1 and 4, respectively. The high pKa values due to these residues promote the electrostatic interaction between the microbial membrane, generally formed by negative charged phospholipids and the positively charged peptide.
- Two apolar residues (red in figure 21), consisting of two Alanine (Ala), at positions 2 and 3. The residue at position 3, unlike the other residues of the chain, is an amino acid of D configuration. This residue probably provides the structure resistance to enzymatic degradation, a defense mechanism used by some microorganisms such as bacteria and fungi against AMP. [72]

Particularly, in this work we use as cationic residues Lys, Arg and His. The lateral chain of these residues are reported in table 4.

**Table 4.** Cation residues used in the preparation of our samples

Amino acid	Lys (K)	His (H)	Arg (R)
Side chain			

### **Antimicrobial activity of D-amino acid-containing peptides**

The use of diastereomeric peptides has some advantages. Peptides constituted by L-amino acids are degraded by some enzymes (such as trypsin and proteinase K) and are thus deactivated in serum. In addition, they are highly hemolytic and sometimes have low water solubility. Peptides containing D-amino acids on the other hand are more soluble in water, show activity in serum, are not hemolytic and their enzymatic degradation can be controlled [73].

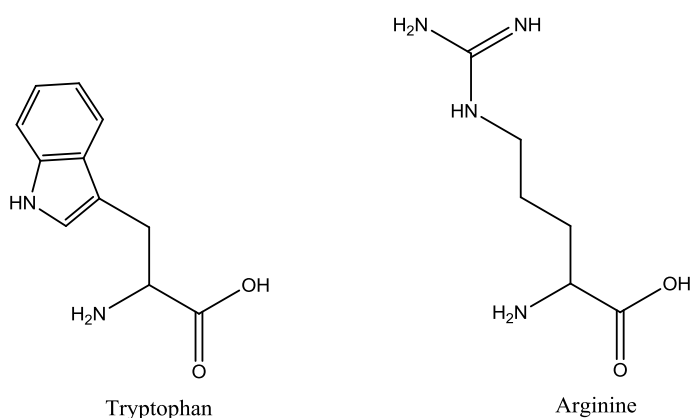
Moreover, the use of D-amino acids in peptides avoid toxic effects on mammals, while maintaining the ability of peptides of spanning bacterial cell membranes, thus increasing selectivity [74].

Unfortunately peptides containing D-amino acids drastically destabilize the helical secondary structure, leading to a decrease in antimicrobial activity in antimicrobial peptides with amphipathic helical structure [75].

However, it has been shown that structure and activity can be maintained by replacing only some L- with D-amino acids in short peptides composed of lysine and leucine and in some amphipathic helical peptides [76].

### **Peptides rich in Tryptophan-Arginine residues**

In this part of the work we focused our attention on short sequence (4 residues) composed only by the residues Tryptophan (Trp) an Arginine (Arg). Activity of AMPs rich in Trp an Arg against bacteria is strong supported and documented in the literature [77,78].



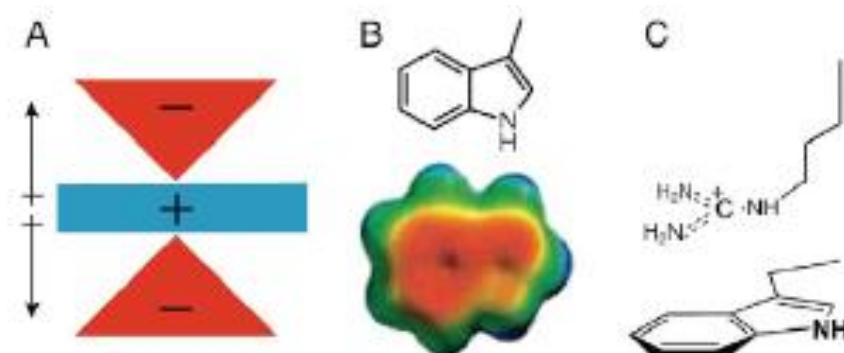
**Figure 23.** Chemical structures of Tryptophan and Arginine.

These residues present some peculiar properties that make them useful for antibacterial purpose:

- Trp show a preference for the interfacial region of phospholipidic bilayer [79];
- Arg provides a positive charge so that the peptide has the possibility to form suitable hydrogen bonding for the interaction with the bacterial membrane, usually negatively charged.



As reported for the AMP lactoferrin the synergism between Trp and Arg is crucial for the interactions with bacterial membrane [80]. In fact the  $\pi$ -electron system of Trp side chain can participate in cation-  $\pi$ -electron interactions between its  $\pi$ -electron and the side chain of Arg that is positively charged (fig.24).



**Figure 24.** A) Dipolar structure of indole ring; B) Disposition of electronic density in indole ring ; C) Mutual cooperation between Arg and Trp lateral chains.

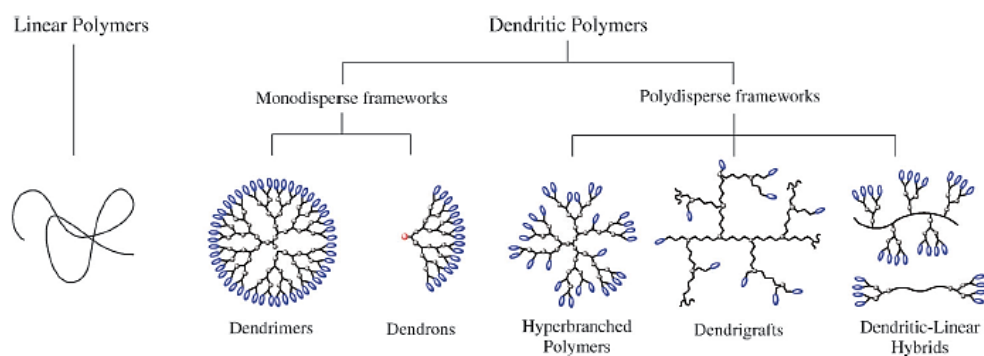
For this reason short sequences rich in Trp and Arg show high activity against bacteria.

Also in this case the N-terminus of the peptides was functionalized with a fatty acid moiety. In this work we prepared tetrapeptides composed only by Arg and Trp varying their mutual position in the sequence.

## Dendrimers

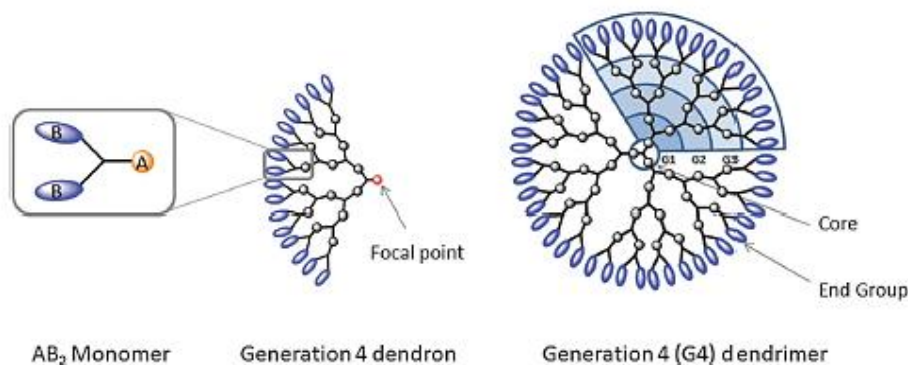
Dendrimers are highly branched dendritic structures that bear a number of precisely controlled functional groups. [81]

The name derived from "Dendro" a Greek word which means tree. The work of synthesis of this class of materials was started by Vogtle et al. in 1978. This research group reported the synthesis of a structure of polypropylene-branched amine, called "molecule cascade", produced by the repetitive addition of the monomer and activation of branched molecules obtained. [82] Although the final branched structure was simple and of low molecular weight, their work is now recognized as a starting point for research of dendritic polymers. Currently, the dendritic structures are typically divided into monodisperse (dendrimers and dendrons) and polydisperse (hyper-branched polymers, dendrimers and dendrigrafts linear hybrid).



**Figure 25.** Dendritic structure.

A dendrimer is formed by monomers  $AB_N$  interconnected, where A and B are two different functions and n is a number greater than or equal to two. A dendrimer consists of a multifunctional central portion, typically di-, tri- or tetrafunctional, from which branches off several layers of monomers, each called a generation (G). The regularly branched structure has an outer layer which is decorated with a large number of activated functional groups which can undergo further growth or post-functionalization. The structure of the dendrimer can also be divided into fragments called dendrons, wedges ranging from the core to the periphery of the dendrimer.



**Figure 26.** Fourth generation dendrimer structure.

It was also discovered that the multi valence of peptide dendrimers could be exploited in the development of species capable of permeating the bacterial membranes. In particular, it is effective ability to amplify charged cationic and hydrophobic cluster as the number of branches of the dendrimer. [83] In fact, the polycationic peptides, both linear and branched, are known for the destruction capacity of the membrane or fusion (permitted by hydrophobic cluster) with the same to facilitate the passage of proteins and genes within a cell [84]. A reasonable

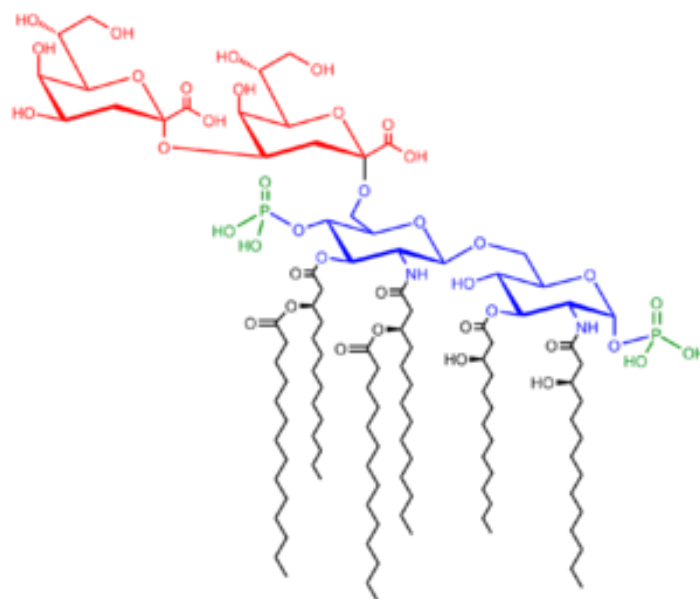
mechanism involves the amplification given by dendrimeric structure increases the effective molarity of monomeric units and decreases the entropy of self-assembly. In this way, the dendrimers mimic the mechanism of action by which antimicrobial peptides with high molecular weight exert their effects of membrane lysis. [85]

### **Mode of action of AMPs**

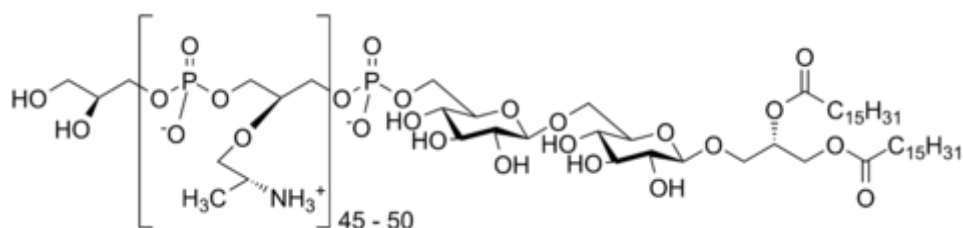
AMPs are generally rich in cationic residues, such as Arg and Lys. This composition confer to the peptide a net of positive charge, that promote the interaction with bacterial membrane, usually negative charged, by an electrostatic interplay. The presence in the sequence of hydrophobic residues favors the insertion in the membrane bilayer.

The presence of sterols in human and fungal membrane cells, cholesterol and ergosterol respectively, can be the reason of the high selectivity shown by AMPs towards bacterial membranes, which on the contrary do not contain sterols. Moreover, while bacterial membranes are mainly composed by anionic lipopolysaccharides (LPS, in Gram negative bacteria) and lipoteichoic acid (LTA, in Gram positive bacteria), conferring an anionic net charge to the system, erythrocyte cell membranes are composed by zwitterionic lipids resulting in an overall uncharged character [86].

Several mechanisms were proposed for membrane disruption strongly related to the nature of the AMP used. In all cases the first step of this action is the same for all the bioactive peptides and is represented by the binding between the AMP and the LPS.

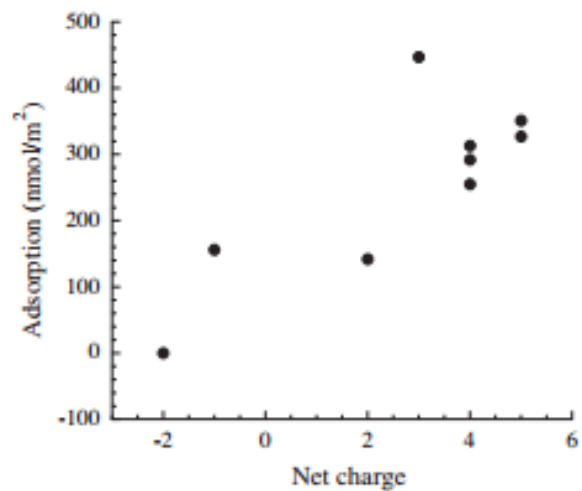


**Figure 27.** Lipopolysaccharide (LPS) chemical structure: i) red color = O-chain; ii) blue color = saccharide core ; iii) black color = Lipid A



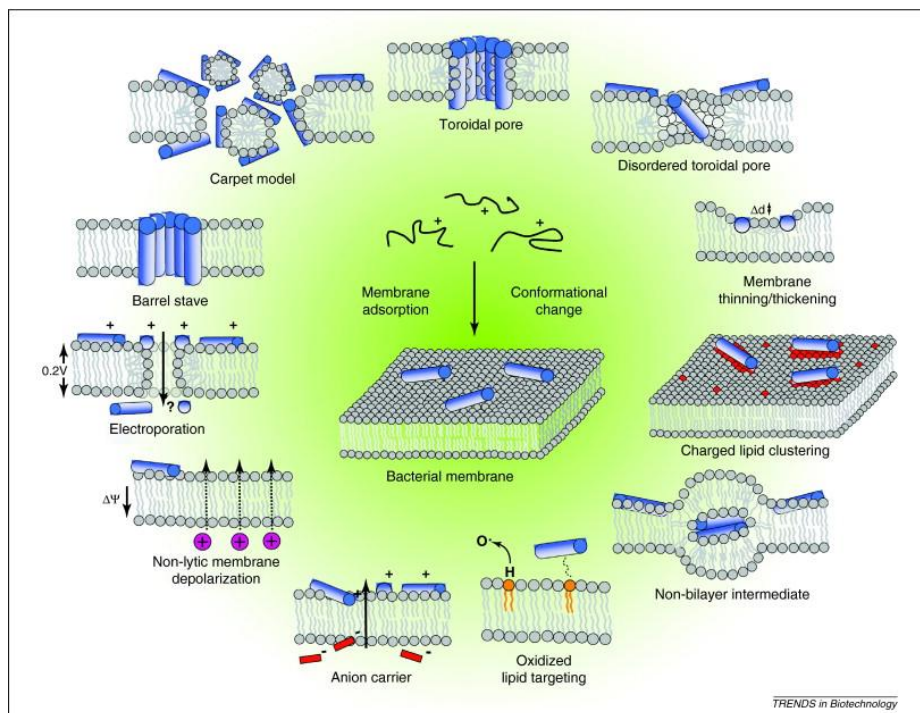
**Figure 28.** Chemical structure of Lipoteichoic acid (LTA).

Numerous studies were performed in the last years about the AMPs-LPS electrostatic interaction. Singh et al. demonstrate that, while phospholipid membrane binding is driven by the amphiphilicity of the peptides, LPS binding is related to their net charges as well as to their hydrophobicity [87]. Similar results were obtained by Andra et al. [88].



**Figure 29.** Correlation between adsorption to *E. coli* LPS and peptide charge density.

It was found that while the hydrophobic part of an AMP acts in the binding with lipid A moiety, their electrostatic moieties bind the polysaccharides part of LPS [89]. Other studies reported by Junkes et al. also demonstrate how cyclic peptides rich in Arg/Trp residues are able to bind LPS, and this pattern also promote the insertion in LPS to lipid A, with the consequently disorder of this region [90]. After the first binding step between AMPs and LPS, membrane disruption can so occur in different proposed ways.



**Figure 30.** Proposed modes of action of AMP after binding with the LPS

### **1.4 Why use cotton?**

An antimicrobial finish can be applied to most types of textiles. However, since 1800, medical textiles are often made by cotton for its comfort and handiness properties. The fiber content of an antimicrobial textile must be chosen carefully. Due to their hydrophobic nature some fabrics, especially synthetic fabrics, may not be appropriate for some uses. This means that fabrics made of synthetic fibers hold a larger amount of perspiration humidity in their structures than do natural fibers. This property can cause an increased chance of irritation and odor due to microbial growth on the body [91].

The use of natural fibers is encouraged because end-use products from natural fibers are biobased. Natural fibers are also good sources for textiles because they are renewable resources and their export can be good for many economies.

Cotton is abundant and its mechanical properties are well suited for garment production. It is easy to care for and takes well to bleaching. The behavior of fibers in bleaching is important when dealing with antimicrobial finishes because many of these finishes bleaching to regenerate their antimicrobial properties [92].

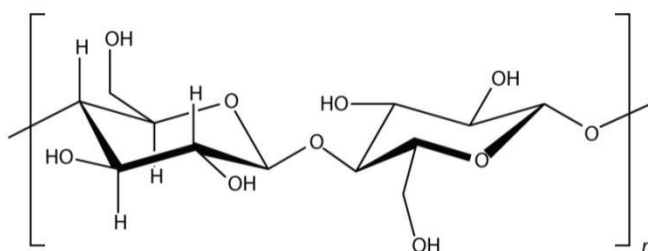
### **Cotton fiber**

Cotton fibers are composed mostly of  $\alpha$ -cellulose (88.0–96.5%) [93]. The noncellulosics are located either on the outer layers (cuticle and primary cell wall) or inside the lumens of the fibers whereas the secondary cell wall is purely cellulose. The specific chemical compositions of cotton fibers vary by their varieties, growing environments (soil, water, temperature, pest, etc.) and maturity. The noncellulosics include proteins (1.0–1.9%), waxes (0.4–1.2%), pectins (0.4–1.2%), inorganics (0.7–1.6%), and other (0.5–8.0%) substances. Being a fiber of vegetable origin, cotton is very resistant to boiling and to ironing (unchanged up to 100° C), has a high power moisture absorption, is a good conductor and promotes the loss of body heat, is not attacked by moths (*falene*), but can be a receptacle of mold and bacteria. Among the defects we find the low elasticity.

The cotton fiber from other fibers for the following factors: its toughness increases with humidity, degrades only at very high temperatures (above 150° C), does not lose elasticity at low temperatures. It can be washed by hand or machine without any

problems as the wet state increases its resistance. The temperature may be high (90°) and detergents can be basic (the strongest). Cotton ignites easily, the flame is supported and there is no smoke emissions. The unpleasant odor during combustion is similar to that of the paper as it burns cellulose.

Cellulose is essential to compose all natural vegetable fibers, it is a polymeric compound consisting of cyclic units deriving from glucose (piranose) condensed through  $\beta$ ,1-4 glucosidic links to form long chains.

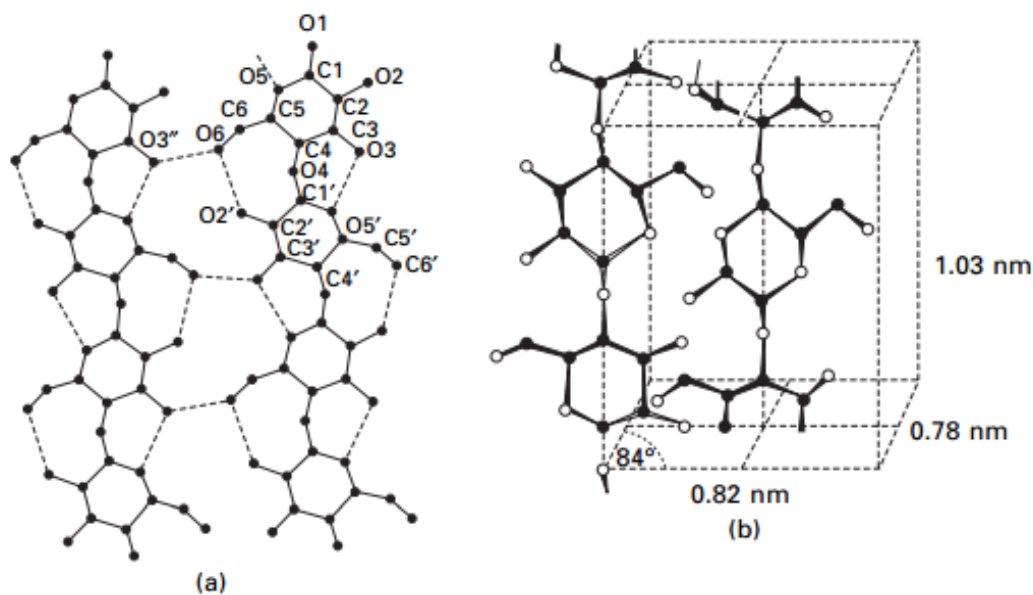


**Figure 32.** Chemical structure of cellulose polymer.

The most important reactions involving the production of artificial fibers implicate mainly hydroxyl groups. In particular, the reaction with caustic soda produces the sodium-cellulose, soluble in water, which is the precursor of the viscose rayon. Other very important reactions are those that lead to the formation of cellulose esters (nitrocellulose, rayon acetate) and ethers (ethyl cellulose, methyl cellulose, used in the adhesives, dressings and dressings).

### **Cellulose chemistry and reactivity**

Cellulose in cotton presents high crystallinity: several types of crystalline forms were found in cellulose. In the solid state, cellulose can exist in seven different allomorphs labelled Ia, Ib, II, III, IIII, IVI, IVII. The  $\beta$ ,1-4 glucosidic link allows favorable O3H/O5 hydrogen bond interactions resulting in a pseudo P2<sub>1</sub> helical conformation of cellulose chains in all seven allomorphs [94]. The most abundant form in vegetal cellulose is cellulose I (fig.33).

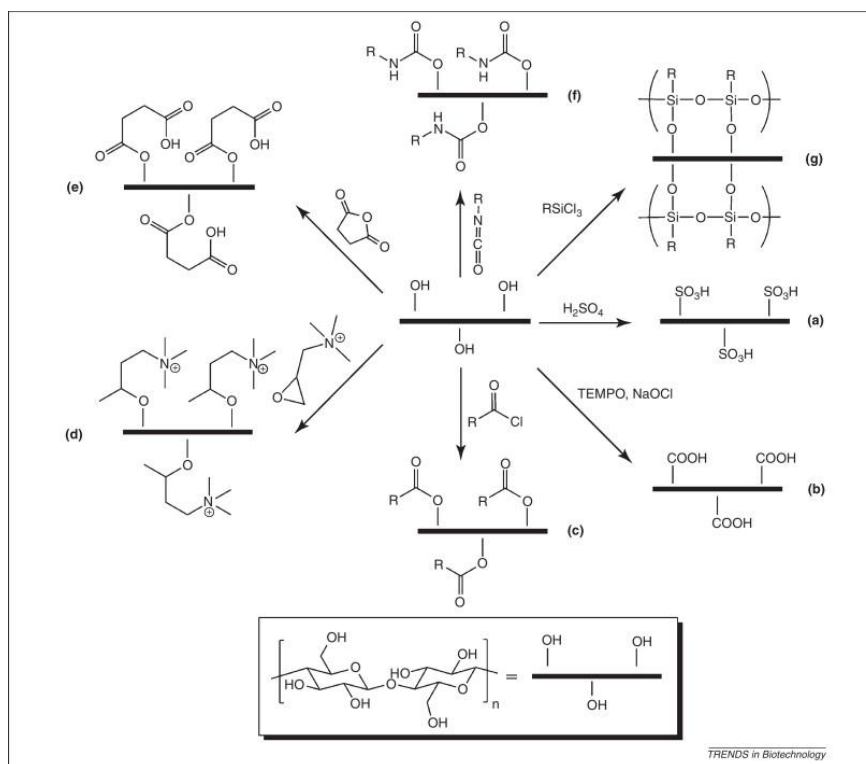


**Figure 33.** Crystallographic representation of cellulose chain with symmetry  $P2_1$ .

Cellulose is a biopolymer composed by glycosides unit link together by  $\beta$ -1,4-glucodidic bonds. Each glucose unit contains three hydroxyl groups, one primary on C-6 and two secondary on C-2 and C-3. The abundant hydroxyl groups and the chain conformation allow extensive inter-molecular and intra-molecular hydrogen bonding to further enhance the rigidity of the cellulose structure and explain the insolubility of the material.

Chemical reactions on cotton cellulose depend on the supramolecular structure as well as the activity of the C-2, C-3 and C-6 hydroxyl groups. Reactions begin in the more accessible amorphous regions and on the surfaces of crystalline domains. Chemical reactivity of the cellulose hydroxyl groups follows those of aliphatic hydroxyl groups, i.e., higher for the C-6 primary than the secondary on the C-2 and C-3.





**Figure 34.** Example of chemical reaction involved cellulose hydroxyl groups.

Etherification and esterification are the two main reactions in which cellulose can be involved. Esterification reactions, such as nitration, acetylation, phosphorylation, and sulfation, are usually carried out under acidic conditions. Etherification, on the other hand, is favored in an alkaline medium.

Cellulose is readily attacked by oxidizing agents, such as hypochlorites, chlorous, chloric, and perchloric acids, peroxides, dichromates, permanganates, periodic acid, periodate salts, and nitrogen tetroxide [95]. Most oxidizing agents are not selective in the way they react with the primary and secondary hydroxyl groups. Oxidation of cellulose can lead to two products, reducing and acidic oxycellulose. In reducing oxycellulose, the hydroxyl groups are converted to carbonyl groups or aldehydes, whereas in acidic oxycellulose, the hydroxyl groups are oxidized to carboxyl groups or acids. The oxycellulose can be further oxidized to acidic oxycellulose.

Reducing oxycellulose is more sensitive to alkaline media and the chain lengths are often reduced. Periodic acid and periodate salts break the anhydroglucose ring between C-2 and C-3, converting the two secondary hydroxyl to aldehydes which can be further oxidized to carboxyl groups. Nitrogen tetroxide reacts specifically

with the primary hydroxyl groups on C-6, oxidizing it to carboxyl group directly or to polyglucuronic acid, an oxycellulose.

In this project, hydroxyl groups of the cellulose have been used as anchor site to covalently bind the desired peptide sequences.

### **Peptide-immobilized fibers**

In recent years the market of antimicrobial materials has increased rapidly, with application ranging from medical devices to nursing care or food packaging. These materials traditionally consist of antimicrobial agents such as silver ions, quaternary ammonium ions or pyridinium salts immobilized on a solid surface [96]. Unfortunately problems of drug-resistance and toxicity arose. Materials functionalized with silver nanoparticles, the prevailing antimicrobial materials which are commercially available, can have adverse effects on human health. The prolonged exposure to silver can cause argyria and is a suspected carcinogen due to its interaction with DNA and RNA [96].

Previous studies show that the covalent immobilization of antibacterial cationic peptides on polymers or metals stops bacterial proliferation and prevent the bacterial adhesion on the surfaces. The advantage of peptides which act through a cell disruptive mechanism is that they can retain activity, even bond to a solid support.

Immobilization of antimicrobial peptides on cotton fibers is interesting, in order to create new antimicrobial textiles for immunocompromised patients and health workers [97].

The correct immobilization of peptides on the support is fundamental to keep the antimicrobial activity. Peptides have many functional groups which can interact with the hydroxyl functions of cotton fibers. Incorrect anchoring can disrupt the correct folding of the peptide or prevent the interaction between the peptide and the bacterial cell membrane. Previous studies tried to solve this problem by introducing a linker between the peptide and the cotton fibers. In our group some antimicrobial peptides have been anchored to cotton fibers. Experiments to test fiber activity were performed in the literature. Immobilized peptide fibers were washed with distilled water and sterilize at 121°C for 15 minutes. Peptides remained anchored on the

cotton fibers and the antibacterial activity was maintained. The result of this test is promising for possible clinical applications.

## *Aim of the work*

- To develop a reproducible and efficient synthetic methodology for covalently link peptides to a natural cotton fabrics.
- To prepare and characterize textile samples covalently linked to peptide or dendrimers displaying antimicrobial properties. Peptides with simple sequences and with wide spectrum of antimicrobial activity were chosen.
- To set up simple protocols in order to characterize and identify the material prepared. Techniques typical of the surface analysis are applied: XPS at N 1s atom, FT-IR, EPR, UV-Vis and TGA.
- To submit peptide-cotton samples to biodegradation through the action of the enzyme cellulase from *Trichoderma reesei* in order to isolate a compound that could be characterized through solution technologies such NMR spectroscopy, HPLC and mass spectrometry. In this way we would be able to unambiguously identify the products of our synthetic efforts.
- To test the antimicrobial activity of the functionalized fabric samples for possible future applications.

The list of the peptide-cotton materials prepared and studied in this work is as follows:

<b>Peptide linked</b>
Palmitoyl-Lys-Ala-D-Ala-Lys- <i>linker</i> -cotton
Palmitoyl-His-Ala-D-Ala-His- <i>linker</i> -cotton
Palmitoyl-Arg-Ala-D-Ala-Arg- <i>linker</i> -cotton
Palmitoyl-Arg(NO <sub>2</sub> )-Ala-D-Ala-Arg(NO <sub>2</sub> )- <i>linker</i> -cotton
Palmitoyl-Trp-Arg-Trp-Arg- <i>linker</i> -cotton
Palmitoyl-Arg-Trp-Trp-Arg- <i>linker</i> -cotton
Palmitoyl-Aib-Gly-Leu-Aib-Gly-Gly-Leu-Aib-Gly-Ile-Leu- <i>linker</i> -cotton
Palmitoyl-Aib-Hyp-Leu-Val-Gln- Leu- <i>linker</i> -cotton
Palmitoil-Leu-Aib-Leu-Aib-Phe- <i>linker</i> -cotton
Palmitoyl-Lys-Aib-Lys-Aib-Phe- <i>linker</i> -cotton
[(Palmitoyl-Lys-Ala-D-Ala-Lys) <sub>4</sub> Lys <sub>2</sub> ]Lys- <i>linker</i> -cotton
[(Palmitoyl-His-Ala-D-Ala-His) <sub>4</sub> Lys <sub>2</sub> ]Lys- <i>linker</i> -cotton
[(Palmitoyl-Arg-Ala-Aib-Arg) <sub>4</sub> Lys <sub>2</sub> ]Lys- <i>linker</i> -cotton
[(Palmitoyl-Arg(NO <sub>2</sub> )-Ala-Aib-Arg(NO <sub>2</sub> )) <sub>4</sub> Lys <sub>2</sub> ]Lys- <i>linker</i> -cotton
[(N-5-Valeroyl-His-Arg) <sub>4</sub> Lys <sub>2</sub> ]Lys- <i>linker</i> -cotton
[(N-5-Valeroyl-Trp-Arg) <sub>4</sub> Lys <sub>2</sub> ]Lys- <i>linker</i> -cotton



## Reference

1. A. Fleming. *Br J Exp Pathol*, **10** (1929) 780-790.
2. S. A. Waksman and R. E. Curtis, *Soil Sci.* **1** (1916) 99-134.
3. W. H. Stewart. *Lancet*, **110** (2008) 372.
4. Powers, J.P.; Hancock, R.E. *Peptides* **24** (2003) 1681–1691.
5. Harrison PW. *Textile Progress*, **32** (2002) 4.
6. Ganz, T.; Lehrer, R.I. *Mol. Med. Today* **5** (1999) 292–297.
7. A. Varki, R. D Cummings, J. D. Esko, H. H Freeze, P. Stanley, C. R. Bertozzi, G. W Hart, M. E. Etzler. *Essentials of Glycobiology* (2009) cap. 20.
8. W. Vollmer, D. Blanot, M.A. de Pedro, *FEMS Microbiol. Rev.*, **32** (2008) 149.
9. T.L. Lemke, W.O. Foye, D.A. Williams, *Principi di chimica farmaceutica* (2009) 873.
10. Van Meer G., Voelker D. R.; Feigenson G. W., *Nat. Rev. Mol. Cell. Biol.* **2** (2008) 112–124.
11. S. T. Cole, *Phil. Trans. R. Soc. B* **369** (2005) 20130430.
12. A. de J. Sosa et al. (eds.), *Antimicrobial Resistance in Developing Countries*, (2009) chapter 2.
13. CDC 2013 Antibiotic resistance threats in the United States, (2013) 1–114. <http://www.cdc.gov/drugresistance/threat-report-2013/>.
14. M.C. Enright, D.A. Robinson, G. Randle, E. J. Feil, H. Grundmann, B.G. Sprat; *PNAS*, **99** (11) (2004) 7687-7692.
15. ECDC/EMA 2009 The bacterial challenge: time to react. London, UK: European Centre for Disease Control & European Medicines Agency
16. Neely, A. N., & Maley, M. P.. *Journal of Clinical Microbiology*, **38**(2) (2000), 724-726.
17. Gao Y, Cranston R. *Textile Research Journal.* **87** (2008) 60-72.
18. White WC, Bellfield R, Ellis J, Vandendaele IP. *Medical and Healthcare textiles*, Woodhead Publishing Limited (2010).
19. Ramachandran T, Rajendrakumar K, Rajendran R. *Antimicrobial Textiles*, **84** (2004) 42-47.

20. Simoncic B, Tomsic B. *Textiles Research Journal*, doi: 10.1177/0040517510363193, 2010.
21. Heine E, Knops HG, Schaefer K, Vangeyte P, Moeller M. *Antimicrobial Functionalization of Textile Materials*. In: Multifunctional
22. O. Bondarenko, K. Juganson, A. Ivask, K. Kasemets, M. Mortimer, A. Kahru, *Arch Toxicol*, **87** (2013) 1181-1200.
23. G. Bedoux, B. Roig, O. Thomas, V. Dupont, B. Le Bot, *Environ Sci Pollut Res*, **19** (2012) 1044-1065.
24. T. McMahan, N. Shamin, S. Gowda, G. Angle, T. Leighton 2008, USEPA, <http://www.epa.gov/oppsrrd1/REDS/2340red.pdf>
25. A. Lindstrom, I.J. Buerge, T. Poiger, P.A. Bergqvist, M.D. Muller, H.R. Buser. *Environ. Sci. Technol.* **36** (2002) 2322-2329
26. J.V. Rodricks, J.A. Swenberg, J.F. Borzelleca R.R. Maronpot, A.M. Shipp. *Crit. Rev. Toxicol.* **40** (2010) 422-484.
27. B.R. Crawford, D. deCatanzaro , *Reproductive Toxicology* **34** (2012) 607–613
28. N. Veldhoen, R.C. Skirrow, H. Osachoff, H. Wigmore, D.J. Clapson, M.P. Gunderson, G. Van Aggelen, C.C. Helbing. *Aquatic Toxicol.* **80** (2006) 217-227.
29. H.L. Zucherbraun, H. Babich, R. May, M.C. Sinesky. *Eur. J. Oral. Sci.* **106** (1998) 628-636
30. G.S. Prins. *Endocr. Relat. Canc.* **15** (2008) 649-656.
31. G. Bedoux, R. Benoit, O. Thomas, V. Dupont, B. Le Bot. *Environ. Sci. Pollut. Res.* **19** (2012) 1044-1065
32. F. Shahidi, Y. Zhong, *Euro J. Lipid Sci Techno* **112** (2010) 930-940
33. C. Beer, R. Foldbjerg, Y. Hayashi, D. S. Sutherland, H. Autrup, *Toxicology Letters* **208**(3) (2012) 286-292.
34. A.F. Aravantinou, *Ecotoxicology and Environmental Safety* **114** (2015) 109–116.
35. I. Entsar Rabea, E. Mohamed, T. Badawy, C. V. Stevens, G. Smagghe, W. Steurbaut, *Biomacromolecules*, **4** (6) (2003) 1457-1465

- 36 M. T. Garcia, I. Ribosa, T. Guindulain, J. Sanchez-Leal, J. Vives-Rego, *Environmental Pollution*, **111** (2001) 169-175.
- 37 F. Harris, S.R. Dennison, D.A Phoenix, *Curr. Protein Pept. Sci.* **10** (2009) 585–606.
38. Harris, F.; Dennison, S.R.; Phoenix, D.A. *Curr. Protein Pept. Sci.* **10** (2009) 585–606.
39. Bradshaw, J. *BioDrugs* **17** (2003) 233–240.
40. Riedl, S.; Zweytick, D.; Lohner, K. *Chem. Phys. Lipids* **164** (2011) 766–781.
41. Huang, Y.B.; Huang, J.F.; Chen, Y.X. *Protein Cell* **1** (2010) 143–152.
42. Dubos, R.J. *J. Exp. Med.* **70** (1939) 1–10.
43. Balls, A.K. *Cereal Chem.* **19** (1942) 279–288.
44. Hirsch, J.G. Phagocytin: *J. Exp. Med.* **103** (1956) 589–611.
45. Groves, M.L.; Peterson, R.F.; Kiddy, C.A. *Nature* **207** (1965) 1007–1008.
46. Radek, K.; Gallo, R. *Semin. Immunopathol.* **29** (2007) 27–43.
47. Conlon, J.M.; *Sonnevend. Methods Mol. Biol.* **618** (2010) 3–14.
48. Powers, J.P.; Hancock, R.E. *Peptides* **24** (2003) 1681–1691.
49. Rozek, A.; Friedrich, C.L.; Hancock, R.E. *Biochemistry* **39** (2000) 15765–15774.
50. Naghmouchi, K.; le Lay, C.; Baah, J.; Drider, D. *Res. Microbiol.* **163** (2012) 101–108.
51. F. Costa, I. F. Carvalho, P. Gomes M.C.L. Martins, *Acta Biomaterial* **7** (2011) 1431-1440.
52. A. Szekeres, B. Leitgeb, L. Kredics, Z. Antal, L. Hatvani, L. Manczinger, *Acta Microbiol. Immunol. Hung.* **51** (2005) 137.
53. H. Brückner, H. Graf, *Experientia* **39** (1983) 528-530.
54. H. Kleinkauf, H. von Döhren, *Eur. J. Biochem.* **192** (1990) 1.
55. S. Rebuffat, M. El Hajji, P. Hennig, D. Davoust, B. Bodo, *Int. J. Pept. Protein Res.* **34** (1989) 200.
56. G. Menestrina, K. P. Voges, G. Jung, G. Boheim, *J. Membrane Biol.* **93** (1986) 111.
57. D. Marsh, *Biochem. J.* **315** (1996) 345.



58. Peggion C., Formaggio F., Crisma M., Epand R.F., Epand R.M. and Toniolo C. *J. Peptide Sci.* **9** (2003) 679–689.
59. Y. S. Tsantrizos, S. Pischos, F. Sauriol, P. Widden, *Can. J. Chem.* **74** (1996) 165.
60. Y. S. Tsantrizos, S. Pischos, F. Sauriol, *J. Org. Chem.* **61** (1996) 2118.
61. T. Fujita, S. Wada, A. Iida, T. Nishimura, M. Kanai, N. Toyama, *Chem. Pharm. Bull.* **42** (1994) 489.
62. C. Toniolo, M. Crisma, F. Formaggio, C. Peggion, R. F. Epand, R. M. Epand, *Cell. Mol. Life Sci.* **58** (2001) 1179.
63. Hülsman, H., Heinze, S., Ritzau, M., Schlegel, B. e Gräfe, U., *J. Antibiot.* **51** (1998) 1055.
64. Crisma M., Barazza A., Formaggio F., Kaptein B., Broxeterman Q.B., Kamphuis J. And Toniolo C. *Tetrahedron* **57** (2001) 2813-2825.
65. Fenical et al. US 2003/0013659 A1.
66. De Zotti M., Biondi B., Formaggio F., Toniolo C., Stella L., Park Y., Hahm K.-S., *J. Pept. Sci.* **15** (2009) 615-619.
67. Improta R., Rega, N. Aleman, C., Barone V., *Macromolecules* **34** (2001) 7550-7557.
68. Toniolo C., Crisma M., Formaggio F., Peggion C., *Biopolymers* , **60** (2001) 396-419.
69. Bavoso A., Benedetti E., Di Blasio B., Pavone V., Pedone C., Toniolo C., Bonora G. M., Formaggio F., Crisma M., *J. Biomol. Struc. Dynamics* **5** (1988) 803-817.
70. Karle I. L. , Balaram P., *Biochemistry* **29** (1990) 6747-6756.
71. 78. D. Avrahami, Y. Shai *J Biol Chem* **279** (2004) 12277.
72. A. Makovitzki, D. Avrahami, Y. Shai. *PNAS* **103** (2006) 15997.
73. Shai, Y., *Curr. Pharm. Des.* **8** (2002) 715-725.
74. Papo N., Oren Z., Pag U., Sahl H.G., Shay Y., *J. Biol. Chem.* **277** (2002) 33913-339321.
75. Arahami D., Shai Y., *Biochemistry* **42** (2003) 14946-14956.
76. Avrahami D., Shai Y., *J. Biol. Chem.* **85** (2004) 12277-12285.
77. A. Wessolowski, M. Bienert, M. Dathe, *J. Peptide Res.* **64** (2004) 159-169

78. M.B. Strom, O. Rekdal, J.S. Svendsen, *J. Pept Sci.* **8** (2002) 431-437.
79. M.P. Aliste, J. L. MacCallum, D. P. Tieleman, *Biochemistry* **42** (2003) 8976-8987.
80. F.N. Petersen, M.O. Jensen, C. Nielsen, *Biophys. J.* **89** (2005) 3985-3996.
81. M.V. Walter, M. Malkoch, *Chem. Soc. Rev.* **41** (2012) 4593.
82. Y.B. Lim, E. Lee, M. Lee, *Angew Chem Int Ed* **46** (2007) 9011.
83. J.K. Ryu, C.B. Park, *Angew Chem Int Ed* **48** (2009)4820.
84. C.Y. Yang, B.B. Song, Y. Ao, A.P. Nowak, *Biomaterials* **30** (2009) 2881.
85. J.P. Tam, Y.A. Lu, J.L. Eur. *J. Biochem.* **269** (2002) 923.
86. E.J.J. Lugtenberg, R. Peters, *Biochim. Biophys. Acta* **441** (1976) 38–47.
87. S. Singh, G. Kasetty, A. Schmidtchen, M. Malmsten, *Biochim. Biophys. Acta* **1818** (2012) 2244–2251.
88. J. Andrä, M.H. Koch, R. Bartels, K. Brandenburg, *Antimicrob. Agents Chemother.* **48** (2004) 1593–1599.
89. S. Singh, M. Kalle, P. Papareddy, A. Schmidtchen, M. Malmsten, *Biomacromolecules* **14** (2013) 1482–1492.
90. C. Junkes, R.D. Harvey, K.D. Bruce, R. Dölling, M. Bagheri, M. Dathe, *Eur. Biophys. J.* **40** (2011) 515–528.
91. S.M. Smith, R.H. Eng, F.T. Padberg, *J of Medicine*, , **27** (5) (1996) 293-302.
92. R. Li, M. Sun, Z. Jiang, X. Ren, T.S. Huang, *Fibers and Polimer*, **15** (2) (2014) 234-240.
93. M. Yatagai, S.H. Zeronian, *Cellulose*, **1** (1994) 205-214.
94. D Ciolacu., V.I.Popa, *Source of the DocumentCellulose Allomorphs: Structure, Accessibility and Reactivity* (2013) pp. 1-69
95. N.M. Bikales, L. Segal *Cellulose and Cellulose derivatives*, **1971**, part IV chapter XIII.
96. Nakamura M., Iwasaki T, Tokino S., Asaoka A., Yamakawa M., Ishibashi J., *Biomacromolecules* **12** (2011) 1540-1545.
97. Zhaoweia L., Guogangb R., Taoc Z., Zhuoa Y., *Toxicology* **264** (2009) 179-184.





## **2. Result and discussion**

### **2.1 Peptide synthesis: synthetic strategy**

Solid phase peptide synthesis was developed by Merrifield in 1963 [1]. In the following years several modifications in the procedure were applied. Introduction of new resins with an increased stability in acidic conditions has limited the presence of sub products during the synthetic steps [2].

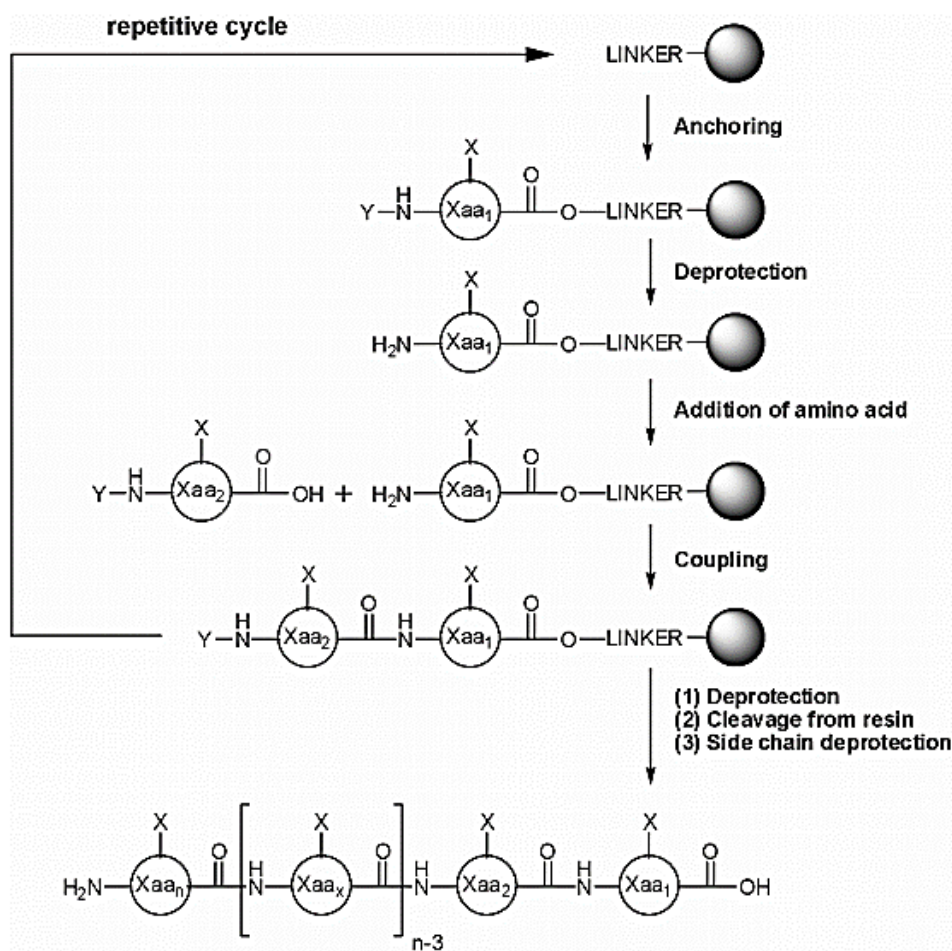
Moreover, the development of new linkers between the polystyrene resin and the C-terminal amino acid improved the ability to link/remove the peptide from the solid support giving final products of good quality [3]. Furthermore, studies regarding the protection of amino acid side chains introduction of new activating agents for the carboxylic moiety, (HOAt, HBTU...) improved the yields of the synthesis and reduced the problems related to epimerization [4].

The first step of the synthesis is the anchorage, through a *linker*, of the C-terminal group of an NH protected  $\alpha$ -amino acid to a polymeric resin composed by styrene with an 1-2% of divinylbenzene as cross-linker. The cross-linker acts by improving insolubility of the resin in organic solvent. The percentage of cross-linker needs to be lower than the 2% because an higher percentage induces problems related to steric effects, such as the formation of secondary rigid structures, in particular the  $\beta$ -sheet structures [5].

To reduce these problems, before adding the reagents the resin needs to be solvated by an opportune solvent in order to obtain a “gel” in which penetration and removal of reagents is favorable.

Contrary to what happens in nature, where peptides are enzymatically synthesized from the N- to the C-terminus, in SPPS the main chain elongation takes place from the C- to the N-terminus. Synthesis takes place, step by step, by adding a residue activated at carboxyl group with the  $\alpha$ -NH, and eventually the lateral chain, protected. When the peptide is completed it is removed from the solid support by different treatments, strongly related to the nature of the *linker* [6].

SPPS can be summarized as a repetition of deprotection steps for N-terminal moiety of the resin bond peptides and coupling steps with the addition of the next amino acid to the solid support.



**Figure 34.** Solid Phase Peptide Synthesis cycles.

Synthetic steps applied in our laboratory are reported below:

- Deprotection: 20 % piperidine in DMF solution;
- Coupling: Fmoc-AA-OH, HOAt/HATU (activating agents), DIPEA (base) in DMF
- Cleavage: acidic condition, TFA and triisopropylsilane (scavenger) in DCM; the percentage of TFA is strongly related to the nature of the resin used.

## Resin

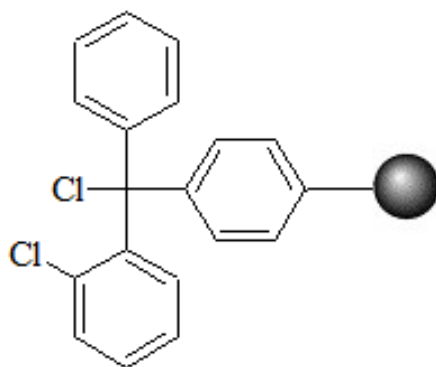
During this work one kind of resins was used: 2-CTC resin.

2-CTC, 2-chlorotriyl resin

Loading = 1.6 mmol/g.

Mesh = 100-200.

Using 2-CTC resin it is possible to obtain a peptide with free C-terminal carboxyl group or with different C-terminal functional groups by adding an opportune nucleophilic group in the first step of the SPPS. Particularly, in our work 2-CTC resin was used to prepare peptides with primary amino or thiol moieties at the C-terminus.



**Figure 35.** 2-CTC resin linker.

2-CTC resin enables the cleavage of the final product in several soft acidic condition

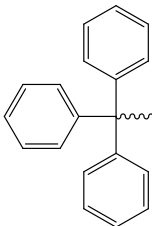
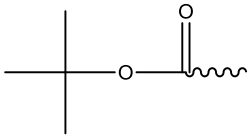
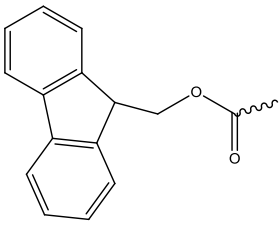
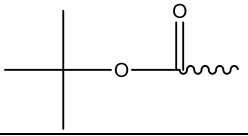
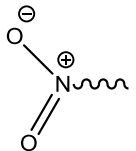
- 1-5% of TFA in DCM solution;
- 30% of hexafluoroisopropanol (HIFP) in DCM solution;
- Trifluoroethanol (TFE).

In the literature it is well reported how the use of 2-CTC resin reduces the formation of diketopiperazine (DKP) [7], decreases the racemization in the introduction of the first amino acid and allows the bond of an amino acid through its lateral chain [8].

### **Protecting group**

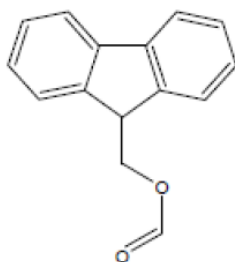
In this work for SPPS we applied the Sheppard approach [9]. Amino acids used present the  $\alpha$ -NH moiety protected by the Fmoc group (9-fluorenylmethoxycarbonyl), removable in alkaline conditions, while the lateral chains are protected by acid labile protecting groups. When needed, different side chain moieties of different amino acids were protected orthogonally.

**Tabella 5.** Protecting group used in this work and their respective cleavage condition

Protected moiety	Protecting group	Structure	Cleavage conditions
Imidazole, His	Trityl (Trt)		5% TFA in DCM, scavengers: triisopropylsilane, H <sub>2</sub> O
ε-Amine, Lys	tert-butoxycarbonyl (Boc)		30% TFA in DCM/ Boiling water overnight
ε-Amine, Lys (for dendrimeric core)	9-fluorenylmethoxycarbonyl (Fmoc)		20% piperidine in DMF, 15 min. (2 cycles)
Indole, Trp	tert-butoxycarbonyl (Boc)		30% TFA in DCM, Boiling water overnight
Guanidinium, Arg	Nitro (NO <sub>2</sub> )		Catalytic hydrogenation, Pd/C 1% in MeOH

Fmoc protecting group

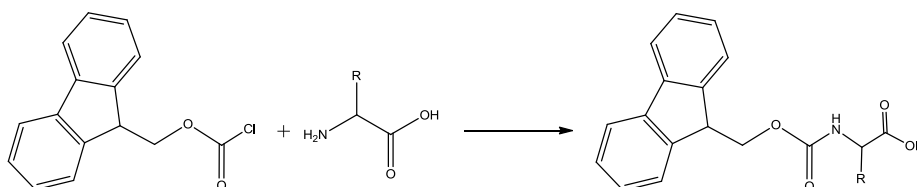
Fmoc group (9-fluorenylmethoxycarbonyl) (fig.36) [10a] was used to protect α-NH group for all the synthesis presented in this work.



**Figure 36.** Structure of Fmoc.

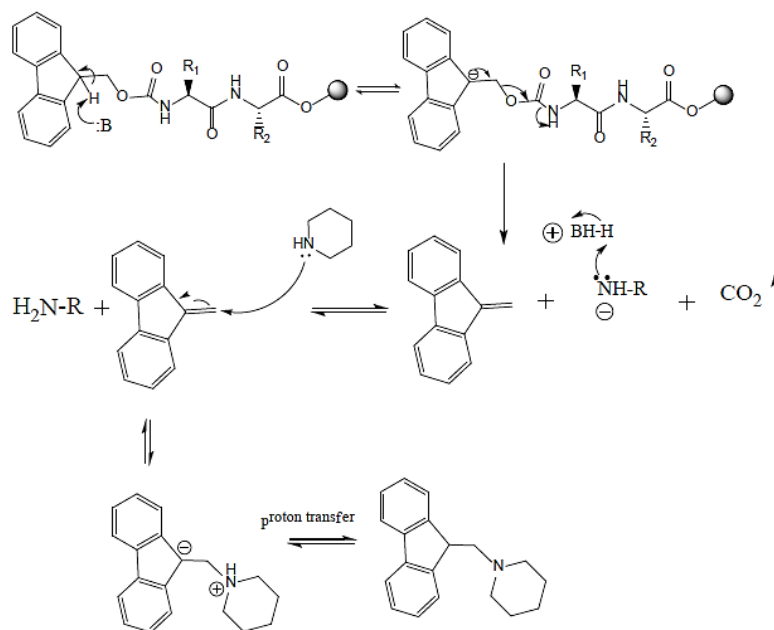


Fmoc group is linked to the amino moiety through an urethane bond. This protection shows a good resistance to acidic conditions, while the cleavage takes place in soft alkaline conditions using secondary cyclic amines, such as piperidine or piperazine.



**Figure 37.** Formation of the urethane bond between Fmoc-Cl and an amino acid.

Anchoring and removal of the protecting groups are quantitative. Moreover, the protection through an urethane bond prevents racemization to the C $\alpha$  [11].



**Figure 38.** Mechanism of Fmoc deprotection using piperidine.

In the Fmoc group the hydrogen linked to the - C $\beta$  in position 9 possesses acidic properties, due to the electron-withdrawing nature of the fluorene system, and can be removed by soft alkali [12]. The first step of the deprotection is the removal of the proton in position 9 by piperidine with the formation of the aromatic intermediate cyclopentadienyl-anion. This is decomposed through  $\beta$ -elimination in

dibenzofulvene and carbonic anhydride (CO<sub>2</sub>) [13]. Then, dibenzofulvene is blocked by the formation of a compound with the secondary amines [14].

As explained below, we used the optical properties of the dibenzofulvene secondary amine compound (UV-Vis absorption) to have information about the quantity of peptide linked to the textile.

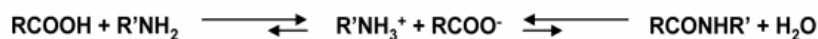
### Boc protecting group

Boc- protecting group was largely used in this work as protection for the Trp and Lys side chains. Removal of this group takes place, usually, in acidic conditions (30 % TFA in DCM solution), but in these conditions cotton fabric samples were rapidly disrupted. To avoid this situation a promising protocol of deprotection was found [10b].

Deprotection of Boc- group by boiling water is not only important for the prevention from the hydrolysis of the glycosidic bond of cellulose, but also permits to start to think about an environmental friendly synthesis approach .

### Activation methods

Direct reaction between a carboxylic group and an amine moiety does not give the formation of an amide bond. In fact, the thermodynamic product is an ammonium carboxylate, a salt obtain after the deprotonation of the carboxyl group and the protonation of the amine [11] (figure 39).



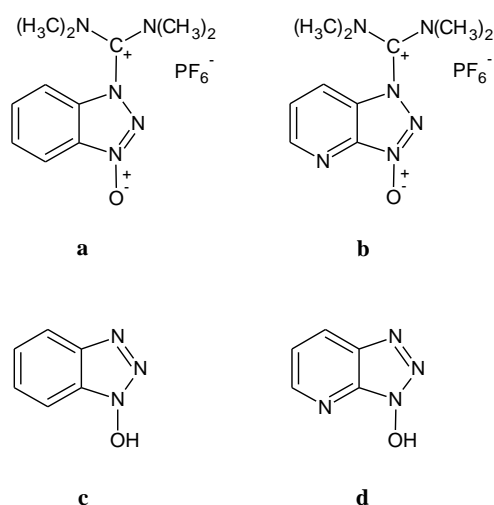
**Figure 39.** Salt formation in the reaction between an amine and a carboxylic group.

Salt condensation requires strong reaction conditions, such as high temperature (160-180°C), with the consequent degradation of the peptide.

Peptide synthesis at room temperature requires rapid and efficient activation methods [15]. Several ways of activation were developed before the introduction of the SPSS approach. From these techniques the products obtained presented often unwanted subproducts resulting by the reaction between the reactive intermediates and the lateral chain moiety or the C α. An example is the Curtius process, the synthesis of

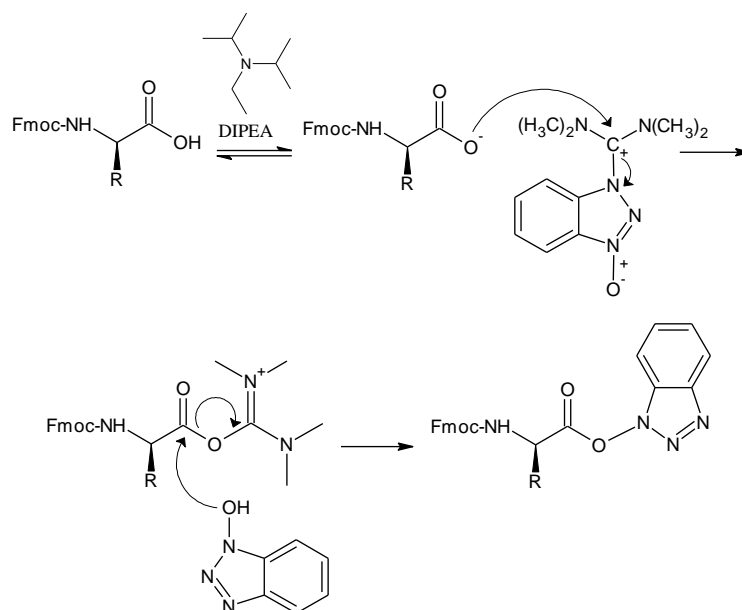
the first N-protected amino acid (benzoylglycine) obtained by treatment of the silver salt of glycine with benzoyl chloride [16]. Another example is the use of azide as activating agent (1904) which allowed the synthesis of peptides with different lengths [17].

Later, several studies have shown how the best activation methods require the preparation of an active ester using HATU/HOAt and HBTU/HOBt as activating agents (fig. 40) [18].



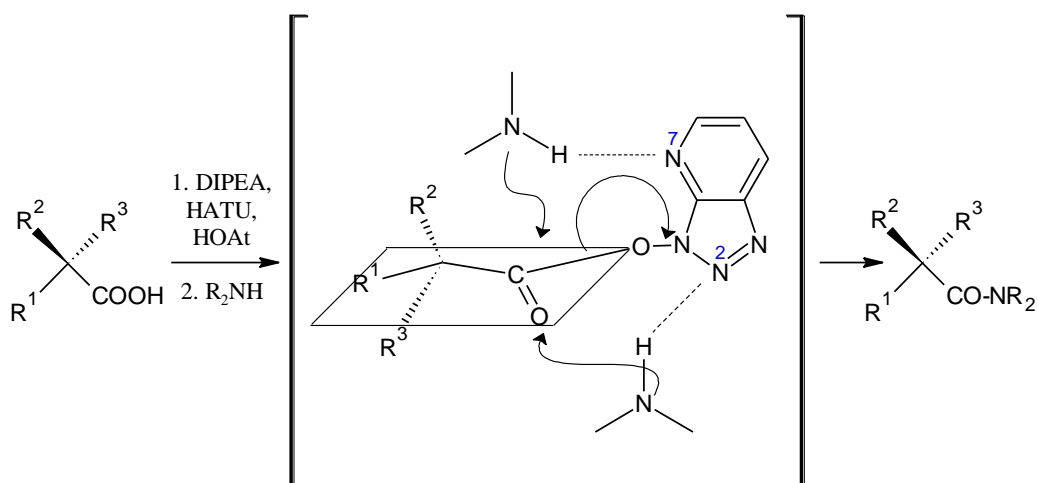
**Figure 40** a) *O*- (benzotriazol-1-yl) -1,1,3,3-tetramethyluronium hexafluorophosphate (HBTU); b) *O*- (7-Azabenzotriazol-1-yl) -1,1,3,3-tetramethyluronium hexafluorophosphate (HATU); c) 1-Hydroxy-1,2,3-benzotriazole (HOBt); d) 1-Hydroxy-7-aza-1,2,3-benzotriazole (HOAt)

The activation process is carried out with the modification of the electron density around the activated carbonyl group, making it more electrophilic and therefore more susceptible to addition of the nucleophilic  $\text{NH}_2$ - terminal group of the chains linked to the support. [19] The activation mechanism used in these synthesis involves the activation of the carboxylic group of the Fmoc-amino acid by the creation of an active ester using HATU/HOAT system. The carboxyl group reacts with HATU leading to the formation of a reactive intermediate which forms, in turn, an activated ester with HOAt. The latter reacts, quickly and without risk of racemization, with the terminal amine function of the growing peptide, being the anions -OBt and -OAt excellent leaving groups. [20-21] The carboxyl group must first be deprotonated by a tertiary amine (DIPEA).



**Figure 41.** Mechanism of the ester active formation.

The catalytic effect of the ester is performed using the assistance that the nitrogen atoms in positions 2 and 7 provide the nucleophilic attack of the amino group to the carbonyl group. [21] Recently it has been shown that, in the crystalline state, the active esters are arranged with the aromatic group perpendicular to the carboxylic acid plane [22] and that this conformation is maintained in solution allowing HOAt to provide the assistance nucleophilic attack through the two nitrogen atoms (Figure 42). Note that HOBt instead has only nitrogen in position 2 and can, therefore, lead the attack from one side only. [23]



**Figure 42.** Assistance in amide bond formation by activation at the carboxylic acid with HOAt.

## Synthesized peptides

We synthesized by SPPS the peptides reported in table 6. These peptides are analogues to peptides prepared on cotton surface and help us to elucidate the structure they adopt using solution techniques. We can envisage that a similar conformation is maintained by the peptides once they are linked to cotton. **Table 6.** Free peptide prepare in this work.

<b>Sample</b>	<b>Sequence</b>	<b>Yield %</b>
AP-1	Pal-Lys-Ala-D-Ala-Lys-NH-(CH <sub>2</sub> ) <sub>2</sub> -NH <sub>2</sub>	63.45
AP-2	Pal-His-Ala-dAla-His-NH-(CH <sub>2</sub> ) <sub>2</sub> -NH <sub>2</sub>	56.82
AP-3	Pal-Arg-Ala-dAla-Arg-NH-(CH <sub>2</sub> ) <sub>2</sub> -NH <sub>2</sub>	60.45
AP-4	Pal-Arg-Trp-Trp-Arg-NH-(CH <sub>2</sub> ) <sub>2</sub> -NH <sub>2</sub>	54.38
AP-5	Pal-Trp-Arg-Trp-Arg-NH-(CH <sub>2</sub> ) <sub>2</sub> -NH <sub>2</sub>	68.47

The yields obtained in the syntheses are around 60%. After the deprotection from the resin the synthesized compounds were purified by flash chromatography on silica gel Merck 60 (particle size 40-63 nm) and precipitated with ethyl acetate/petroleum ether.

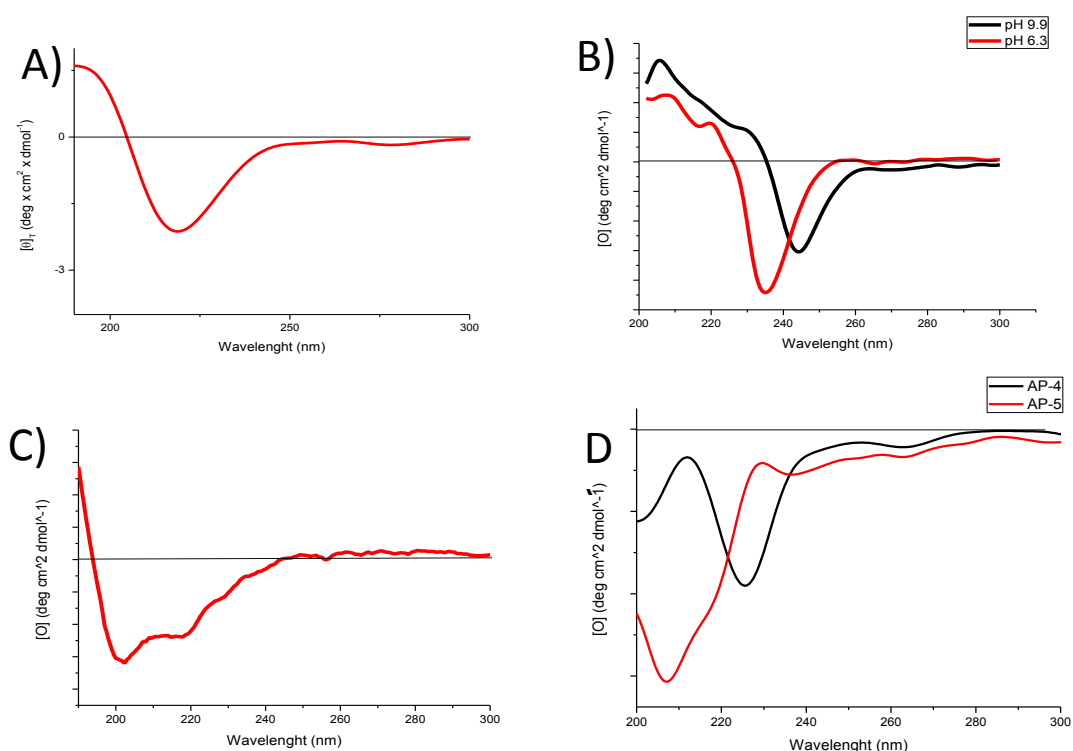
The purity was determined by analytical HPLC analysis, using a C18 analytical column. The products were characterized by mass spectroscopy with a time of flight mass spectrometer (ESI-TOF) and by <sup>1</sup>H-NMR spectroscopy at 200 MHz.

## Circular Dichroism

Synthesized peptides were analyzed by Circular Dichroism in order to determine their conformation. Previous work showed that there is a strong relationship between the ability of the peptides to assume a secondary defined structure, mostly helical, and their antimicrobial activity [24]. The spectra series of cationic peptides prepared (**AP-1**, **AP-2**, **AP-3**) were recorded in water at a concentration of 10<sup>-4</sup> M, while for peptides of the series Arg/Trp, hardly soluble in water, methanol was used as solvent, working at the same concentration.

The measurements were carried out using a quartz cell with a thickness of 1 mm. The spectral region analyzed was between 190 and 270 nm, where the bands related to transitions  $n \rightarrow \pi^*$  and  $\pi \rightarrow \pi^*$  of the peptide chromophore unit are located.

The spectra of sample **AP-2** was also recorded at two pH values (6.3 and 9.9) to determine the variations of conformation in relationship with protonation and deprotonation of the imidazole side chain ( $pK_a = 6.04$ ).



**Figure 43.** Circular dichroic spectra of synthesized peptides: **AP-1**, **AP-2**, **AP-3**, **AP-4**, **AP-5**. Spectra A, B and C were registered in water while spectrum D in methanol. Optical length: 0,1 cm, Peptide concentration:  $4,5 \cdot 10^{-4}$  M

Sample **AP-1** (fig. 43, A) show a negative maximum around 230 nm that moves to a positive maximum values around 200 nm. The peptide seems to adopt a parallel  $\beta$ -sheet conformation.

In the spectra of sample **AP-2**(fig. 43 B) we did not observe remarkable changes in function of pH. For both pH values, the sample displays a  $\beta$ -sheet like conformation, confirmed by the presence of a negative maximum around 230 nm that moves toward positive values at about 220 nm. In particular, the peptide seems to prefer an antiparallel  $\beta$ -sheet conformation, as the negative maximum is blue shifted.

Circular dichroism spectrum of **AP-3** (fig. 43, C) indicates that the peptide adopts a conformation of the helical type pointed out by the presence of the two negative maxima at 208 nm (corresponding to the transition  $\pi \rightarrow \pi^*$ ) and 222 nm (corresponding to the  $n \rightarrow \pi^*$  transition). From the relationship between the intensity of the two maxima ( $R = [\Theta]_{222} / [\Theta]_{208}$ ), we can identify the type of helix assumed by peptide. For a ratio  $R < 0.4$  peptides adopt a  $3_{10}$ -helical conformation, while for  $R \sim 1$  the preferred structure is the  $\alpha$  helix. In Table 4 the values of R found for the samples analyzed are reported: Arg-A has an  $R = 0.65$  (table x). Peptides bearing the arginine residues have a mixed  $\alpha/3_{10}$  helical structure.

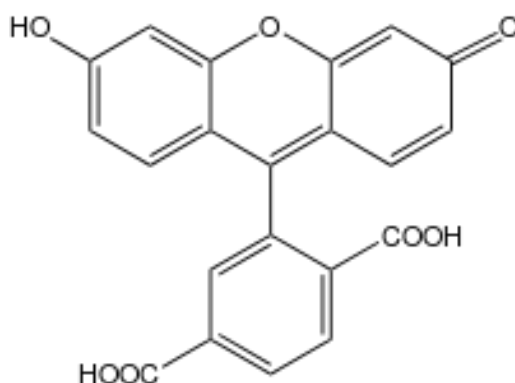
Finally, figure 43 D shows the dichroic spectra recorded for the samples of the series Arg-Trp. The spectra, recorded in methanol, demonstrate that compound **AP-4** adopts a disordered conformation, while peptide **AP-5** assumes a helical conformation at which competes a value of  $R = 0.68$  (table 7). This value indicates that the peptide assumes a mixed helical  $3_{10}/\alpha$  conformation with a predominance of the  $\alpha$ -helical character.

**Table 7.**  $R = [\Theta]_{222} / [\Theta]_{208}$  value obtain from CD spectra.

<b>Campione</b>	<b>R = <math>[\Theta]_{222}/[\Theta]_{208}</math></b>
Arg-A	0.65
Arg-Trp-B	0.68

## Leakage test

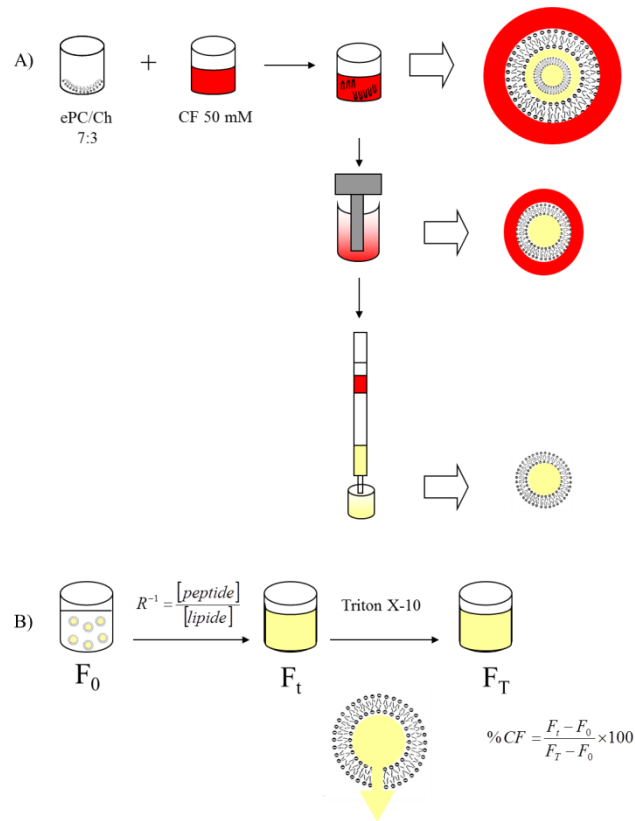
The ability of the peptides to permeate membranes was analyzed through a *leakage* test. This test consists in the preparation of liposomes, double layer phospholipid vesicles (SUV, small unilamellar vesicles), containing a fluorescent probe, the carboxyfluorescein (CF) (fig. 44).



**Figure 44.** Chemical structure of carboxy fluorescein.

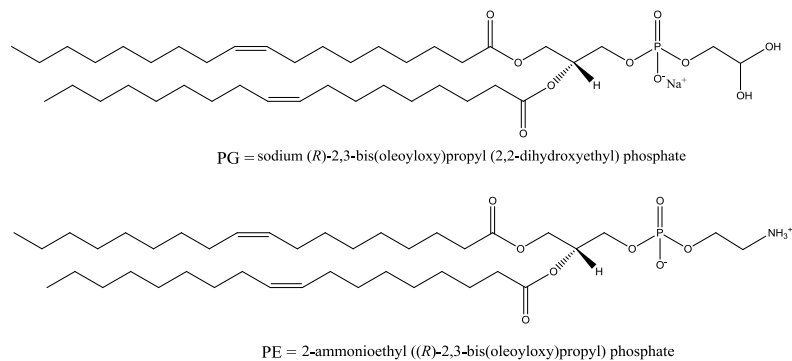
The molecules of the fluorophore that are encapsulated in the liposome give the phenomenon of self-quenching fluorescence showing modest emission values. When the double layer is disturbed and the permeation of the liposome membrane is changed by interaction with a peptide, the CF leaks in the surroundings and increased fluorescence emission is detected. At the end of the experiment the surfactant Triton X is added to the system leading to the complete destruction of the membranes; in this condition the maximum value of fluorescence of the system is determined. The scheme of preparation of the vesicles and the scheme of the experiment are shown in Figure 45.





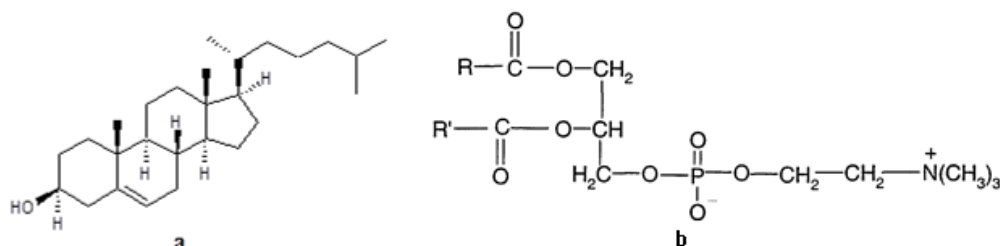
**Figure 45.** *Leakege assay*

This procedure allows to simulate different types of membranes according to the choice of the phospholipid used to prepare the liposomes. The test was conducted on liposomes mimicking Gram negative bacterial membranes and erythrocyte membranes. Phosphatidylethanolamine (PE) and phosphatidylglycerol (PG) in mutual relationship 7: 3 were used for mimicking Gram negative membranes (fig. 46).



**Figure 46.** *Chemical structure of PE and PG phospholipids*

For the preparation of erythrocyte-like membranes phosphatidylcoline (PC) and cholesterol (Ch) in mutual relationship 7: 3 (wt/wt) were used (fig. 47).



**Figure 47.** Chemical structure of PC and Cholesterol

In the procedure, peptides are added to a fluorescence cuvette containing a solution of liposomes in HEPES buffer (pH = 7.4) at a known concentration. Increasing amounts of peptides are added to the liposome solution and release of CF is detected by fluorescence.

Fluorescence of the liposome solution is recorded before the addition of the peptide ( $F_0$ ), 20 minutes after the addition of the peptide, and after Triton X addition ( $F_{tot}$ ) ( $\lambda_{exc} = 488 \text{ nm}$ ,  $520 \text{ nm} = \lambda_{emi}$ ). The percentage of CF released is calculated as follows:

$$\%CF = \frac{F_t - F_0}{F_T - F_0} \times 100$$

With:  $F_0$ : intensity of fluorescence of the liposomes in absence of peptide

$F_t$ : intensity of fluorescence of the liposomes after 20 minutes from the addition of the peptide

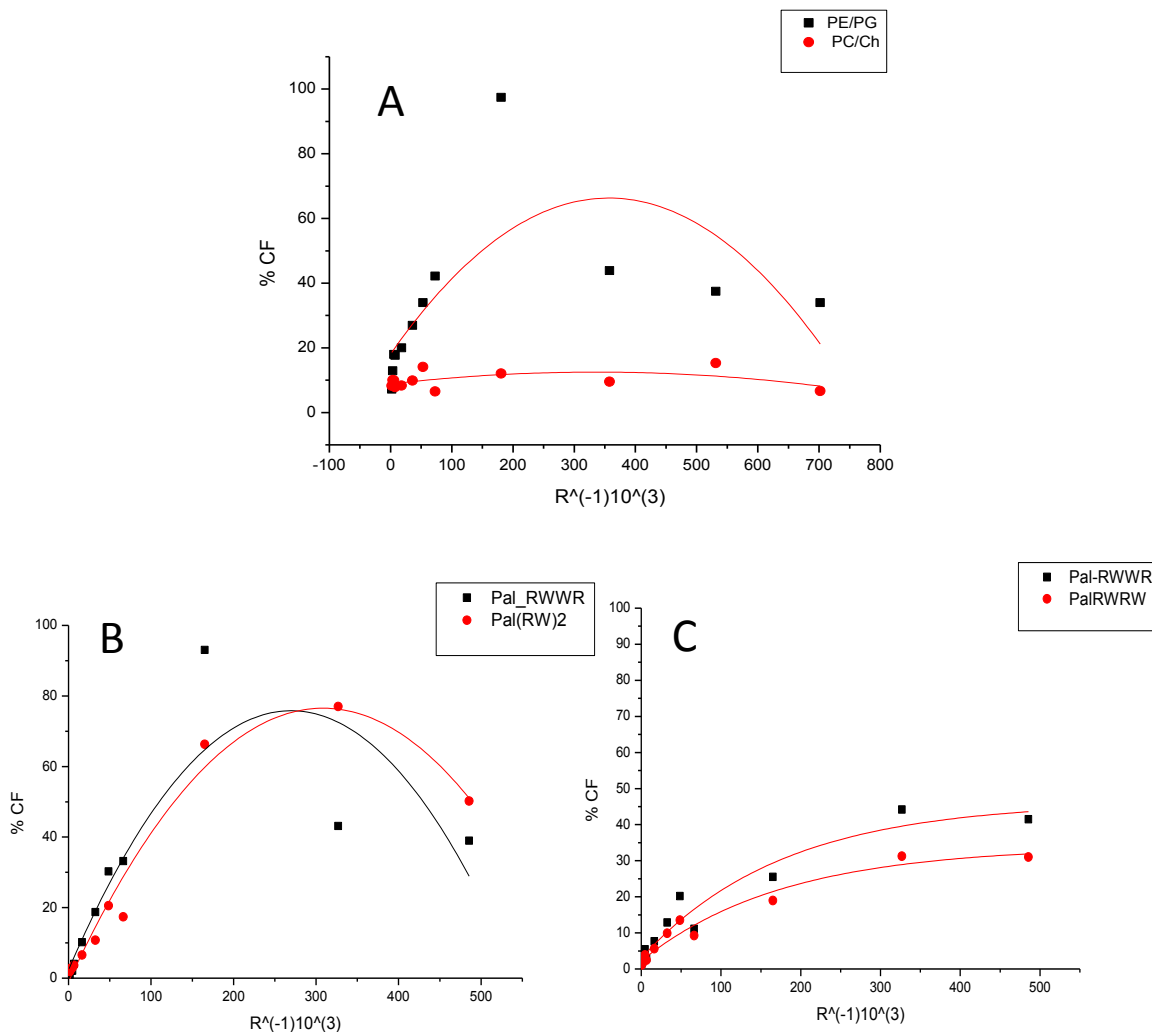
$F_T$ : intensity of fluorescence after liposome destruction by adding Triton-X 100 in water

The amount of peptide that was added was calculated as ratio considering the amount of lipids:

$$R^{-1} = \frac{[peptide]}{[lipids]}$$

To analyze the activity of the analogues bearing His residue, we chose to take the test even under acidic conditions, working in HEPES buffer at pH 6.3. This choice is related to the pKa value of the imidazole ring (pKa = 6.04): at alkaline pH the ring in

the side chain is deprotonated, while in acidic condition imidazole results protonated, then assuming one of the basic requirements to interact with membranes.



**Figure 48.** Leakage assay for sample AP-3 (A) and AP-4 and AP-5 (B = PE/PG liposomes) (C = PC/Ch liposomes)

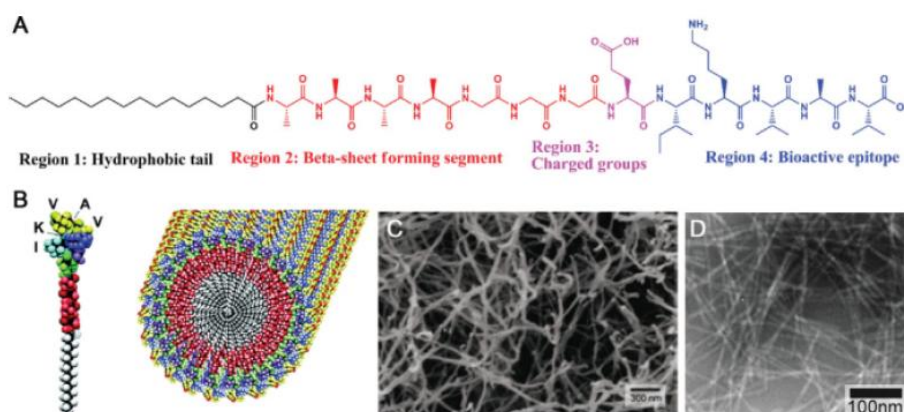
Graphs in figure 48 represent some examples of the results obtain by the *leakage* test. No all data are reported because for some samples, especially for the peptides bearing the His residues, high poydispersion of data is observed. However, from the trend of CF release we stretch the following conclusions.

As expected, the ability of permeation of membrane models of the peptides bearing His residues increases going from basic to acidic condition. The observed effect is more pronounced in interaction with PE/PG liposomes, while for the test with the PC/Ch, the activity does not seem to undergo major changes.

Sample **AP-3** shows a very low interaction with the PC/Ch erythrocyte liposomes, In contrast, interaction with PE/PG membranes results to be quite evident.

Peptides **AP-4** and **AP-5** show a similar trend in the interaction with different liposomes tested. Also in this case there is a certain selectivity, being the ability to permeate PC/Ch liposomes much less than that shown towards the PE/PG liposomes.

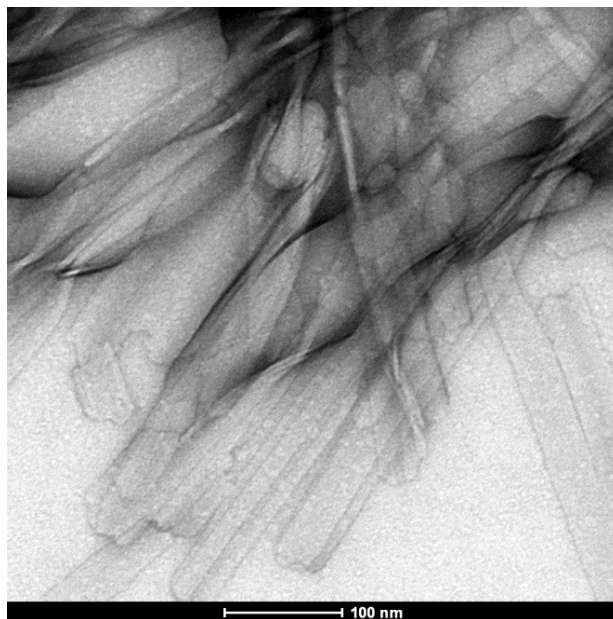
All the samples show a bell-like trend. This situation can be explained considering the aggregation properties of these peptides. It is well reported in the literature how lipopeptides characterized by the presence of both charged and hydrophobic residues in the sequence are able to self-assemble in supramolecular structures, such as nanowires and nanotubes [25]. Self-assembly properties were also reported for both cationic [26] and anionic charged peptides [25].



**Figure 49.** Examples of self-assembly lipopeptide and their TEM images from Science (<http://www.sciencemag.org>) (VVC 2003 American Chemical Society)[25].

Particularly, Shai et al. demonstrated that short lipopeptide sequences, composed mainly by Lys and Palmitoyl fatty acid at the N-terminus (C16-KKK; C16-KLK and C16-KGK), are able to rearrange in nanofibrils or nanotubes [27].

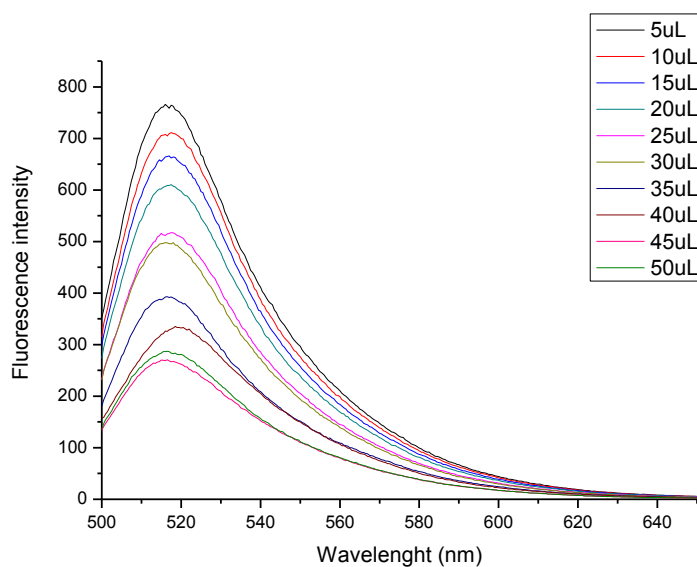
During the leakage test of our synthetic cationic peptide Pal-Lys-Ala-D-Ala-Lys-NH-(CH<sub>2</sub>)<sub>2</sub>-NH<sub>2</sub> we observed the decrease in fluorescence accomplished by the formation of naked eyes visible wires in the cuvette. These structures were characterized using TEM microscopy (fig. 50) From the image we observed the presence of nanotubes.



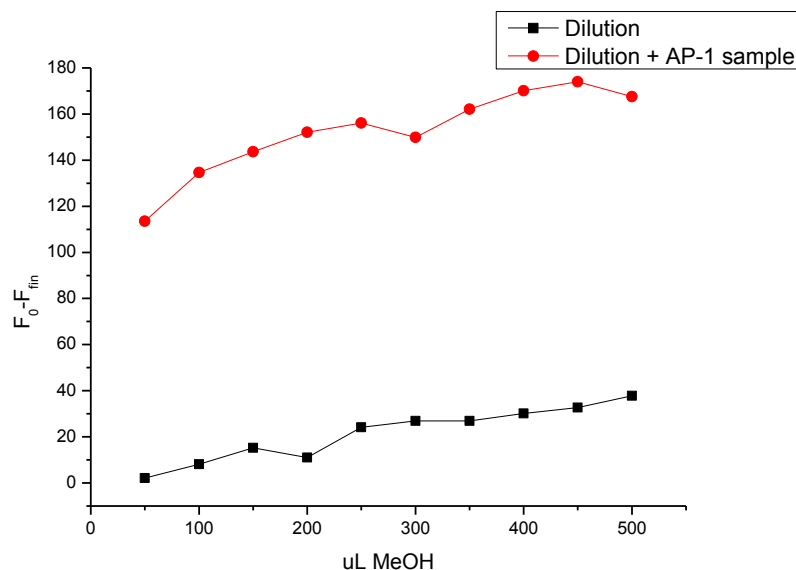
**Figure 50.** TEM image of nanotube like structure formed by sample **AP-1** in water.

In order to correlate the decrease of fluorescence with the amount of peptide present in the system, we performed two titration experiments.

In the first we added an increasing amount of peptide **AP-1** (solubilized in methanol) to an aqueous solution of carboxyfluorescein. A progressive decrease in fluorescence emission is observed (fig. 51).



**Figure 51.** Fluorescence intensity of carboxyfluorescein in presence of different amounts of peptide **AP-1**. Peptide solution concentration:  $10^{-3}$  M in MeOH.



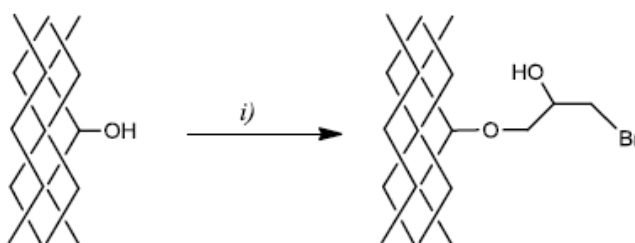
**Figure 52.** Effect of dilution of a CF solution ( $\dots M$ ) by addition of methanol with and without peptide **AP-1** in the system ( $\dots mM$ ).

Graph confirms that when peptides are added to the CF solution a strong decrease in fluorescence emission is observed. As previously supposed, while the wires became from white to pale-red, the solution passes from yellow to uncolored, probably because the chromophore is encapsulated in these tubes and here, due to the concentration effect, the phenomena of *auto-quenching* takes place.

In a second experiment we intended to demonstrate that the decrease of fluorescence was not due to dilution effects. The difference between the initial value of fluorescence ( $F_0$ ) and the fluorescence detected after methanol addition ( $F_{Fin}$ ) are plotted versus amount of methanol added. This was performed once in a cuvette containing only CF and once in a cuvette containing the same CF solution and the peptide (figure 52). As small effect of dilution is observed in both cases, allowing us to conclude that the great decrease in fluorescence emission of the previous experiment can be really attributable to the presence of the peptide. It probably self assembles and encapsulates CF molecules.

## 2.2 Textile functionalization

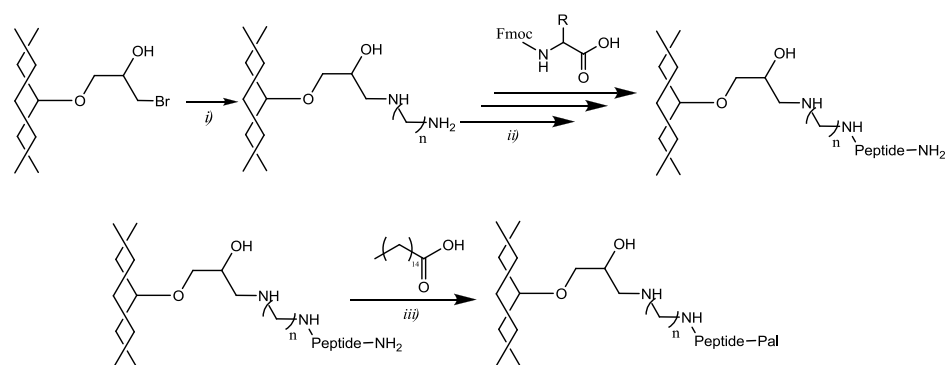
The synthetic approach used to prepare peptides covalently linked to cotton fibers is based on the work of M. Nakamura published in 2011 [28]. He describes the early development of a peptide-immobilized fiber, the D-9-mer, showing lasting antibacterial activity against MRSA (methicillin-resistant *Staphylococcus aureus*) and antitumor activity against myeloma in mice and against human leukemia cells (*Jurkat*). Following his methodology (figure 53), we used the fabric as a support for solid phase synthesis and we built the peptide on it using the step by step synthesis of Sheppard (*via* Fmoc) [9].



**Figure 53.** Reaction conditions: (i) Epibromohydrin, 60% HClO<sub>4</sub> in DMF.

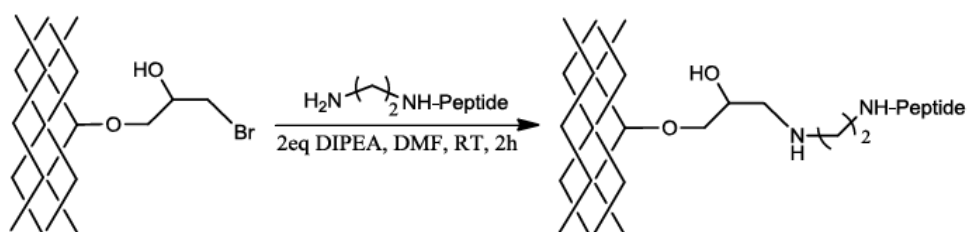
In the first step (*i*, figure 53) hydroxyl groups of the cellulosic support, soaked in DMF, react with epibromohydrin in the presence of HClO<sub>4</sub>. The epoxide opens forming an ether bond and introducing a halogen at the same time. Bromine is then substituted by reaction with a nucleophilic moiety. At this point we have followed two different paths to tie the peptide to the textile:

- **M-1)** Halogenated cotton reacts with a diamino compound, which replaces bromide allowing us to obtain the amino-functionalized fiber. At this point, we proceed with the construction of the peptide *step by step* working with Fmoc- N- $\alpha$  protected amino acids, activated *via* active ester using HOAT / HATU as coupling reagents (figure 54).



**Figure 54.** Reaction conditions for the synthesis using M-1 method (i) 20% Ethylenediamine in DMF solution; (ii) step by step SPPS with the conditions of i), iii) Palmitic acid coupling with the same condition of i).

- **M-2)** The peptide analogs bearing the primary amine moiety to the C-terminus react, under alkaline conditions, with the "halogenated" fabric. The amino terminal nucleophile group, replaces the bromide through nucleophilic substitution, thus allowing the direct anchoring the entire peptide to the textile.



**Figure 55.** Reaction condition the synthesis using M-2 method.

The sequences bearing the primary amine at the C-terminus have been previously prepared using SPPS.

The choice of this second synthetic strategy comes from the desire to prepare samples interacting as little as possible with the fabric, thus avoiding any contamination; on the other hand, we aimed at binding the peptide or the dendrimer in a single step. The *one pot* attack of peptide/dendrimer would be more compatible with an industrial approach.



## **Samples prepared using M-1 approach**

Samples prepared using the *step by step* (M-1) approach will be described in this chapter. Samples are divided into four classes, according to the characteristics of the peptides. These classes are the following:

- Synthetic peptides based on the FA-YXXY pattern (Y, cationic residues; X, hydrophobic residues);
- Short peptides rich in Arg and Trp;
- Peptaibols;
- Peptide dendrimers.

### **FA-YXXY Peptides**

The idea of using this class of peptides is due to their peculiar antimicrobial characteristics well reported in the literature. The most studied peptide of the class is the analogue Pal-Lys-Ala-D-Ala-Lys-NH<sub>2</sub>. This peptide is characterized by the presence of cationic residues in the sequence that promote the interaction between the peptide itself and a bacterial membrane, often negatively charged [27]. Furthermore, both theoretical and empiric works demonstrated that this sequence is able to adopt in aqueous solution an helical amphiphilic conformation [28]. In addition, the presence of a lipophilic alkyl chain at the N-terminus is an efficient method to increase the affinity of the peptide for the membrane, thus increasing its biological activity [27].

Starting from these purposes we prepared cotton samples functionalized with the sequences reported in table 8:

**Table 8.** Samples of cotton fabric functionalized with cationic AMPs.

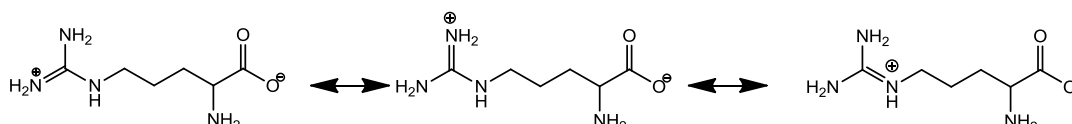
	Sample	Peptide sequence linked to textile
<b>Cationic AMP</b>	<b>AO-1</b>	Pal-Lys-Ala-D-Ala-Lys-
	<b>AO-2</b>	Pal-His-Ala-D-Ala-His-
	<b>AO-3</b>	Pal-Arg-Ala-D-Ala-Arg-
	<b>AO-4</b>	Pal-Arg(NO <sub>2</sub> )-Ala-D-Ala-Arg(NO <sub>2</sub> )-

Cationic peptide-cotton materials including cationic residues of different types were prepared. Our choice was made considering the properties of the cationic amino

acids and the defense mechanism developed by bacteria against positively charged antibiotics.

### Arginine

Arginine, similarly to Lysine, is a cationic amino acid bearing guanidinium group as lateral chain.

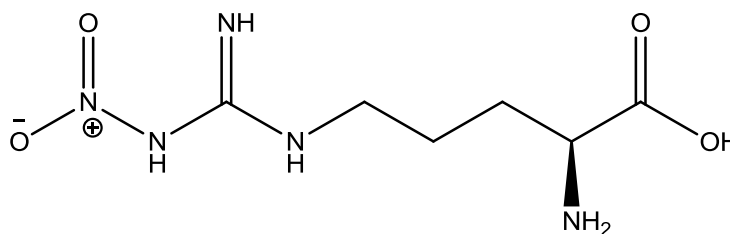


**Figure 56.** *Electronic resonance of Arginine side chain.*

While Lysine present a  $pK_a$  of 9.05, Arginine has a  $pK_a$  of 12.48. The guanidinium group is positively charged in neutral, acidic, and even most basic environments, and thus imparts basic chemical properties to arginine. Because of the conjugation between the double bond and the nitrogen lone pairs, the positive charge is delocalized, enabling the formation of multiple H-bonds.

The major cationic character of Arginine, compared with Lysine, promotes a better binding with bacterial membranes; moreover, peptides rich in arginine are able to maintain their cationic nature in different environments, from acidic to alkaline so they can perform their biological activity both towards negatively and positively charged bacterial membranes.

The presence of Arginine residues also offers an easy way to insert in the peptide a nitro ( $NO_2$ ) moiety. Nitro protected Arginine is in fact commercially available. (fig.57).



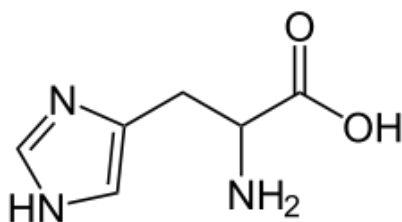
**Figure 57.** *Chemical structure of nitro protected Arginine*

It is reported in literature how the addition of a nitro group to bioactive molecules increases the ability the peptides to interact with bacterial membranes [29].

For this consideration fabrics functionalized with the peptide Pal-Arg-Ala-D-Ala-Arg- are tested both with and without the nitro protection at the guanidinium moiety.

### Histidine

Likewise Lysine and Arginine, Histidine is a cationic residue. This amino acid is characterized by the presence of an imidazole group in the side chain.



**Figure 59.** Chemical structure of Histidine

Imidazole is a five terms ring, two of them are nitrogen atoms one pyrrole and one piridine like. Imidazole is a weak base with  $pK_a$  conjugate acid equal to 7.00. It is also a weak acid with a  $pK_a$  of 14,52 for the deprotonation of the pyrrole nitrogen. The molecule then has an overall amphoteric character.

We decided to use this residue considering the defense mechanism of bacteria which involve changes in the membrane potential. In opposition to the analogues displaying an Arg, where the high  $pK_a$  of guanidinium moiety maintains the cationic nature of the peptide, sequences containing His are able to modulate their nature from cationic to nucleophilic nature and so to maintain the interaction with bacterial membrane.

### **Short peptides rich in Arg and Trp**

As described in the *Introduction*, the Arginine- Tryptophan couple is able to form an adduct involving the guanidinium and indole moieties. This adduct is reported to be a good promoter of membrane permeation.

In our work we linked three Arg/Trp containing peptides to textile changing the position of the amino acids in the sequence.

**Table 9.** Samples of cotton fabric functionalized with short AMPs rich in Arg and Trp residues.

Short Arg and Trp sequence	Sample	Peptide sequence linked to textile
	<b>RW-A</b>	<b>Palmitoyl-Trp-Arg-Trp-Arg-</b>
	<b>RW-B</b>	<b>Palmitoyl-Arg-Trp-Trp-Arg-</b>

### Peptaibols

Peptaibols represent a large class of peptides mainly characterized by the presence of one or more Aib residues. Aib is well known to be an helix inductor [30]. Usually peptides containing Aib residues have an  $\alpha$ -helical,  $3_{10}$ -helical or mixed  $\alpha/3_{10}$ -helical conformation, as discussed in the *Introduction*.  $\alpha$ -Helical conformation is favored in long peptaibols, while  $3_{10}$ -helix is favored in short ones (less than 7-8 residues). . Peptaibols can be divided into two mainly classes: acetylated peptaibols and lipopeptaibols.

In this work we choose to use lipopeptaibols as antimicrobial agent to be linked to fabrics. This choice was done as they are short compared with the acetylated members of the class.

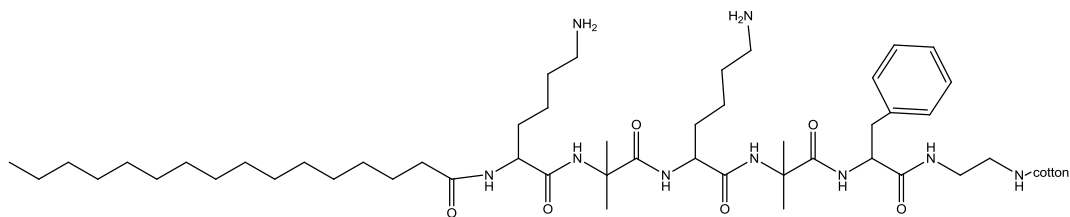
In all the lipopeptaibols prepared we introduced palmitoyl as the fatty acid.

Particularly, in this work we prepared the samples reported in the table below:

**Table 10.** Samples of cotton fabric functionalized with peptaibols.

Peptaibols	Sample	Common name	Peptide sequence linked to textile
	<b>AB-1</b>	Halovir	Pal-Aib-Hyp-Leu-Val-Gln-Leu-
	<b>DC-1</b>	Peptaibolin	Pal-Leu-Aib-Leu-Aib-Phe-
	<b>AO-5</b>	Tricogin GA IV	Pal-Aib-Gly-Leu-Aib-Gly-Gly-Leu-Aib-Gly-Ile-Leu-
	<b>DC-2</b>	K-Peptaibolin	Pal-Lys-Aib-Lys-Aib-Phe-

Sample **DC-2** corresponds to a modification of Peptaibolin, particularly the two Leu residues were replaced by two Lys residues. In this way we tried to prepare an hybrid peptide that combines the structural properties of peptaibols with the cationic nature of Lys.



**Figure 60.** Chemical structure of a peptaibolin analogues with Lysine in place to Leu residues.

### Dendrimers

The last class of AMPs linked to cotton fabrics is represent by dendrimers. We choose to employ these peptides in order to increase the number of peptide chains on the textile surface and to promote an interaction between near sequences. Several literature reports describe that the cytotoxic activity displayed by some AMPs is strongly reduced if they are inserted in a dendrimeric structures [31].

Sample prepared are reported in table 11:

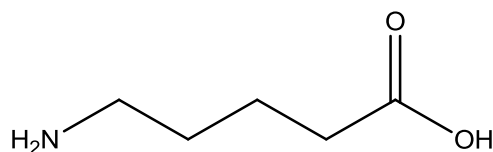
**Table 11.** Samples of cotton fabric functionalized with dendrimers.

<b>Dendrimer</b>	Sample	Peptide sequence linked to textile
	D1	[(Pal-Lys-Ala-D-Ala-Lys) <sub>4</sub> Lys <sub>2</sub> ]Lys-
	D2	[(Pal-His-Ala-D-Ala-His) <sub>4</sub> Lys <sub>2</sub> ]Lys-
	D3	[(Pal-Arg-Ala-D-Ala-Arg) <sub>4</sub> Lys <sub>2</sub> ]Lys-
	D4	[(Pal-Arg(NO <sub>2</sub> )-Ala-D-Ala-Arg(NO <sub>2</sub> )) <sub>4</sub> Lys <sub>2</sub> ]Lys-
	D5	[(N-5-Valeroyl-His-Arg) <sub>4</sub> Lys <sub>2</sub> ]Lys-
	D6	[(N-5-Valeroyl-Trp-Arg) <sub>4</sub> Lys <sub>2</sub> ]Lys-

Two types of dendrimers linked to cotton fabrics were prepared, both based on the same lysine dendrimeric core. In the first class we create a dendrimer using the cationic AMP sequences previously described. The second dendrimer is made of dipeptide sequences linked to the lysine core. Sample **D-5** was prepared to investigate the interactions between His and Arg side chains considering their different pK<sub>a</sub> values, as in the Trp-Arg couple. Sample **D-6** was prepared considering the properties of the peptides rich in Arg and Trp residues.

For both **D-5** and **D-6** samples a  $\gamma$ -amino acid (5-N-amino valeric acid, fig. 61) replaces the palmitoyl fatty acid moiety. This choice was done considering the low number of positive charges present in the structure that is further reduced by the reciprocal interaction between the cationic Arg side chain and the Trp/His side chain.

The introduction of the 5-N-amino valeric acid contributes with an additional charge to the overall charge of the final compound.



**Figure 61.** Chemical structure of 5-amino-valeric acid

### **Samples prepared using M2 approach**

We try to apply AMPs to cotton fabrics using a *one-pot* method to try a technology that could be more appealing for an future industrial application. For this synthesis C-terminal diamino peptaibolin was prepared using SPPS on 2-CTC resin, before linking to cotton, while methyl ester C-terminus peptaibolin was prepared by peptide synthesis in solution. Both peptides **OPP-1** and **OPP-2** were synthesized by Dr. Daniele Canaglia during his thesis stage. The peptide sequences prepared are reported in table 12.

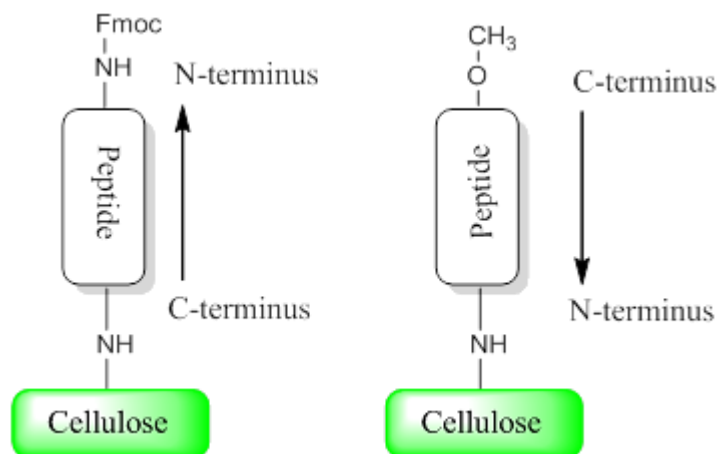
**Table 12.** Samples of cotton fabric functionalized with AMPs using M-2 method.

Sample	Peptide sequence	Yield %
<b>OPP-1</b>	Fmoc-Leu-Aib-Leu-Aib-Phe-NH(CH <sub>2</sub> ) <sub>2</sub> NH <sub>2</sub>	65%
<b>OPP-2</b>	H <sub>2</sub> N-(CH <sub>2</sub> ) <sub>4</sub> CO-Leu-Aib-Leu-Aib-Phe-OCH <sub>3</sub>	-----

Samples **OPP-1** and **OPP-2** present a primary amino moiety as anchoring site for textile bonding, at C-terminus and N-terminus respectively.

We made this synthetic choice to demonstrate that the biological activity of an immobilized AMPs bearing lysine residues vary by the site of attach used [32]. In some literature works it is asserted that AMPs show the higher activity when they are C-terminally anchored to a surface, while the activity decreases if the bond between the peptide and surface is at the N-terminus. Often AMPs are inactive if the AMPs is linked by the ε-NH<sub>2</sub> of the lysine side chain.

From these premises we tried to fix peptides to fabrics directly in one-step and we also investigated the relationship between biological activity and the direction of peptide anchoring (fig. 62).



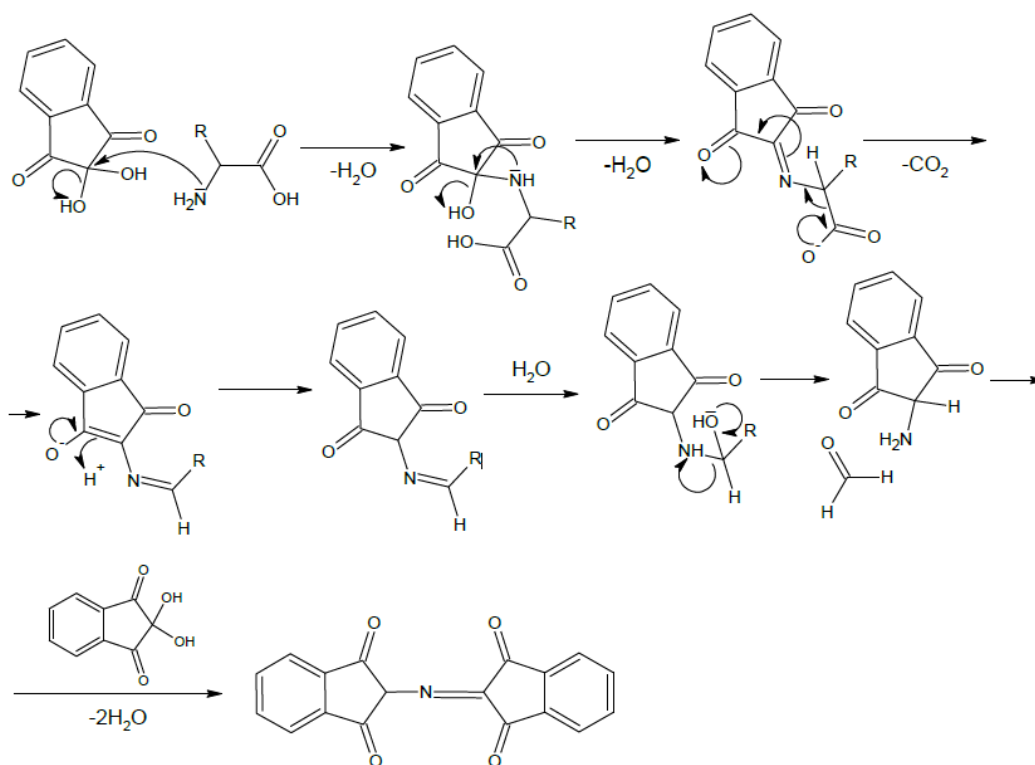
**Figure 62.** Schematic representation of the peptide anchoring to cotton through C- and N-terminus.

In our work AMPs were linked to textile by direct nucleophilic substitution of the bromide group present on the textile surface- a primary amino moiety located in the AMPs.

Peptides **OP-1** and **OP-2** were purified by HPLC. In sample **OP-1** a diamino linker was linked via amide bond to the C-terminal group. To have the amino group at the N-terminus in sample **OP-2** we exploit 5-amino-valeric acid. In this way we obtained two samples with a similar spacer between the peptide and the fabrics.. Fmoc-protective group in sample **OP-1** allow us to determinate the loading of the peptide on the surface, while for sample **OP-2** we do not have a method to determine the loading.

## Qualitative determination of textile functionalization

Kaiser test is commonly used in SPPS to rapidly check the Fmoc protection/deprotection step [33]. We applied the same test to have a rapid qualitative information on textile functionalization. This test allow to identify the presence of a primary amino moiety by reaction with ninhydrin. Ninhydrin is able to react with amines to form a compound called *Ruhemann purple* or *Ruhemann blue* depending on the source [34]. This molecule is a strong chromophore and colors the solution of an intense violet, indicating qualitatively the presence of amines. The check carried out through this test is the main indicator to assume the success or failure of a reaction. Kaiser test was applied in each coupling and deprotection step during the building of the peptide on the cotton surface.

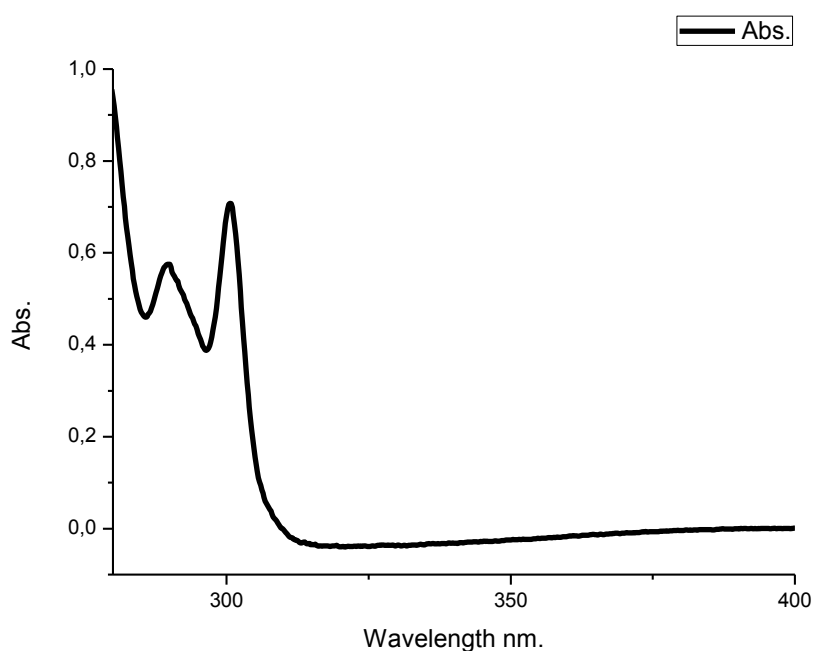


**Figure 63.** Mechanism of Ruheman purple compound formation.



## Quantitative determination of textile functionalization

The quantitative determination of the anchorage of the peptide on the support of cotton was performed through the analysis of the solution of deprotection of the Fmoc group by UV-Visible spectroscopy. From the values of absorbance obtained registering UV-Vis spectra ( $\lambda_{\text{max}} = 301\text{nm}$ ;  $\epsilon = 7800 \text{ cm}^{-1}/\text{M}$ ) we determinate the concentration of the piperidine-dibenzofulvene adduct present in the deprotection solution with the relevant annexes washes. We then correlated this value to the number of peptide sequences present on the fabric.



**Figure 64.** UV-Vis absorption spectra of the adduct *piperidine-dibenzofulvene* registered in *DMF*.

The loading values obtained by UV-Vis spectroscopy are reported in the table below.

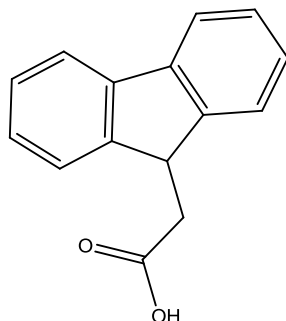
**Table 13.** Sample of cotton fabrics functionalized with peptides/dendrimers using both the synthetic method **M-1** and **M-2** and loading obtain by UV-Vis determination

Class of functionalization	Sample	Loading (mmol/g)
Cationic AMPs	AO-1	0.72
	AO-2	0.63 - 0.36 - 0.52
	AO-3	0.44 - 0.59
	AO-4	0.44
AMPs rich in Arg and Trp	RW-A	0.71
	RW-B	0.61
Peptaibols	AB-1	0.20
	DC-1	0.35
	AO-5	0.78
	DC-2	0.43
Dendrimer	D1	2.79
	D2	1.56
	D3	1.63
	D4	1.63
	D5	2.36
	D6	2.48
Peptaibols ( <b>M-2</b> )	OP1	0.63

The data confirm a functionalization degree in the range 0.1-1.0 mmol/g. The values relative to cotton fabrics functionalized with dendrimers correspond to the quadruple of the anchoring sites on the textile. Samples **AO2** and **AO3** were prepared twice and the loading value obtained is slightly different each time. The difference, anyway, remain in a reasonable extent that can be justified with manality and experimental errors. In the literature there is not a clear correlation between immobilized peptides concentration and biological activity was found. Gabriel et al. [35] demonstrated how the bactericidal activity of LL37 fixed on a titanium surface is independent by its concentration. In opposition, Humblot et al [36] correlate a low peptide (magainin I) concentration with a bacteriostatic effects and an higher concentration with a bactericidal effect.

In our experience we found that for samples functionalized with the same peptide at different concentration (according to UV loading determination) the biological activity does not vary significantly.

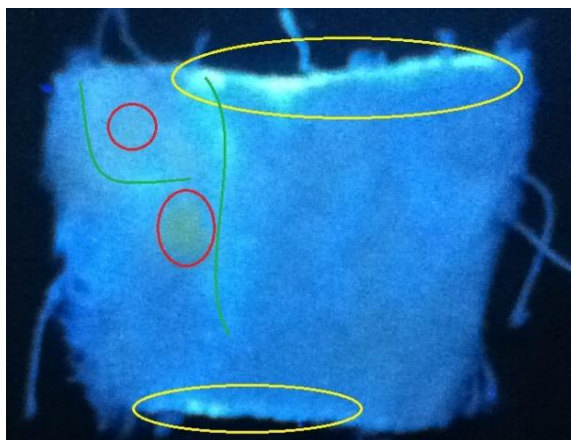
In order to understand the superficial homogeneity of the functionalized cotton fabrics we prepared a cotton sample where we linked 9-fluorenic acid (opportunately activated) directly on the cotton surface



**Figure 65.** Chemical structure of 9-fluorenyl-acetic acid.

This compound present the same chromophore of the Fmoc, and gives photoluminescence phenomenon that allowed us to observe what macroscopically happens to the cotton surface.

We observed the final material under UV irradiation at 365 nm (fig. 66).

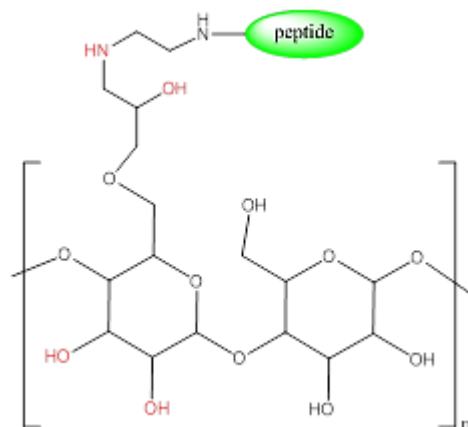


**Figure 66.** Cotton fiber functionalized with 9-fluorenyl acetic acid under UV irradiation at 365 nm.

The material shows an higher functionalization at the extremes of the piece of cotton in comparison to the internal parts that result lower but more homogenously functionalized.

We confirm that the loading determined by UV-Vis spectroscopy is over-estimated. In fact, every coupling step takes place by adding an activated ester to the modify cotton fabrics This activated ester reacts in presence of nucleophile species, on any kind. Beside the primary amines that we want to react, also the hydroxyl

groups of the cellulosic matrix can react forming esters. In this way, some peptides would be linked to the cotton surface not via amide bond, but via ester bond directly on the cellulosic hydroxyl groups. (fig.67).



**Figure 67.** Schematic representation of cellulose-linker-peptide system focused on the possible nucleophilic reactive sites

This hypothesis is confirmed by FT-IR spectroscopy, see next chapter.

Apparently, these undesired esters don not influence the biological activity of the final sample, as we will be discuss better in the following part of this thesis.

We tried to quantify the amount of this over functionalization. To this aim, we prepared a piece of cotton functionalized with epibromohydrin and then we reacted it directly with Fmoc-NH-(CH<sub>2</sub>)<sub>2</sub>-NH<sub>2</sub> in DMF.

The presence of the Fmoc-protection allowed a successive step in which we inactivated cellulosic hydroxyl moieties by acetylation with acetic anhydride and also blocked the secondary amine formed in the nucleofilic substitution step.

We then deprotected the Fmoc group and quantified the loading by UV. The results obtained was compared with a sample prepared in a similar way but without the acetylation step. Anyway the sample shows a lower functionalization, probably due to the lower concentration of the Fmoc- diamine respect to the large excess used with the unprotected ones.

We built on both fiber samples a dipeptide with the sequence Fmoc-Ala-Ala. we proceed with the loading determination by UV-Vis spectroscopy at each step of the synthesis. Results are reported in table 14.

**Table 14.** UV-Vis loading data of tested sample to verify the effect of acetylation before the first coupling process.

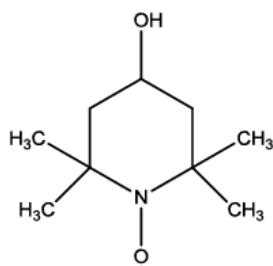
	<b>Non-Acetylated sample</b>	<b>Acetylated sample</b>
<b>Ala 1</b>	0.027	0.014
<b>Ala 2</b>	0.067	0.023

The data in the table above confirm, especially for the first anchored Alae, the possibility to have a bond formation with the secondary amine moiety. In fact the loading obtained for the non-acetylated sample is quite the double respect to the acetylated one.

The increasing in loading, for both samples from the first to the second step confirm the formation of bond nucleophiles different from the primary amine.

## Electron Paramagnetic Resonance (EPR)

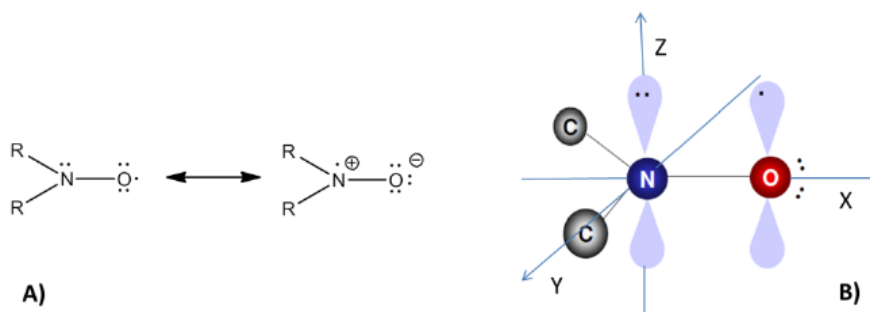
Functionalized cotton samples were also analyzed using EPR spectroscopy. This technique is the most known and used for the detection of radicals. To perform this test it was necessary to introduce in peptide sequences a paramagnetic probe. To this end the 4-hydroxy-TEMPO (fig. 68) was used. This experiment test uses the spin labeling approach, method that exploits stable free radicals (nitroxides) to label various types of biomolecules with a diamagnetic probe [37].



**Figure 68.** Chemical structure of 4-hydroxy-TEMPO.

This molecule is an ideal spin label because it is a free radical stable structure and with a reactivity that allows its introduction in macromolecules. The efficiency of this function depends on the intrinsic properties of the radical nitric oxide:

- The g factor reflects the characteristics of size, geometry and symmetry of the orbital where there is the unpaired electron. Therefore in most cases, it is anisotropic. Considering that in one of the limit forms of resonance of the nitroxide radical the unpaired electron is located in the orbital  $p_z$  of nitrogen (fig. x) it assumes axial symmetry, it is then described by a parallel ( $g_{\parallel}$ ) and perpendicular ( $g_{\perp}$ ) component to the field.

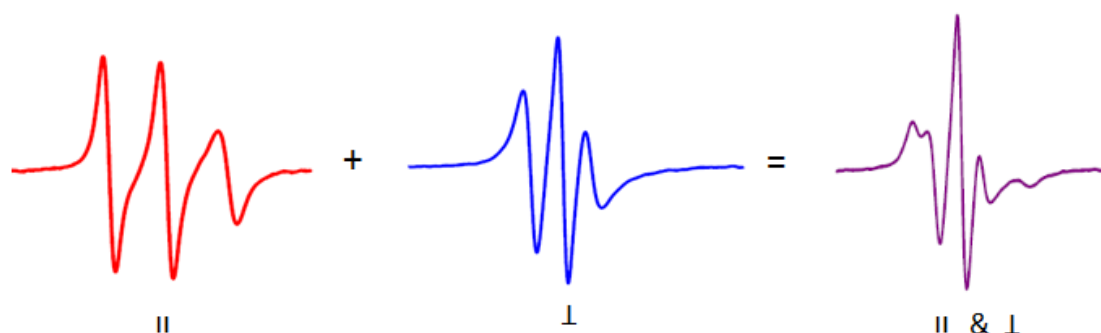


**Figure 69.** A) Limit forms of resonance of the nitroxide radical. B) Representation of nitroxide radical inserted in a Cartesian layer.

- The hyperfine coupling constant ( $A$ ) is the equivalent of the coupling constant  $J$  in NMR. It is the moment of interaction between the electron spin and spin moments of nuclei in the system. When the unpaired electron is in an orbital with  $L > 0$ , as in the  $p_z$  orbital of the nitrogen in the nitric oxide, the interaction depends on the orientation with respect to the external magnetic field. Then this factor is usually described by a component parallel ( $A_{||}$ ) and a perpendicular ( $A_{\perp}$ ) to the field.

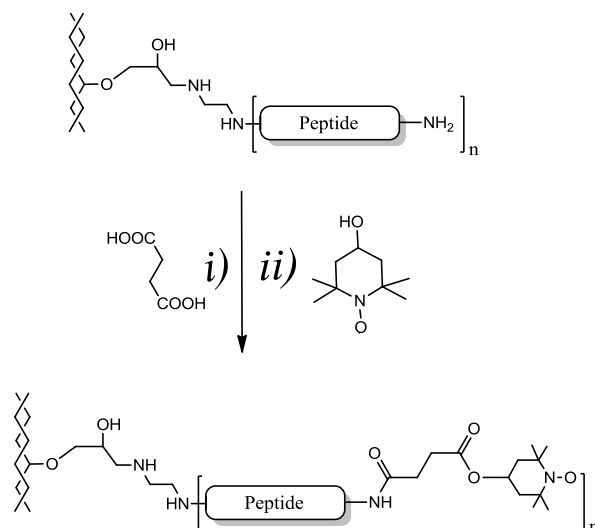
Because of these properties, the EPR spectrum of the nitroxide is sensitive both to the structural characteristics of the labeled peptide and to the interactions of the labeled biomolecule with its environment. The resulting changes in the spectral bands allow the detection and measurement of such characteristics.

The anisotropy of  $g$  and  $A$  makes the nitroxide sensitive to the mobility of the labeled biomolecule. The molecular mobility causes the mediation of the diagonal elements main tensors  $g$  and  $A$ , resulting in a spectrum characterized by three EPR bands. A lower motion prevents the averaging time and allows for the simultaneous visibility of the perpendicular and parallel components of the signal in the EPR spectrum. The spectrum then presents five overlapping bands.



**Figure 70.** Generalization of the amount between the perpendicular component (blue) and parallel (red) of the nitroxide spectra

In this work we used the hydroxyl functionality of the probe to tie it to the peptide using succinic acid as a linker.



**Figure 71.** Schematic synthetic approach applied for the synthesis of the sample prepared for EPR analysis.

To test the different mobility of the nitroxide probe linked to different peptide structures the following compounds were prepared:

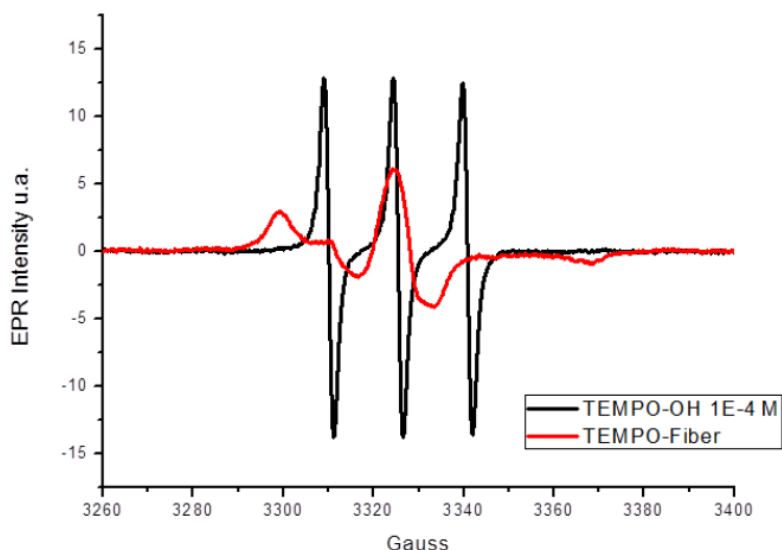
- TEMPO-Lys(Boc)-Ala-D-Ala-Lys(Boc)-NH-CH<sub>2</sub>-CH<sub>2</sub>-NH-cotton (**A**)
- [TEMPO-Lys(Boc)-Ala-D-Ala-Lys(Boc)]<sub>2</sub>-Lys-NH-CH<sub>2</sub>-CH<sub>2</sub>-NH-cotton (**B**)
- {[TEMPO-Lys(Boc)-Ala-D-Ala-Lys(Boc)]<sub>2</sub>-Lys}<sub>2</sub>-Lys-NH-CH<sub>2</sub>-CH<sub>2</sub>-N(Ac)-cotton (**C**)

Figure 72 represents the comparison between the EPR spectra of 4-hydroxy-TEMPO in toluene solution and that of compound **A** at room temperature. The solution spectrum (black line) is about 30 Gauss wide. It shows three components, because of the hyperfine coupling with the <sup>14</sup>N nucleus (hyperfine constant  $a_N = 15.4$  Gauss), with equal line widths, as expected for a nitroxide species free to rotate in a nonviscous solvent (fast motional regime, i.e. rotational correlation time  $\tau < 109$  s) [38].

On the contrary, the spectrum of peptide-cotton **A** (red line) is wider ( $\approx 70$  Gauss) and shows contributions by two spin probe populations. The main one is in the slow motion regime with rotational correlation time  $\tau = 16.5$  ns, whereas the marginal



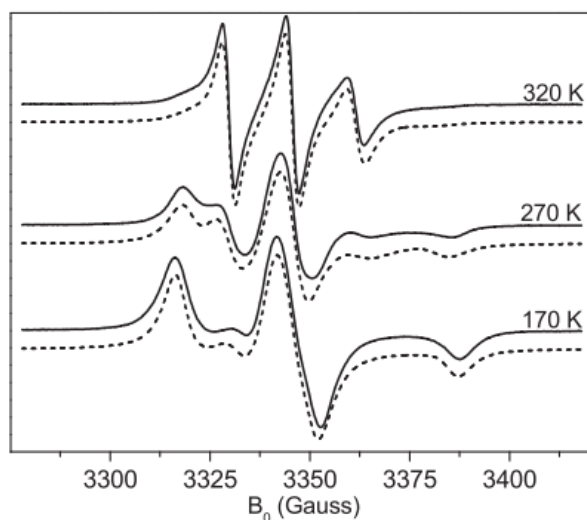
population is characterized by  $\tau=2$  ns. This mobility difference, compared with 4-hydroxy-TEMPO in liquid toluene, shows the lower rotational freedom of the textile-linked nitroxide probe and confirms the actual covalent linking of the peptide to the cotton.



**Figure 72.** Comparison of the spectra of a solution of  $10^{-4}$  M TEMPO-OH in toluene (black curve) and the spectrum of the nitroxide linked to mono-peptide (LysAlaDAlaLys) fixed on cotton.

Multiple contributions to the EPR spectra coming from 4-hydroxy-TEMPO in different motional regimes have been reported even for a spin probe adsorbed into the cotton (not covalently bound) [39]. With the aim at better understanding the features of nitroxide spin probes on cotton, we started a preliminary investigation on the effect of temperature on the EPR spectra of sample **A** (Figure x). At 170 K, the spectrum is about 70 Gauss wide, and its aspect is typical of a nitroxide probe immobilized in the timescale of X-band EPR [38]. Indeed, the 170 K simulation (Figure x) is obtained using  $\tau=84$  ns (Table x). In this case, the spectral shape is due to both isotropic (constant  $a_N$ ) and anisotropic hyperfine interactions and to the anisotropy of the  $g$  tensor. As the temperature is raised, the spectrum shrinks as expected. In fact, the nitroxide label gains mobility that averages the anisotropic contributions, thus reducing their effect on the spectrum. Anyway, for  $T \geq 270$  K, the spectra show two contributions coming from two different spin-label populations (Table x). One of them reaches at 320 K, the fast motion regime, while the other one is in the slow motion regime at all temperatures. At 320 K, the averaging of the anisotropic magnetic interaction is therefore almost complete only for the population

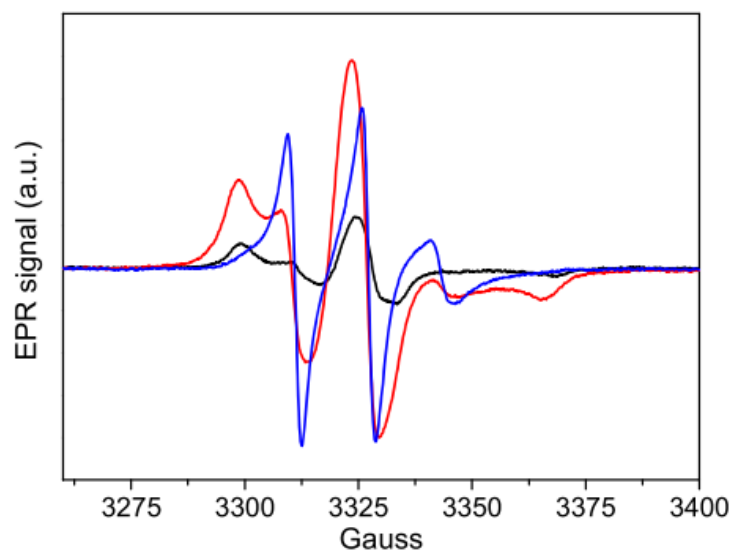
of nitroxides in the fast motion regime. Its spectrum extends for about 30 Gauss and shows three well-resolved hyperfine lines, separated by  $aN = 16$  Gauss. The other population gives still a slow motion spectrum ( $\tau = 7.4$  ns), which contributes to about one half of the total intensity.



**Figure 73.** Electron paramagnetic resonance spectra of 1b at temperatures ranging from 170 K to 320 K (solid lines). Calculated electron paramagnetic resonance spectra of cotton-peptide 1b (dashed black lines) obtained with the parameters reported in Table 4. Spectra are shifted vertically for clarity.

Figure 73 reports the EPR spectra of the three spin-labeled peptides at 290 K. The spectra of **A** and **B** extend through about 70 Gauss and had the typical shape of slow moving nitroxide probes, even if double slow contributions are present in the traces. Conversely, the EPR spectrum of 3b is narrower, covering only ~40 Gauss, and has a line shape (three hyperfine lines) that resembles much that of **A** at high temperature.

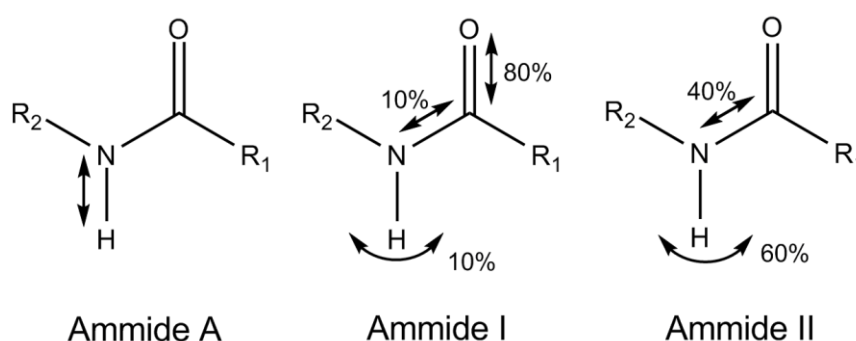
Once more, the EPR spectrum of **C** shows that there have been contributions from slow moving spin labels but also substantial contributions from fast moving nitroxides. This finding indicates a more mobile spin label. Indeed, in sample **C**, two Lys residues move the peptides and the nitroxyl probes farther from the cotton surface.



**Figure 74.** Comparison of EPR spectra recorded for the textile samples functionalized with peptide units and dendrimeric compound

### **FT-IR characterization**

In this work the IR absorption spectroscopy was used to determine the presence of the peptide on the cotton used as a support for our synthesis. To this end we have sought the typical signals related to the absorption of infrared amide functions. Generally the ranges of the most significant research are between 3500-3200  $\text{cm}^{-1}$  (relating to the amide A) and between 1700-1450  $\text{cm}^{-1}$  (relating to the amide I and II) [12].

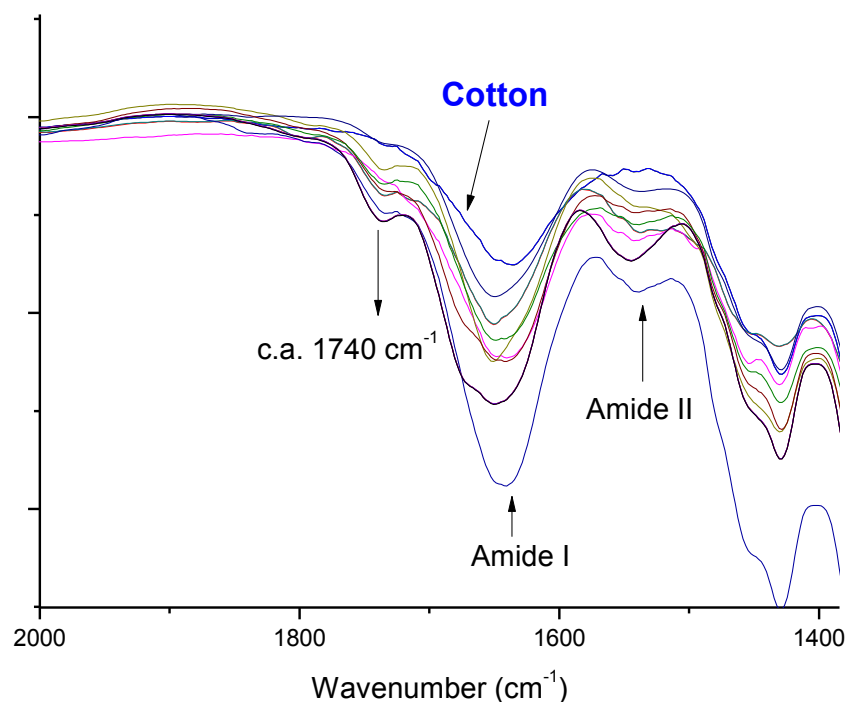


**Figure 75.** Typical vibrational modes of the amide group.

For the type of sample used only the area between 1700-1450  $\text{cm}^{-1}$  was observed, because the area around 3400  $\text{cm}^{-1}$  is also characteristic of the stretching of the hydroxyl groups of which the cellulose is rich, and that of the water present in the

sample, and then the signals attributable to absorption of the amide A are not easily recognizable.

The fabric samples functionalized with peptides were characterized by infrared spectroscopy in a KBr pellet. The spectra obtained are shown in figure 76.



**Figure 76.** *Overlap of the FT-IR spectra of all sample prepared using method M-I and simple cotton.*

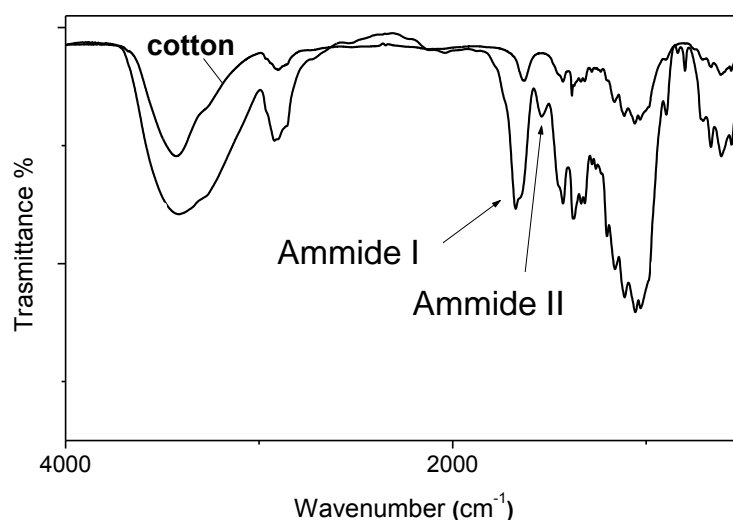
In fig.76 the FT-IR spectral region from 1800 to 1500  $\text{cm}^{-1}$  is reported. All the spectra confirm the presence of both signals related to the absorption of the amide I and II, respectively. It is also noted that the intensity of the absorption signals amide increases with the length of the peptide chain. The signals relative to amide I are more intense for cotton functionalized with Tricogin GA IV (consisting of 11 residues, red curve) and for the cotton functionalized with dendrimeric structure, while in the cotton samples functionalized with shortest sequences the absorption values are lower. These characteristic signals are a proof of the presence of the peptide on the textile surface.

From the spectra there is also evidence that some ester bonds are present.. Spectra of functionalized cotton is in fact present an absorption band around 1740  $\text{cm}^{-1}$ , absent in the spectrum of simple cotton, attributable to an ester bond.

It is reasonable to say that the activated carboxylic acid reacts mainly with the amine functionality forming the desired amide bond, but partly it reacts also with the hydroxyl sites of the cellulose forming an ester bond.

The case leaves therefore be assumed that on the surface of the tissue are present some incomplete sequences in addition to the desired peptides. These truncated and undesired peptides do not necessarily create an interference in the biological activity of the final material, which is the final focus of this project.

Anyway, to avoid the formation of these unwanted sequences it was tried to prepare a sample of cotton functionalized with peptaibolin applying the *one-pot* synthetic approach already mentioned in the previous process. An analogous of peptaibolin, Pal-Leu-Aib-Leu-Aib-Phe-NH-(CH<sub>2</sub>)<sub>2</sub>-NH<sub>2</sub>, bearing a linker ending with an amino function, was prepared by liquid phase peptide synthesis by Dr. Daniele Canaglia during his thesis. This peptide was successively bound to cotton in a single step. The comparison between a cotton sample (functionalized with the bromine moiety) and the cotton bearing the peptaibolin analogues shown in Figure 77.



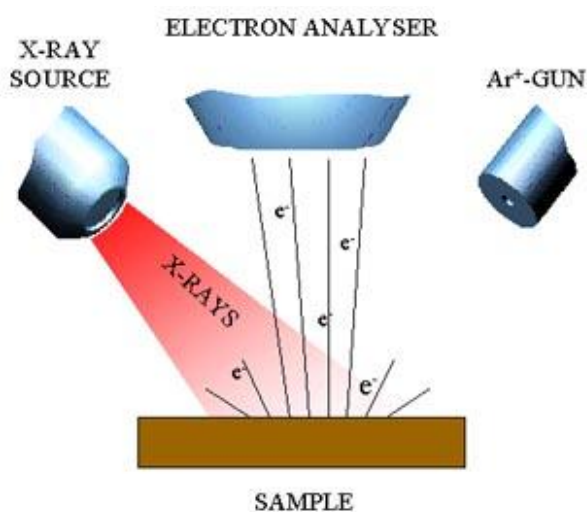
**Figure 77.** FT-IR spectra of sample OP-1 compared with the spectra of simple cotton.

In the spectrum signals due to ester bonds are completely absent, as expected. Indeed, in the one-pot approach the anchoring occurs through a nucleophilic substitution reaction between the bromine moiety of " halogenated cotton " and the primary amine pendant from the C-terminus of the peptide, thus excluding the possibility of ester formation.

## X-Ray Photoelectron Spectroscopy characterization (XPS)

Peptide-cotton samples were analyzed by XPS in order to confirm the presence of the desired peptide on the cotton support.

This technique, based on the photoelectric effect, provides a beam of X-rays that impacts on the surface under examination: by photoelectric effect the surface emits photoelectrons that are solved by an analyzer and subsequently quantified by a detector that determines the intensity (fig. 78).



**Figure 78.** Schematic representation of XPS assay

For each photo emitted electron a kinetic energy ( $E_k$ ) can be calculated using the Einstein relationship:

$$E_k = h\nu - E_b - \phi_{\text{spectr}}$$

$h\nu$  is the energy of the incident radiation,  $\phi_{\text{spectr}}$  is a constant feature of the instrument used and  $E_b$  is the binding energy (binding energy of the electronic level from which photoemission is originated). The  $E_b$  is slightly affected (though slightly) from the chemical neighborhood of the element that can induce shifts in the energy of the peaks of a few eV (called chemical shift). This information can be used to identify the chemical state in which a certain element is found.

The analysis was carried out by the group of Dr. Silvia Gross using the Perkin-Elmer XPS  $\Theta$  5600ci. The tool uses a standard source-based Al, it leverages 13 K $\alpha$  emission line due to the decay  $2p_{3/2} \rightarrow 1s$  developing a radiation with energy of

1486.6 eV. The instrument works in a range of pressure between  $5 \cdot 10^{-8}$  and  $10^{-11}$  torr.

In table 15 an example of the results obtained by XPS analysis on C 1s electrons:

Sample	%C	%N	%O	C/N	O/C
Cotton	78.0	0.4	21.6	-	0.28
Cotton-NH <sub>2</sub>	59.78	1.66	38.56	36.0	0.64
Pal-Arg(NO <sub>2</sub> )-Ala-ala-Arg(NO <sub>2</sub> )-linker-cotton	69.21	4.84	25.95	14.3	0.40
[Pal-Arg(NO <sub>2</sub> )-Ala-ala-Arg(NO <sub>2</sub> )] <sub>4</sub> (Lys) <sub>2</sub> Lys-linker-cotton	72.6	6.3	21.1	11.5	0.29

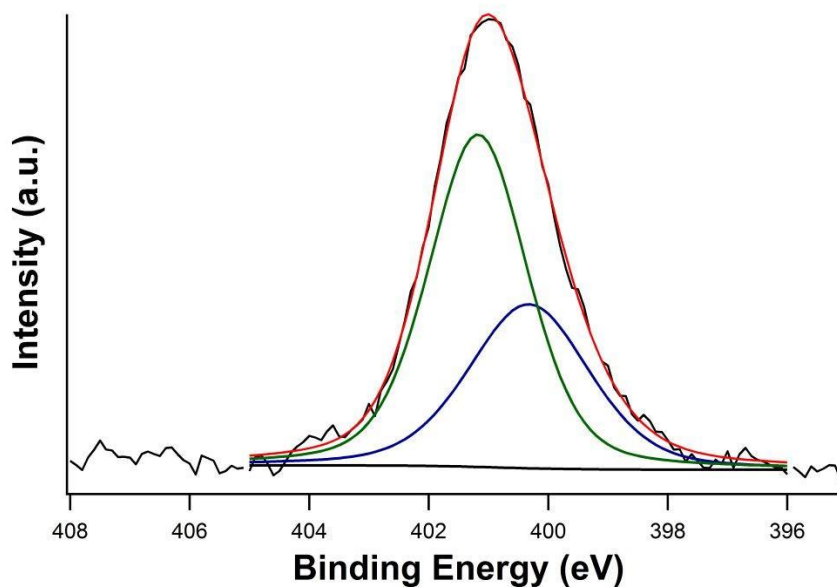
The goal of the XPS analysis on our samples is the identification of the presence of an element normally absent in cellulose matrix and instead present in the bound peptides. This element is nitrogen (N). As evident from the results obtained, the quantity of nitrogen is approximately equal to zero only in the cotton itself. The obtained value (0.4%), is attributable to the small amount of air present, regardless of the instrumentation works in vacuum conditions. But moving from simple cotton to functionalized-cotton, the percentage of nitrogen present increases from 1.6% for the sample containing the amino linker (NH<sub>2</sub>-CH<sub>2</sub>CH<sub>2</sub>-NH<sub>2</sub>) to 4-5% for samples having a tetrapeptide bound on the surface and to a percentage of 6 - 8% for samples functionalized with dendrimeric sequences. These results are consistent with what we expected by building gradually longer peptide sequences and dendrimers.

In this elaborate we prefer to omit the results of the binding energy obtained, because the chemical environment for the C1s observed does not change sufficiently to be able to discriminate between C-N and C-O or between C = O and O-C = O. XPS analysis was also performed to study N 1s electrons.

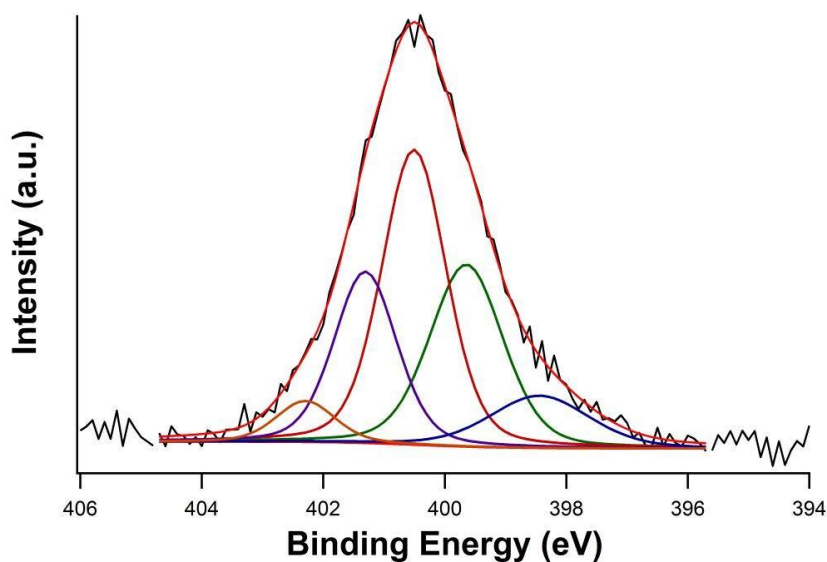
The binding energies relative to the N 1s are in the area between 405-395 eV so the results are not influenced by the structure of the cotton –matrix.

The analysis of the N 1s XPS was also particularly significant to distinguish samples of the series **AO-x** by comparison with data report in literature [40]. The peptides used to functionalize these samples in fact belong to the pattern of Shai already illustrated in the previous years consisting of two charged residues at positions 1 and 4 and two residues of apolar Ala at positions 2 and 3. Peptide analogs of this series keeping the apolar component but varying the charged residues were synthesized on cotton support. In particular, sample **AO-2** bears two His residues at positions 1 and

4, sample **AO-3** bears Arg, while the **AO-1** has two residues of Lys at positions 1 and 4.. The three amino acids, all cationic, bear a N in the side chain with different chemical environments. The analysis allowed us to confirm the presence of residues on the cotton support.



**Figure 79.** XPS spectra of sample **DC-1** in the range of 405-395 eV.



**Figure 80.** XPS spectra of sample **AO-3** in the range of 405-395 eV.



- Pal-His-Ala-D-Ala-His-linker-cotton

Bond	Binding Energy (eV)	% Area
Imino imidazole	398.3	11.0
Amino imidazole	399.5	9.2
Amide	400.9	77.7
Protonated amide	403.4	2.1

- Pal-Arg(NO<sub>2</sub>)-Ala-D-Ala-Arg(NO<sub>2</sub>)-linker-cotton

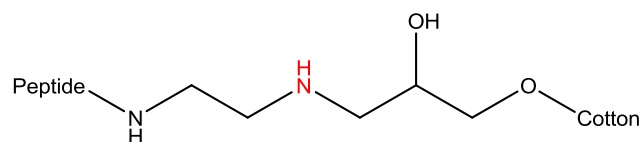
Bond	Binding Energy (eV)	% Area
Imino	398.4	3.0
Amine arginine	399.8	24.2
Amide	400.9	43.2
Amine	401.7	25.3
Nitro	402.8	4.3

- Pal-Lys-Ala-D-Ala-Lys-linker-cotton

Bond	Binding Energy (eV)	% Area
Amide	400.6	28.6
Amine	401.5	34.1
Alkyl ammonium	401.8	37.3

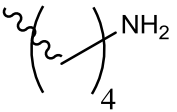
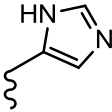
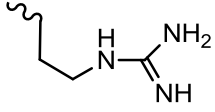
From the results shown in the table we can observe that:

- All samples present the peak typical of the amide bond, at about 400 eV;
- In all the samples examined at about 401.5 eV there is a signal relative to amines, attributable to the N amino linker



**Figure 79.** Schematic chemical representation of the linker between peptide and cotton draw attention to the secondary reactive amine moiety (red colored).

- The presence of cationic residues in samples AO-1, AO-AO-3 and AO-5 is confirmed, as it is possible to recognize the side chains of imidazole (His), guanidinium (Arg) and a primary amine (Lys), respectively.

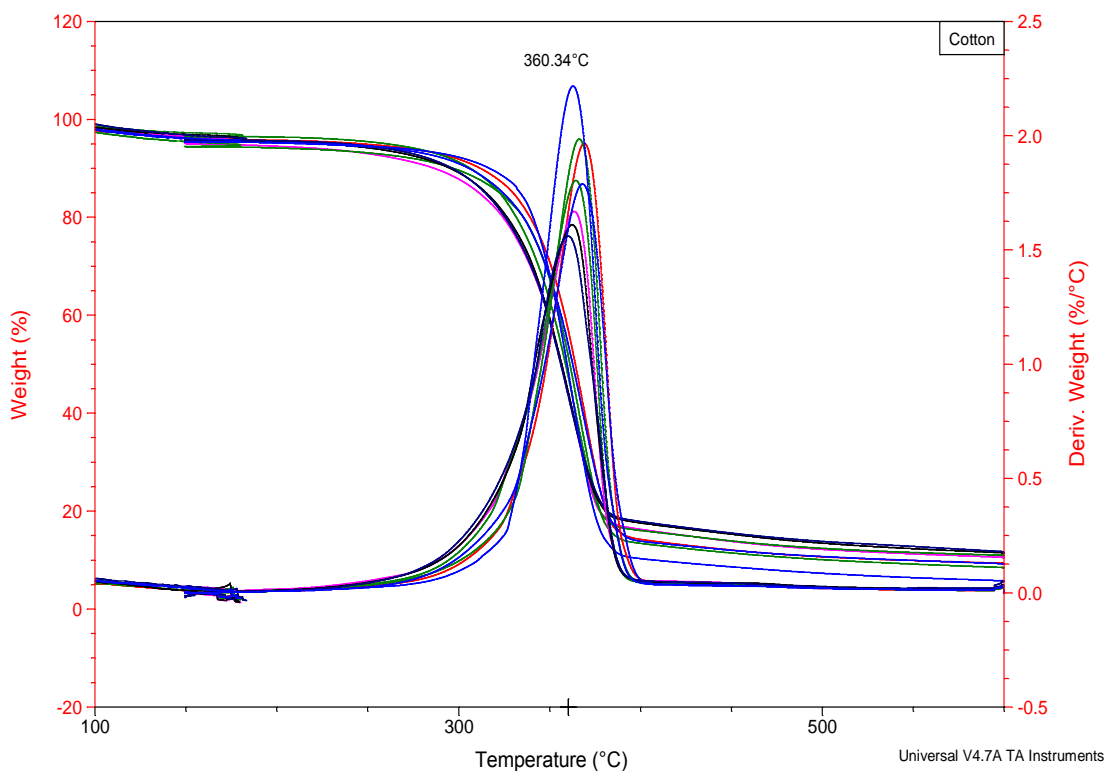
Amino acid	Lys (K)	His (H)	Arg (R)
Side chain			

## Thermo gravimetric analysis (TGA)

The properties of our products were also tested by thermo gravimetric analysis (TGA). This technique allows to determinate how the functionalization of textiles modify the characteristics of the fabrics, such as the improvement of flame retardant properties. The complete mechanism of cellulose pyrolysis is not yet fully understood. This technique provides information regard the loss of mass of a sample related to time or temperature [41]. The first derivative of TGA called DGT gives information about the difference of TGA curves.

Analysis were performed, in a range of temperature from 100 to 600°C with a slope of 10°C/min. The mass of the tested sample was around 2-3 mg for each ones. Samples were stabilized at 100°C for 5 minutes to remove the adsorbed water.

The obtained results are reported in figure 80.



**Figure 80.** Thermogravimetric analysis of our functionalized fabric samples.

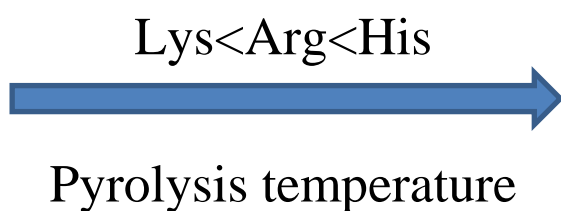
From the analysis it is clear that for every sample pyrolysis takes place in one step only.

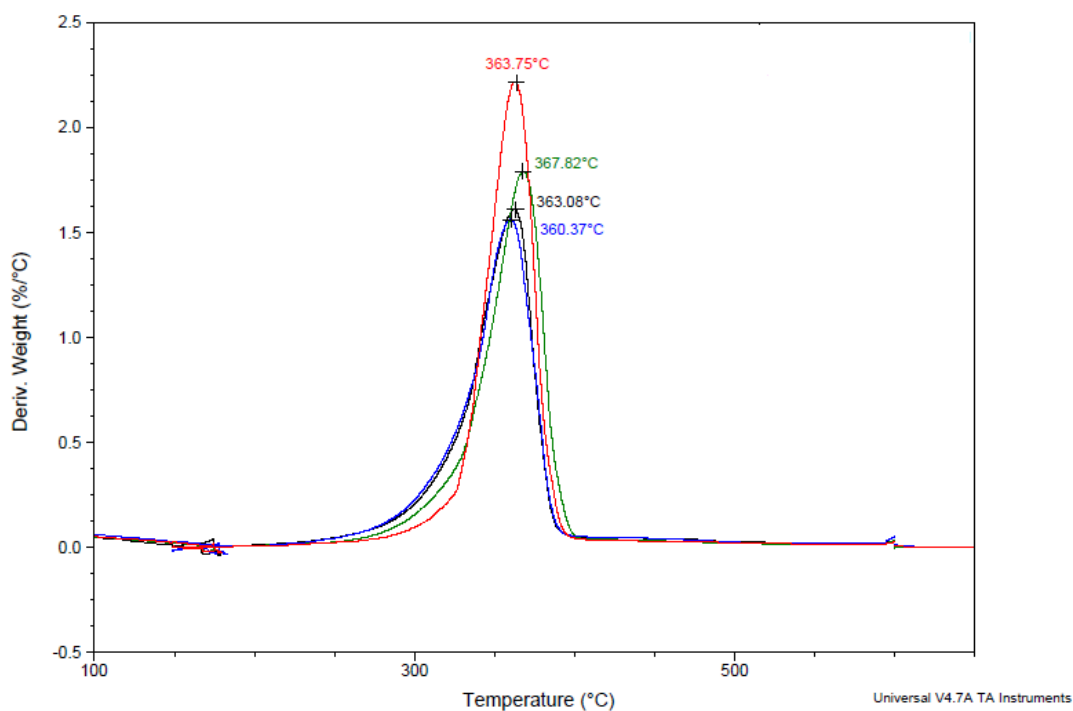
Functionalization of textile promotes an increase in the temperature of pyrolysis that arises from 360.34°C for the simple cotton to 367.82°C for sample **D-2**. The others samples show a temperature of pyrolysis contained in this range. Analysis data confirm that this increase of temperature is strongly related to nature of the compound linked to cotton fabric, particularly to the kind of residues present in the sequence.

Generally, fabrics functionalized with peptides or dendrimers bearing His residues show the highest temperature of pyrolysis respect to samples containing Lys or Arg residues.

So, the increase in temperature can be related to the mechanism of pyrolysis of the peptides investigated [42]. This process takes place firstly through the formation of a diketopiperazine and much longer is the peptide linked more energy for the formation of these products is required.

By the comparison of the DGT results of the fabrics functionalized with dendrimer based on cationic AMPs (fig. 81) we can find a relationship between the temperature of pyrolysis and the number of cationic residues located in the peptide:





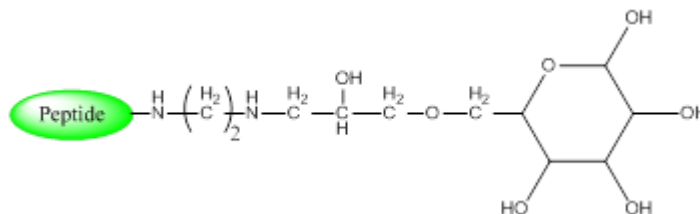
**Figure 81.** Comparison between the DGT of the sample D-1 (black), D-2 (green), D-4 (red) and simple cotton (blue)

From figure 81 we also obtain information regard the loss in weight of the tested sample. As expected the variations in weight loss for the samples are strongly related to the molecular weight of the linked compounds and to the extent of the functionalization.

So TGA and DGT analysis confirm the presence of a functionalization on the fabrics, and also the capacity of bond peptides to improve flame retardant properties that are better than that performed by the simple cotton.

## Enzymatic degradation of cotton fabrics

An enzymatic degradation experiment was conducted on the functionalized peptide-cellulose material. The experiment aimed at obtaining a single glucose unit with the peptide bound to it. In this way we should be able to examine the material by means of the classical techniques used to characterize chemical compounds in solution. In particular, we could identify the peptide-glucose degradation product by NMR spectroscopy. Theoretically, if the cellulose support could be completely digested by cellulase, we should obtain the compound described in Figure 82. If the cellulose degradation is not complete, we could obtain a peptide unit linked to a cellobiose unit or to a higher oligomer of glucose. Also, we can envisage to obtain a mixture of the described compounds.

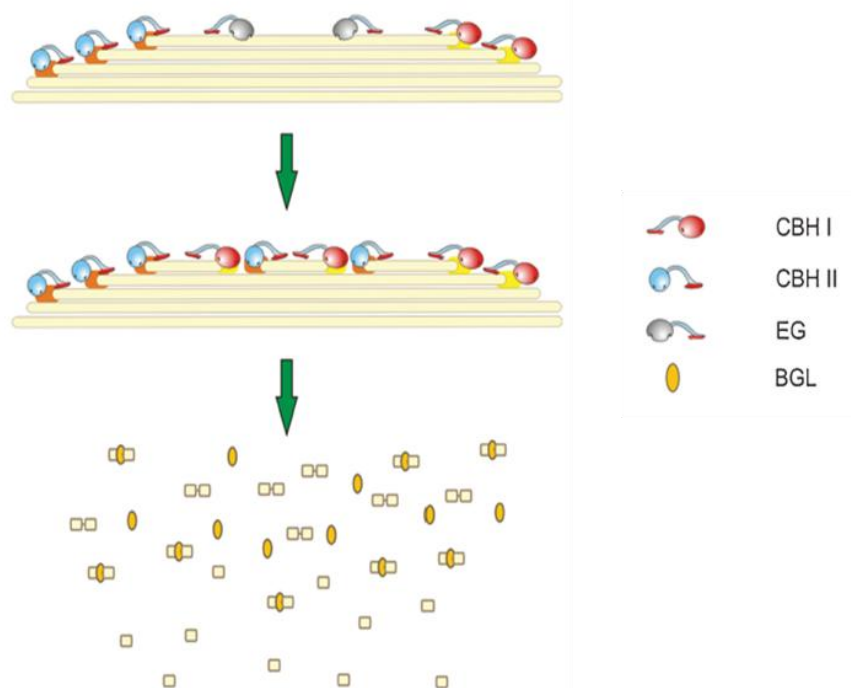


**Figure 82.** Desired compound after enzymatic degradation composed by peptide-linker-glucose

In nature cellulose is degraded by fungi and bacteria to obtain cellulose with low polymerization degree and/or single glucose units as metabolites. For this purpose these live organisms developed a series of enzymes able to degrade the cellulose chains.

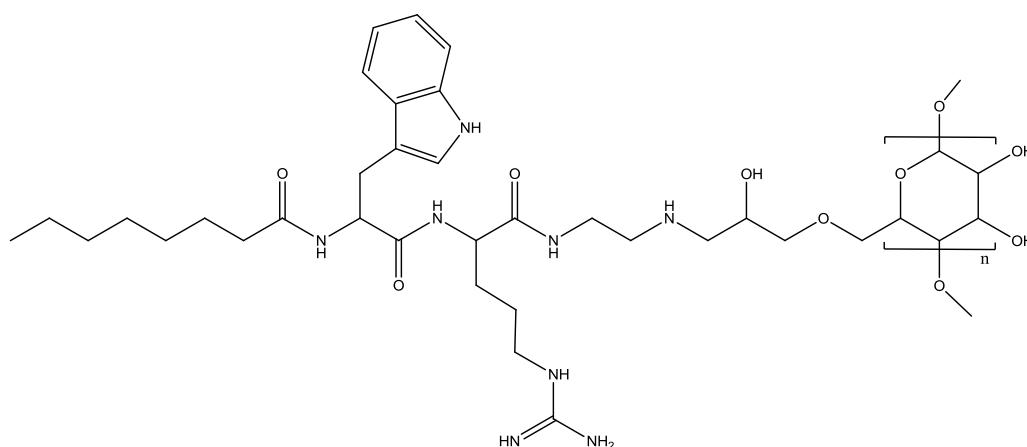
The cellulolytic systems are composed by several enzymes that act in different zones of the cellulose polymer: *exogluconase* acts at the end of the polymer and *endogluconase* acts in the middle of the cellulose polymer [43].

In our experiment we used cellulase obtained by *Trichoderma reesei* fungi. It is the most industrially used cellulolytic system. Several studies were conducted on these enzymatic system elucidating its composition. *Trichoderma reesei* cellulase is composed by two *exogluconases* (CBHI and CBHII) [46], six *endogluconases* (EGI...EGVI) and two  $\beta$ -*glucosidases* [Saloheimo, 1992-2002] that complete the hydrolysis of cellulose to glucose.



**Figure 83.** Schematic mode of action of cellulase from *Trichoderma reesei*.

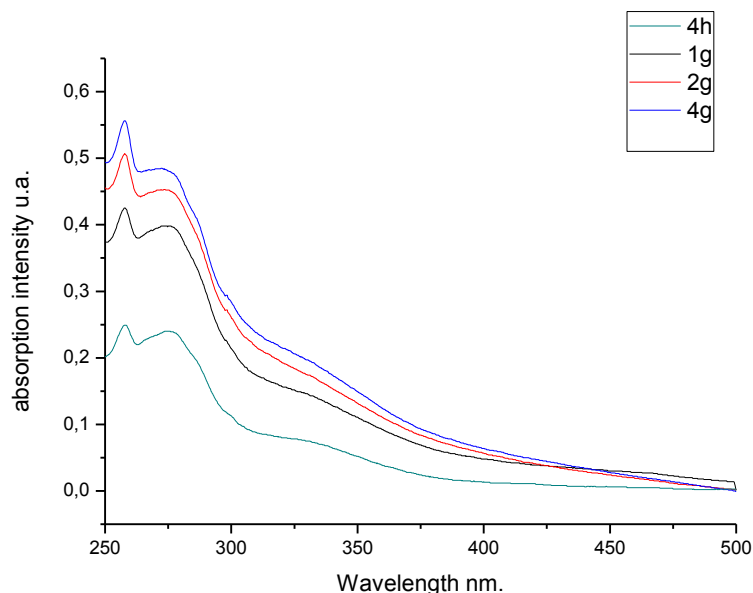
Several works are report in literature to determinate the optimal condition for enzymatic degradation of cellulose [44,45]. The best conditions found are acidic conditions and a mild heating, more specifically pH = 5.5 and 55°C for one week. For our test a functionalized fabric sample was prepared *ad hoc* (fig.84).



**Figure 84.** Sample prepared *ad hoc* for the cellulase assay.

As a model compound or the test we a short lipo-dipeptide containing Arg and Trp. These two amino acids possess characteristics side chains, adapt to be identified by

NMR and UV techniques. Trp residues allow to follow by UV-Vis spectroscopy the action of the cellulolytic system by the release in solution of this amino acid ( $\lambda_{\max}=280$  nm,  $\varepsilon = 5690$  cm<sup>-1</sup>/M) (fig. 85). Moreover, Arg and Trp lateral chain have characteristic signals useful for the protonic NMR analysis.



**Figure 85.** UV-Vis absorption spectra of the enzymatic degradation solution at measured different time.

The fatty acid linked to the N-terminus of the peptide is an octanoyl moiety whose aliphatic chain is easy to be identified by NMR analysis. The sample tested was prepared using **M-1** approach with a loading, measured at the end of the synthesis by UV-Vis determination, of 0.39 mmol/g. The concentration of Trp measured by UV spectroscopy released in solution after 7 days of enzymatic degradation was found to be 0.25 mmol/g. The two concentration values are not very far apart and the moderate difference observed can be due to an incomplete decomposition of the sample. A proof of this is the fact that the solution after the 7 days of incubation is not limpid and needs to be filtered. The filtered solid suspension is reasonably made of cotton fibers not yet degraded.



## <sup>1</sup>H-NMR characterization

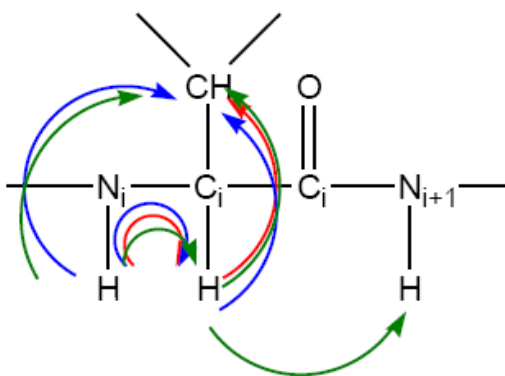
In this work NMR spectroscopy was used to obtain information regarding the conformational preferences of the synthesized peptides in order to establish whether a correlation between conformation and bioactivity exists. Once built on the cotton surface, some peptides were “detached” from the cellulosic support by enzymatic degradation of the cellulose matrix. NMR was used to identify the products resulting from this enzymatic degradation.

Mono- (1D) and two-dimensional (2D) <sup>1</sup>H-NMR experiments were performed to characterize the peptides of the His and Arg series. *Correlation Spectroscopy* (COSY), *Total Correlation Spectroscopy* (TOCSY) and *Nuclear Overhauser Effect Spectroscopy* (NOESY) experiments were acquired.

COSY and TOCSY are homonuclear 2D techniques used to correlate the chemical shift of <sup>1</sup>H nuclei which are J-coupled to each other. These spectra were used to assign the chemical shifts of the backbone protons and of the side chains.

In NOESY experiments, direct dipolar coupling provides the primary means of cross-relaxation. Spins undergoing cross-relaxation are those which are close to each other in space. The cross peaks of NOESY spectra indicate which protons are close, giving an indication of the three dimensional structure adopted by peptides.

The correlations COSY, TOCSY and NOESY of a generic residue are represented in Figure 86.



**Figure 86.** Correlations COSY (red), TOCSY (blue) and NOESY (green) of a generic residue.

The area representing the correlations between amide protons and  $C\alpha$  protons is very important to determine the conformation of the peptides. Correlation peaks  $C^\alpha H_i \rightarrow HN_{i+n}$  are useful to determine the presence of helical structures and the nature

of the helix. In general,  $C^{\alpha}H_i \rightarrow HN_{i+1}$  cross-peaks confirm the presence of a helical structure.  $C^{\alpha}H_i \rightarrow HN_{i+2}$  cross-peaks represent  $3_{10}$ -helices, whereas  $C^{\alpha}H_i \rightarrow HN_{i+4}$  cross-peaks represent  $\alpha$ -helices. The presence of  $C^{\alpha}H_i \rightarrow HN_{i+3}$  signals are compatible with  $3_{10}$ -helices as well as  $\alpha$ -helices.

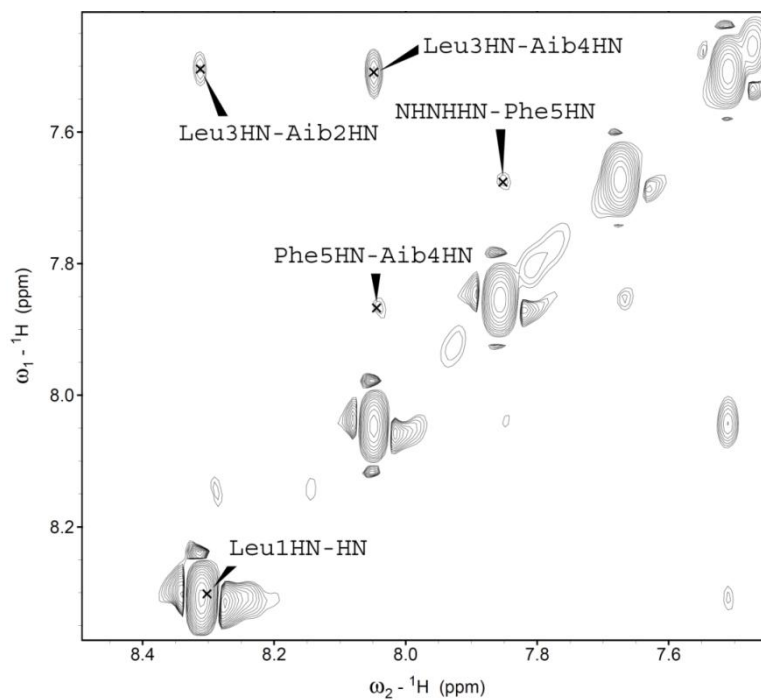
NMR conformation investigation was performed for the samples reported in table 16. Their sequences correspond to that of the most active peptide-cotton samples (see *Biological Activity*).

**Table 16.**

Sample	Sequence
AP-2	Pal-His-Ala-D-Ala-His-NH <sub>2</sub> CH <sub>2</sub> CH <sub>2</sub> NH <sub>2</sub>
AP-4	Pal-Arg-Ala-D-Ala-Arg-NH <sub>2</sub> CH <sub>2</sub> CH <sub>2</sub> NH <sub>2</sub>
OPP-1	Pal-Leu-Aib-Leu-Aib-Phe-NH <sub>2</sub> CH <sub>2</sub> CH <sub>2</sub> NH <sub>2</sub>

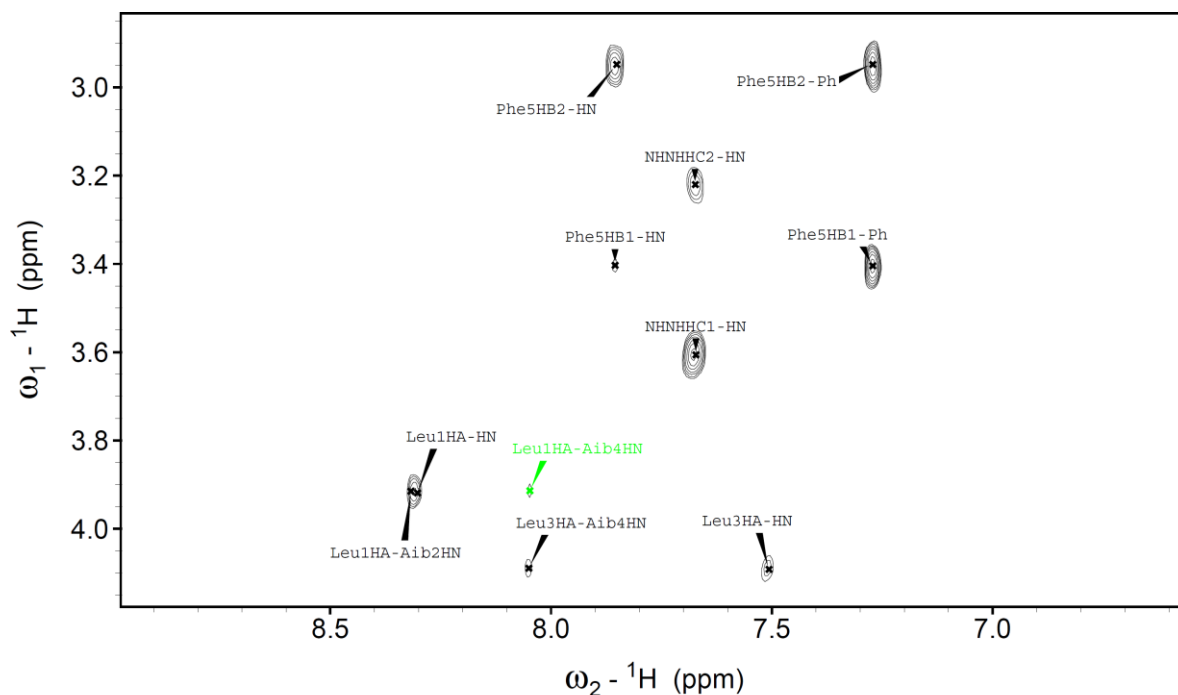
NMR spectra were recorded at about 10 mM peptide concentration in DMSO-d<sub>6</sub> or in MeOH, solvents in which the peptides studied show a good solubility. Spectra of AP-2 and AP-4 were recorded and allowed the assignment of all the signals. However, an accurate analysis of the NOESY spectra indicate the absence of significant cross-peaks indicative of a defined secondary structure. In all probability the two tetrapeptides studied are too short to fold in a well-defined three dimensional structure.

Regions from NOESY spectra of Pal-Leu-Aib-Leu-Aib-Phe-NH<sub>2</sub>CH<sub>2</sub>CH<sub>2</sub>NH<sub>2</sub> (**OPP-1**) in CD<sub>3</sub>OH are reported in the following figures (600 MHz). Figure 87 shows the cross-peaks in the amide protons region. The presence of all the sequential NH(i)→NH(i+1) correlations is diagnostic of the presence of an helical structure.



**Figure 86.** Region of the NOESY spectrum of *Pal-Leu-Aib-Leu-Aib-Phe-NH<sub>2</sub>CH<sub>2</sub>CH<sub>2</sub>NH<sub>2</sub>* in  $CD_3OH$  (1.6mM, 600 MHz, 298K). All  $NH_i \rightarrow HN_{i+1}$  correlation peaks are observed.

In the fingerprint region ( $\alpha H \rightarrow NH$  correlations) this observation is confirmed by the presence of  $CH_i \rightarrow HN_{i+3}$  correlations, also diagnostic of helical structures (Figure 87).

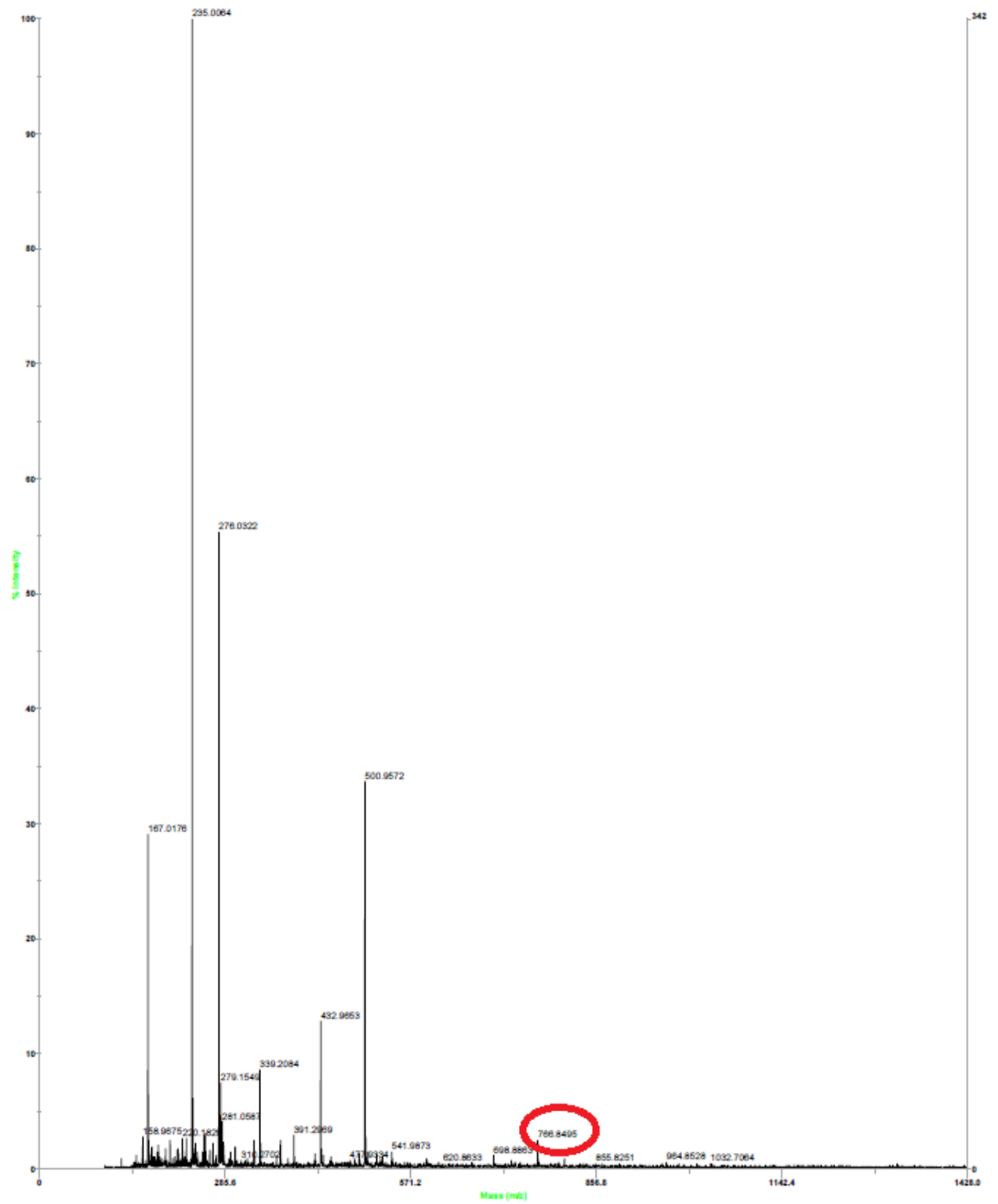


**Figure 87.** Region of the NOESY spectrum of Pal-Leu-Aib-Leu-Aib-Phe-NH<sub>2</sub>CH<sub>2</sub>CH<sub>2</sub>NH<sub>2</sub> in CD<sub>3</sub>OH (1.6mM, 600 MHz, 298K). A CH<sub>i</sub> → HN<sub>i+3</sub> correlation peak is observed.

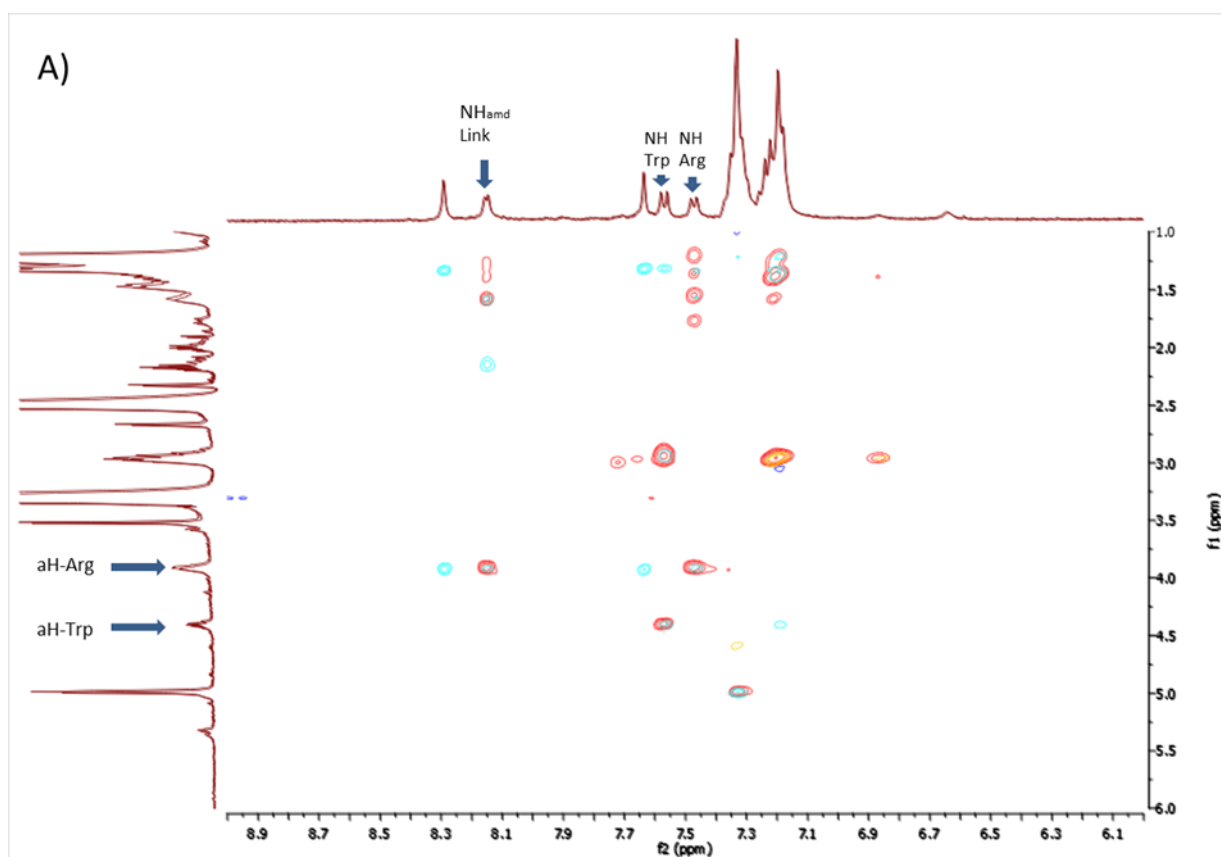
The presence of a helical secondary structure was so confirmed by the analysis of two-dimensional NMR. Although the sequence of peptaibolin is formed by only five residues, the presence of two Aib residues is sufficient to stabilize two turns of the helix. Most likely the presence of an additional amide at the C-terminus may contribute to the stabilization of the structure.

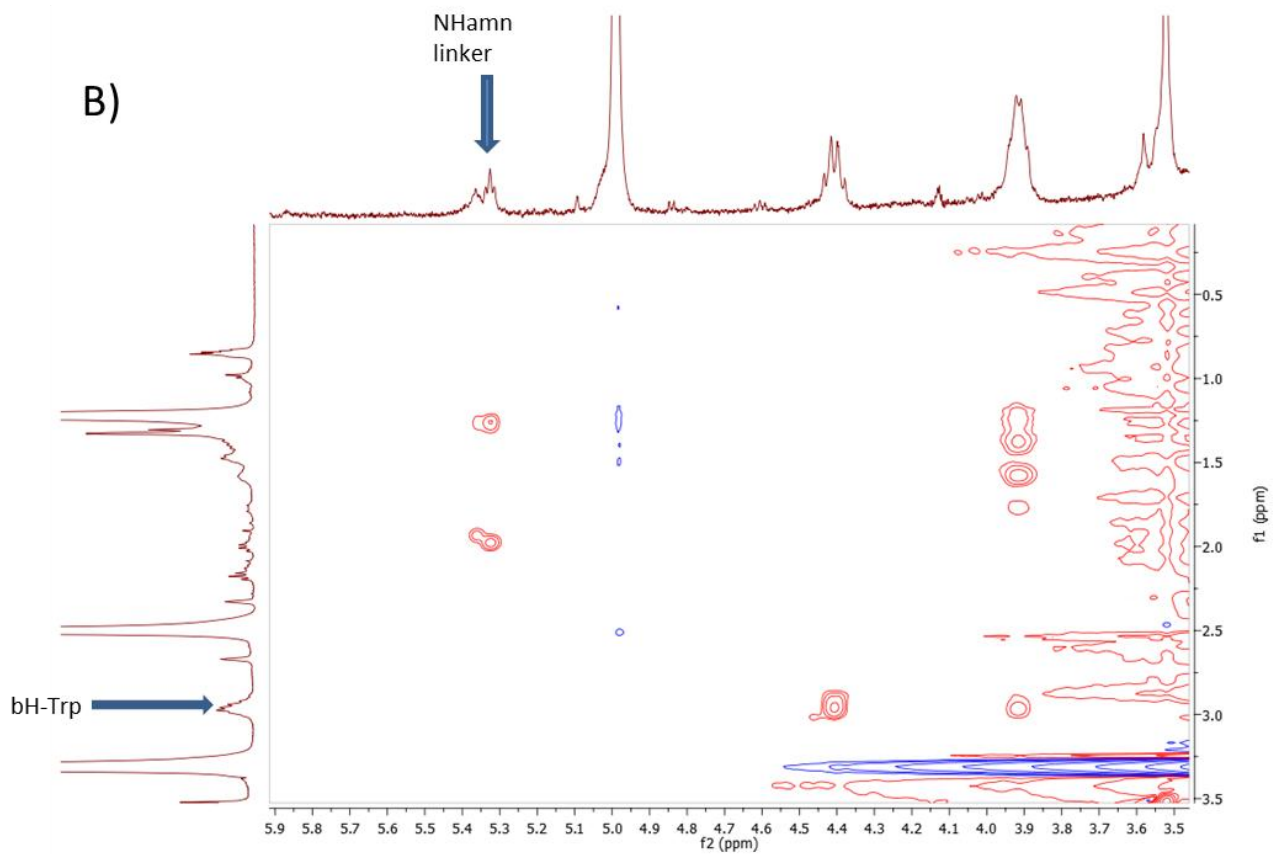
The second application of the <sup>1</sup>H-NMR spectroscopy concerns the qualitative analysis of the products obtained from the enzymatic degradation of some peptide-cotton samples, specifically Oct-Trp-Arg-*linker*-cotton and Pal-His-Ala-D-Ala-His-*linker*-cotton. The products were identified by mass spectroscopy and isolated by HPLC purification.

In the following figures the results of the analysis of the compound resulting from the enzymatic degradation of Oct-Trp-Arg-*linker*-cotton are presented. In the mass spectrum we could identify a peak having the mass of the product corresponding to a complete break-down of the cellulosic matrix: the mass obtained at 766.84 (non riesco a leggere il valore), in fact, corresponds to Octanoyl-Trp-Arg-NH-CH<sub>2</sub>CH<sub>2</sub>-NH-CH<sub>2</sub>CH(OH)CH<sub>2</sub>-Glucose. This compound was isolated in HPLC and NMR spectra collected in DMSO.



In Figure 88 regions of TOCSY and COSY spectra are reported. Signals confirm the presence of the peptide that before was anchored to the cotton and now is presumably linked to only one unit of glucose. All signals for residues Arg and Trp (table 18) and the signals relative to the fatty acid chain were identified. Signals probably attributable to glucose were also found. They were identified at about 3.9 ppm (Figure 88), but this assignment further verification.





**Figure 88.** 2D NMR of a compound referable to Octanoyl-Trp-Arg-NH-CH<sub>2</sub>CH<sub>2</sub>-NH-CH<sub>2</sub>CH(OH)CH<sub>2</sub>-Glucose. (A) Region of the TOCSY and COSY spectra overlapped, COSY is in cyan, TOCSY in red. (B) Region of the TOCSY spectrum where the linker can be identified.

From the information obtained, we can claim to be close to the focus of this analysis, that is, obtaining by enzymatic degradation, the lipopeptide linked through the linker to a single glucose unit.

**Table 18.**  $^1\text{H-NMR}$  signal assegnation of sample Octanoyl-Trp-Arg-NH- $\text{CH}_2\text{CH}_2\text{-NH-CH}_2\text{CH(OH)CH}_2\text{-Glucose}$ .

Octanoyl-Trp-Arg-NH- $\text{CH}_2\text{CH}_2\text{-NH-CH}_2\text{CH(OH)CH}_2\text{-Glucose}$

Residue	NH	$\alpha\text{H}$	$\beta\text{H}$	$\gamma\text{H}$	Other H
Oct					$\text{H}_3\text{C}$ 0.85 - $\text{CH}_2\text{-CO-}$ 2.15 Altri $\text{CH}_2$ 1.47
Trp	7.56	4.42	2.95		$\text{H}_{\text{aromatic}}$ 7.20 $\text{NH}_{\text{aromatic}}$ 6.87
Arg	7.47	3.94	1.55	1.79	$\epsilon\text{NH}$ 8.29 = $\text{NH}$ 7.64 - $\text{NH}_2$
Linker	8.15				$\text{NCH}_2\text{CH}_2\text{NH-}$ 5.32 $\text{CH}_2\text{CH}_2\text{NH-}$ 1.98



### 2.3 Biological Activity

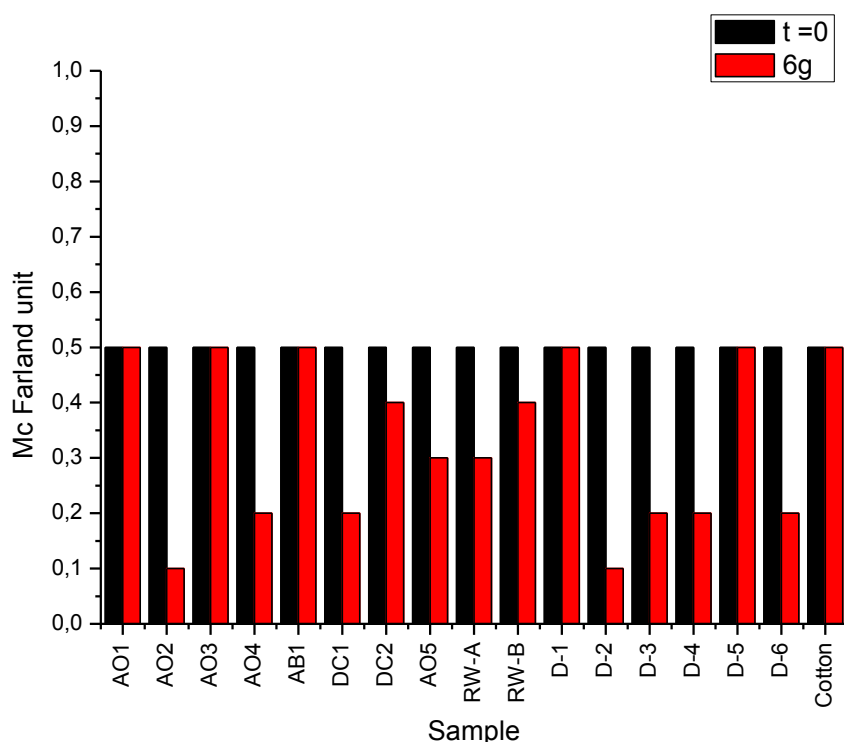
Textile samples were tested in order to determine their antimicrobial activity against Gram positive and Gram negative bacteria. Tests were performed at the University "Lucian Blaga" of Sibiu (RO) under the supervision of Dr. Simona Oancea and Dr. Getta Hilma. In Gram positive bacteria *Staphylococcus aureus* ATCC 25923 was used while for the Gram negative *Escherichia coli* ATCC 25922 was used.



**Figure 89.** Instrumentation used for the biological test.

Tests are based on a turbidimetric approach that allows the measurement of the cell concentration in solution. The data obtained are reported in the histogram shown below, the results of cell concentrations are expressed in McFarland units, where 0.5 McFarland units correspond to a concentration of  $1.5 * 10^8$  ColonyFormationUnit / ml (CFU / ml).

Both for the test performed against Gram positive and Gram negative bacteria, we consider active samples that after six days of incubation show a bacterial concentration equal or lower than 0.2 McFarland units.



**Figure 90.** Antimicrobial activity of the samples of peptide/dendrimer bound to cotton against *Staphylococcus aureus* ATCC 25923.

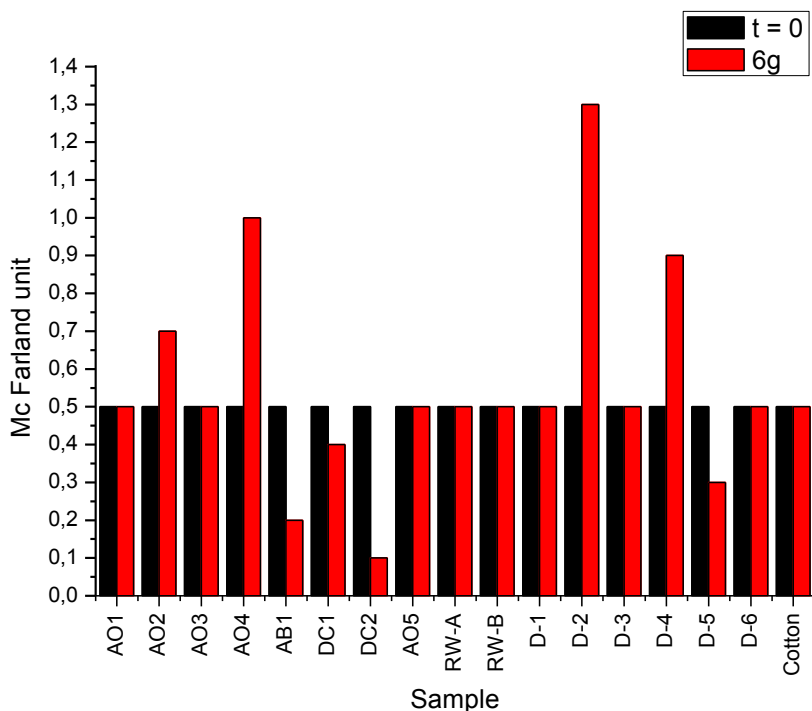
Our samples present a good activity against *S. aureus* (Gram positive bacteria). In particular, sample **AO-2** shows the best bioactivity confirming that the substitution of Lys residues with His is useful for our end-use. This result is confirmed by the results obtained for sample **D-2**, which also contains histidine.

Comparison between the results obtained for samples **AO-3** and **AO-4** against *S. aureus* indicates how the presence of the nitro (NO<sub>2</sub>) protecting group at the Arg lateral chain enhances the antibacterial activity if compared to peptides containing unprotected Arg.

This relation between antibacterial activity and presence of a nitro group is not maintained for the dendritic samples **D-3** and **D-4**, in fact in this case the presence/absence of nitro protecting group at the guanidinium moiety do not modify their activity.

Another good result was obtained for sample **D-6**, characterized by the presence of the pattern Arg/Trp. This peptide show a promising activity against *S. aureus* bacterial strands

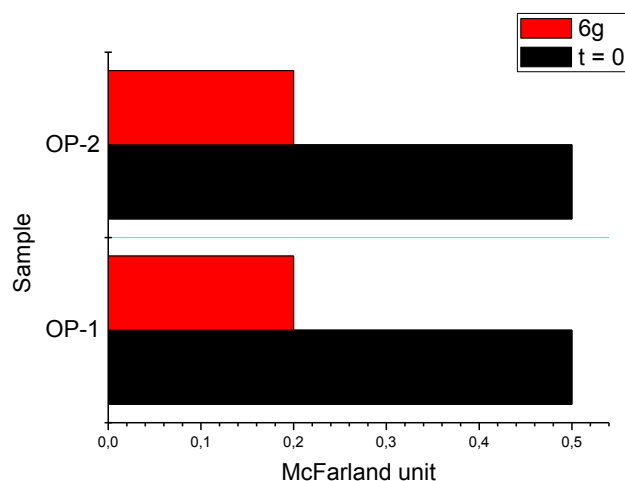
Among the samples functionalized with peptaibols, only sample **DC-1** show a good activity against *S. aureus*, while its positive charged analogue, sample **DC-2**, is inactive in opposition of what was expected.



**Figure 91.** Antimicrobial activity of the samples of peptide/dendrimer bound to cotton against *Escherichia coli* ATCC 25922

The results obtained for Gram negative *E. coli*, reported in figure x, show that only sample **AB-1** and **DC-2** are active against this bacterial strain.

Anyway, the most widespread infections in hospital environment are caused by Gram positive bacteria and our work is focused to the preparation of antimicrobial textiles for medical end-use. So the bioactivity found against *S. aureus* is itself an important result, independently form the results obtained on Gram negative bacterial strands. Biological activity were also tested for the samples prepared using method **M-2** and the result are reported in figure 92.



**Figure 92.** Antimicrobial activity of the samples prepared using **M-2** method against *Staphylococcus aureus* ATCC 25923.

It is clear that the biological activity against *S. aureus* of the cotton sample bearing Peptaibolins not related to the anchoring direction, in fact both samples **OP-1** and **OP-2** show the same antibacterial activity. These two samples are made with the same peptide once linked through its C-terminus and once through its N-terminus. . Probably the conformation adopted by Peptaibolin (discussed in *NMR Section*) is quite stable in both the Peptaibolin-cotton samples and plays a role in the final antibacterial activity, independently from the orientation of the peptide on the cotton surface.

The biological activity of samples **DC-1** and **OP-1** against *S. aureus* , samples containing the same Peptaibolin sequence build with different methods (**M1** and **M2**, respectively) turned out to be the same. Apparently, the possible incomplete sequences formed synthesizing sample **DC-1**, (with a methodology that does not exclude the formation of ester bonds on cellulose hydroxyl groups or the growth of chains on the secondary amine moiety of the *linker*) do not interfere with the antimicrobial activity. Both the samples show an encouraging good activity.

Antibacterial activity were measured four times for all samples giving the same results. Before every test fabric samples were sterilized using autoclave at 121°C for 15 minutes.

## **2.4 Conclusions**

Several samples of cotton fabric functionalized with immobilized peptides were obtained using two different methods of preparation.

We were able to build peptides *step-by-step* on cotton fibers using **M-1** approach, while we applied the **M-2** synthetic method to anchor the desired compounds directly on cotton (*one-pot*). The main difference between these two synthetic ways stays in the possibility to have or not unwanted/uncomplete peptide sequences linked to the fabrics.

In **M-1** preparation method, in fact, an activated amino acid was added, in each coupling step, to the cellulosic support rich in hydroxy groups; the parallel reaction of activated amino acids with secondary amines of the diamino *linker* and with hydroxyl groups of cellulose is also observed. The esters and tertiary amides thus formed have been detected by FT-IR spectroscopy. From a comparison of the loading values obtained in peptide-cotton samples were the undesirable nucleophile sites were blocked by acetylation, we could confirm that side reactions do occur and need to be avoided (i.e., by acetylation). Through the application of the **M-2** approach, which consist in *one pot* direct reaction between the brominated fiber and the peptide (opportunistically modified with an amino moiety at the C-terminus), we can avoid the formation of undesirable chains and esters.

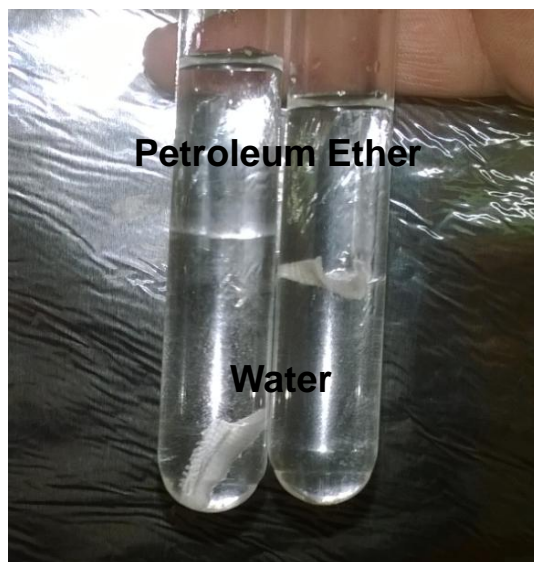
In any case, antimicrobial tests performed on *S. aureus* strains for a sample prepared using both **M-1** and **M-2** approaches (peptaibolins **DC-1** and **OP-1**), showed that undesirable side-products (truncated peptides and esters) do not affect the bactericidal properties of the final material.

The characterization techniques applied to our samples confirm the presence of peptide sequences anchored onto the cotton fabric surface. In particular, the FT-IR spectra and XPS analyses allowed to identify the characteristic signals of amide bonds. Moreover, an accurate study of the binding energies of nitrogen atoms performed by XPS let us to distinguish different kinds of nitrogen atoms, revealing the presence of residues with characteristic side chains, such as His, Arg and Lys.

Enzymatic degradation was another important experiment performed during this work. This assay allowed to decrease the degree of polymerization of cellulose giving soluble compounds that could be characterized applying the analyses typical of the liquid phase, such as  $^1\text{H-NMR}$  spectroscopy.

Immobilization of peptides onto the textile surface induced modifications to the macroscopic properties of the fabrics. TGA analysis reveals an increase in the pyrolysis temperature, compared to the results obtained for the simple cotton. The amount of this alteration seems related to the kind of residues located in the immobilized peptides.

For some samples, particularly for fabrics bearing dendrimers, the presence of the functionalization promotes the develop of super hydrophobic properties.



**Figure 93.** *Demonstration of the superhydrophobic property develop by some fabric sample after functionalization*

This point is not described in detail in this thesis because it is part of a patent on which we are working.

Anyway, we reached our focus as some of our samples look very promising displaying an encouraging antimicrobial activity against *S. aureus*. They are a good materials that can be used for the production of medical devices, health care workers uniforms and in generally to produce safe aseptic fabrics.

An activity against Gram negative *E. coli* was also detected for some samples (peptaibol-containing cotton samples **DC-2** and **AB-1**) indicating that the work done

up to now is anyway a good base to start a more deep develop of the peptide-based antimicrobial textile research field.

It is, also important to stress, the resistance shown by samples to autoclave sterilization. This is a very promising property of durability, one of the most important characteristics required for an antimicrobial fabrics which act *by contact*.





## Reference

1. M. Lebl, et al., *J. Comb. Chem.* **1** (1999) 474
2. L.A. Carpino, *Acc. Chem. Res.* **20** (1997) 401.
3. R. Bollhagen, M. Schmiedberger, K. Barlos, E. Grell, *Chem. Comm.* **22**, (1994), 2559.
4. P. Rovero, S. Vigano`, S. Pegoraro, L. Quartara, *Lett. Pept.Sci.* **2** (1995) 319.
5. N. Bayo´ -Puxan, A. Ferna´ndez, J. Tulla-Puche, E. Riego, C.Cuevas, M. A´lvarez, F. Albericio, *Chem. Eur. J.* **12** (2006) 9001.
6. P. Alenka, *Can. J. Chem.* **60** (1982) 976.
7. T. Curtius, *J. Prakt. Chemie* **26** (1882) 145.
8. E. Fischer, *Ber. Dtsch. Chem. Ges.* **38** (1905) 605.
9. E. Atherton, C. J. Logan and R. C. Sheppard *J. Chem. Soc., Perkin Trans.* **1** (1981)538-546
10. a) F. Albericio, *Curr. Opin. Chem. Biol.* **8** (2004) 211. b) J. Wang, Y-L. Liang, J.Qu *Chem Commun* (2009) 5144-5146.
11. C. A. G. N. Montalbetti, V. Falque, *Tetrahedron* **61** (2005) 10827.
12. L. A. Carpino, A. El-Faham, F. Albericio, *J. Org. Chem.* **60** (1995) 3561.
13. W. Konig, R. Geiger, *Chem. Ber.* **103** (1970) 788.
14. G. Jou, I. Gonzlez, F. Albericio, P. Lloyd-Williams, E. Giralt, *J. Org. Chem.* **62** (1997) 354.
15. C. Toniolo, M. Crisma, F. Formaggio, *Biopolymers* **40** (1996) 627.
16. M. Crisma, G. Valle, V. Moretto, F. Formaggi, C. Toniolo, F. Albericio, *Lett. Pept. Sci.* **5** (1998) 247.
17. L. A. Carpino, *J. Am. Chem. Soc.* **115** (1993) 4397.

18. E. Fischer, E. Fourneau, *Rer. Dtsch. Chem. Ges.* **34** (1901) 2668.
19. T. I. Al-Warhi, H. M. A. Al-Hazimi, A. El-Faham, *J. Saudi Chem. Soc.* **16** (2012) 97.
20. P. Lloyd-Williams, F. Albericio, E. Giralt. *Chemical Approaches to the Synthesis of Peptides and Proteins* (1997) 97.
21. R. Rebek, D. J. Feitler, *Am. Chem. Soc.* **96** (1974) 1606.
22. N.L. Benoiton, F. M. F. Chen, *J. Chem.* **59** (1981) 384.
23. W. KOonig, R. Geiger, *Chem. Ber.* **103** (1970) 788.
24. S.Y. Hong, T.G. Park, K.H. Lee. *Peptides.* **22**, (2001),1669-1674.
25. X. Zhao, F. Pan, H. Xu, M. Yaseen, S. Zhang, J.R. Shan *Chem. Soc. Rev.*, **39** (2010), 3480–3498
26. A. Makovitzky. J. Baran, Y. Shai. *Biochemistry* **47** (2008) 10630–10636.
27. A. V. Eberhard, A. Makovitzki, A. Beauvais, J.P. Latge´, S. Jung, and Y. Shai . *ANTIMICROB. AGENTS CHEMOTHER.* **52** (2008) 9 3118-3126.
28. M.E. Selsted, A.J. Ouellette, *Nat. Immunol.* **6** (2005) 551.
29. K. Gholivand, N. Dorosti. *Chemical Papers* **2012**,66 (8), 765–771.
30. Toniolo C., Benedetti E. *Trends Biochem. Sci.* **16** (1991) 350-353.
31. A.W. Young, Z. Liu, C. Zhou, F. Totsingan, N. Jiwrajka, Z. Shi. *Med. Chem. Commun.* **2011**, 2, 308.
32. M. Bagheri, M. Beyermann, M. Dathe. *Antimicrob. Agents Chemother* **2009**, 53, 1132-1141.
33. D. E. Discher, R. D. Kamien, *Nature* , **430** (2004) 519-520
34. C. Hyde, T. Thomson, *In Peptides 1971*, Nesvabda H (ed.). North Holland: Amsterdam, (1973) 111.
35. M.Gabriel, K. Nazmi, E.C. Veerman, A.V. Nieuw Amerongen. *Bioconj Chem.* **17** (2006) 548-550.

36. V. Humblot, J.F. Yala, K.Boukerma, A. Hequet, J.M. Berjeaud. **30** (2009) 3503-3512.
37. R. Lowell Fey, M. Workman, H. Marcellos and M.J. Burke. *Plant Physiol.* **63** (1979) 1220-1222.
38. Fajer PG. *Encyclopedia of Analytical Chemistry*, John Wiley & Sons, Ltd, (2006) 5725–5761.
39. Frantz S, Hübner GA, Wendland O, Roduner E, Mariani C, Ottaviani MF. Batchelor SN. *J. Phys. Chem.* **109** (2005) 11572–11579.
40. J. S. Stevens, A. C. de Luca, M. Pelendritis, G. Terenghi, S. L. M. Schroeder, *Surf. Interface Anal.* **45** (2013) 1238-1246.
41. N. Abidi, L.Cabrales, E. Hequet. *Thermochimica Acta* **498** (2010) 27–32.
42. C.L. Liu, F. Basile, *J. Anal.Appl.Pyrol.* **92** (2011) 217-223.
43. L. Cabrales, N Abidi. *J Therm Anal Calorim* **102** (2010) 485–491
44. cellulasi
45. Wood, J.D., Wood, P.M., *Biochim. Biophys. Acta* **1119**(1) (1992) 90–96.
46. Bower, B., Clarkson, K., Collier, K., Kellis, J., Kelly, M. and Larenas, E. **1998**. WO 98/15619, PCT/US97/18402.
47. M. Saloheimo, M. Palheimo, S. Hakola, J. Pere, B. Swanson, E. Nyysönen, A. Bhatia, M.Ward, M. Penttila, *Euro. J. of Biochemistry*, **269** (17) ( 2002) 4202-4211.

### **3. Experimental Part**

#### **Reagents and solvents**

**Acros Organics (New Jersey, USA):** H-L-Leu-OH, H-L-Val-OH, H-Arg(NO<sub>2</sub>)-OH.

**Applied Biosystems:** Kaiser test solution (A-phenol in ethanol solution 76% w/w, B-KCN 0.0002 M in pyridine, C-ninhydrin in ethanol 0.28 M).

**Baker (Mumbai, India):** NaHCO<sub>3</sub>.

**Carbosynth (Compton-Berkshire, UK):** HATU.

**Carlo Erba (Milano, Italia):** HClO<sub>4</sub>, triethylamine (TEA).

**Euriso-top (Saint Aubin, Francia):** CDCl<sub>3</sub>, DMSO d<sub>6</sub>.

**Fluka (Buchs, Svizzera):** Ethylendiamine.

**GL Biochem (Shangai, Cina):** Fmoc-Aib-OH, HOAt.

**Iris Biotech (Marktredwitz, Germania):** Fmoc-L-Lys(Boc)-OH, Fmoc-OSu.

**Merck (Darmstadt, Germania):** CaCl<sub>2</sub>, Na<sub>2</sub>SO<sub>4</sub>.

**Serva (Heidelberg, Germania):** L-Ala-OH, L-Lys ·HCl, L-Hyp-OH.

**Sigma-Aldrich (St. Louis, USA):** Ethyl Acetate, Acetone, Acetonitrile, HCl 37% v/v, Palmitic acid, 9 fluorenic acid, chloroform, Dichloromethane, Diethylether, 1,4-dioxane, di-tert-butyl dicarbonate, Epibromohydrine, Fmoc-L-Gln-OH, Methanol, N,N-dimethylformamide, Piperidine, Fmoc-His(Trt)-OH, Fmoc-Lys(Boc), Fmoc-Ala-OH, Fmoc-Trp(Boc)-OH, Fmoc-Arg(Pbf)-OH, DIPEA.

**VWR (Radnor, USA):** NaCl, Petroleum Ether, NaOH, KHSO<sub>4</sub>.

Textile used is a mercerized cotton without bleaching.

## **Instrumentation and methods**

### FT-IR spectroscopy

The FT-IR absorption spectra of cotton samples were recorded by tearing some fibers from the samples and incorporating them in a KBr pellet. The measurements were performed with a spectrophotometer Perkin-Elmer model 1720X operating in the Fourier transform. The room which houses the sample is maintained under constant flow of nitrogen in order to minimize the contributions due to water vapor. The data obtained by the instrument were analyzed using the software Origin 8.

### UV-Vis spectroscopy

UV measurements were performed by means of a Shimadzu UV-2501PC spectrometer using quartz reduced optical path cell.

### <sup>1</sup>H-NMR spectroscopy

Bruker AV-200 (200 MHz) and Bruker AV-400 (400 MHz) instruments have been used. Solvents (chloroform or DMSO) were deuterated.

Multiplicities of signals are pointed out as: s - singlet, d - doublet, t - triplet, q - quartet, m - multiplet. Chemical shifts ( $\delta$ ) are expressed in ppm.

Residual peaks of solvents have been used as reference for setting of chemical shifts.

### Mass spectroscopy

To record the mass spectra a mass spectrometer was used, TOF (Time of Flight) and as ESI ionization technique was used, positive ions formed were accelerated to 10, 15, 20 or 30 keV and analyzed linearly. The ESI generates the spray from an aqueous medium acidified with formic acid to improve the ionization of the molecules; that environment corresponds to that needed to remove the Boc protecting group, therefore molecules without their Boc group are detected.

### X-ray Photoelectron Spectroscopy (XPS)

In order to characterize the composition of the surface of cotton XPS investigations were performed, carried out by the group of Surface Science, Prof. Gaetano Granozzi of the Department of Chemical Sciences. A Perkin-Elmer instrument 5600 using  $\Phi$  radiation K<sub>3</sub> of a aluminum electrode operating at 350 W 38 (1486.6 eV) was used. The working pressure is less than  $5 \cdot 10^{-8}$  Pa. Calibration was performed on the basis of the binding energy of the line 4f<sub>7/2</sub>, located at 83.9 eV with respect to the Fermi level. The standard deviation for the binding energy is 0.15 eV. The survey was obtained from scans from 0 eV to 1350 eV (187.5 eV pass energy, 1.0 eV / step, 25 ms / step). Were scanned carefully (29.35 eV pass energy, 0.1 eV / step, 50-150 ms / step) peaks O 1s, C

1s and N 1s. The atomic composition after Shirley background subtraction was performed on the basis of the sensitivity factors supplied by Perkin-Elmer. Charge effects were offset in part using a floodgun as neutralizer. The investigations were carried out on a scrap of fabric size 5x5 mm, pasting the same crop in the sample holder with a special adhesive tape. Before the measurement the samples were left 12 hours in vacuum in order to clean them from any species adsorbed pollutants.

### HPLC analysis

The HPLC measurements were performed using an Agilent 1200 series apparatus, equipped with a UV detector at variable wavelengths.

*HPLC conditions:* wavelengths 254 nm and 214 nm.

*Eluents:* **A:** 90% H<sub>2</sub>O, 10% MeCN + 0,05% TFA; **B:** 10% H<sub>2</sub>O, 90% MeCN + 0,05% TFA.

*Column:* Agilent C18 (stationary phase)

### Circular Dichroism (CD)

CD measurements have been accomplished at room temperature on a J-715 Jasco spectropolarimeter. Quartz cell (0,1 cm pathway length - HELLMA) or cylindrical quartz cell (0.2 cm or 0,01 cm pathway length - HELLMA) were used.

Values are reported in total molar ellipticity (deg x cm<sup>2</sup> x dmol<sup>-1</sup>):

$$[\Theta] = \frac{(100 \times \theta)}{(l \times c)} = 3300 \times \Delta\epsilon = 3300 \times (\epsilon_L - \epsilon_R)$$

Θ = observed ellipticity

MW = molecular weight

l = pathway length (cm)

C = concentration (M)

Δε = ε<sub>L</sub> - ε<sub>R</sub> = difference between left- and right-handed component of extinction coefficients of polarized light

### Permeation of artificial membrane

The measures of the permeability of artificial lipid membranes have been performed following the release of carboxyfluorescein (CF) from unilamellar vesicles (SUV), phosphatidylcholine (PC) / cholesterol (Ch) 7: 3. The total lipid concentration (0.06 mM) was kept constant for all experiments, which were performed in polystyrene cuvettes (1 × 1 cm) containing 2.5 ml of the lipid suspension. The CF released was determined by fluorescence measurements by repeating the experiment at different ratios:

$$R^{-1} = [peptide] / [lipid]$$

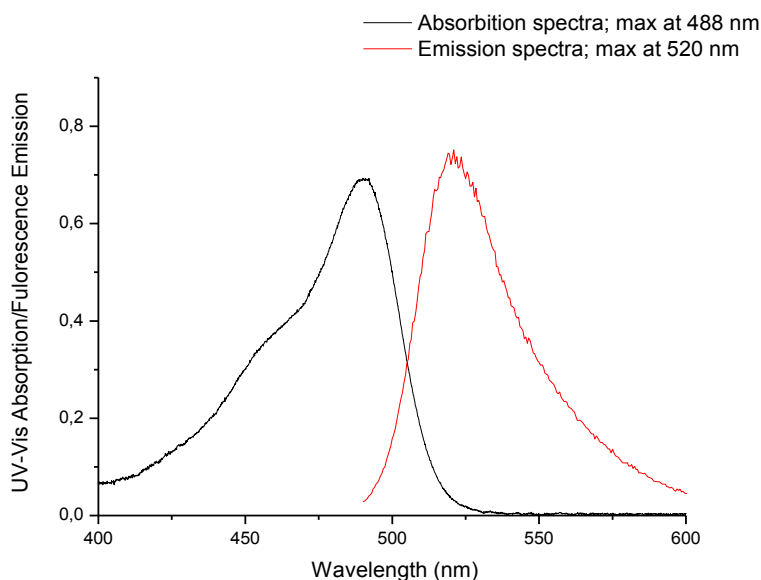
which were obtained by adding aliquots of a methanolic solution of the peptide.

The fluorescence measurements were performed with a Perkin-Elmer LS50B spectrofluorimeter at room temperature, by setting  $\lambda_{exc} = 488 \text{ nm}$  and  $\lambda_{em} = 520 \text{ nm}$ . The percentage of CF released after 20 minutes after addition was determined as:

$$\%CF = \frac{F_t - F_0}{F_T - F_0} \times 100$$

where:

- $F_0$  = fluorescence intensity of the vesicles in the absence of the peptide;
- $F_t$  = fluorescence intensity at time t (20 minutes) in the presence of the peptide;
- $F_T$  = total intensity of fluorescence determined destroying the vesicles by addition of  $50 \mu\text{l}$  of a solution of Triton X-100 at 10% in water.



**Figure 93.** Adsorption and Emission spectra of carboxyfluorescein

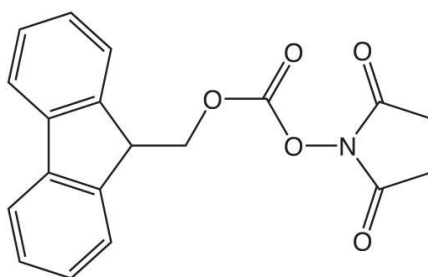
Fluorescence spectra were recorded on a Perkin-Elmer MPF-66 spectrofluorimeter or on a Fluoroskan Ascent FL (Thermo Labsystem).

### Antibacterial test

Textile samples with anchored peptides were tested in order to determine their antimicrobial activity against Gram positive and Gram negative bacteria. The tests were performed at the University "Lucian Blaga" of Sibiu (RO) under the supervision of Dr. Simona Oancea and Dr. Getta Hilma. In particular for Gram positive *Staphylococcus aureus* ATCC 25923 was used while for Gram negative *Escherichia coli* ATCC 25922 was used.

## Protection of amino moiety with Fmoc

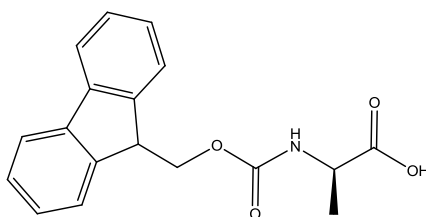
HCO<sub>3</sub><sup>-</sup> and H-AA-OH in equimolar ratio were dissolved in 100 ml of water under stirring. The mixture was cooled down to 0°C and then an equimolar ratio of Fmoc-OSu (respect to the number of free amino moieties present in the molecule) previously dissolved in 100ml of 1,4-dioxane was added. The pH of the solution was maintained between 8 and 9 by addition of a 1M NaOH solution.



The mixture temperature was raised up to r.t. and the reaction followed by TLC. After 24 hours 1,4-dioxane was removed under vacuum and the aqueous solution diluted with 100 ml of water. The solution was washed with 20 ml of Et<sub>2</sub>O, acidified slowly with solid citric acid and extracted with EtOAc (3x100 ml). The organic layers were combined and washed with water (6 x 50 ml) and brine. The organic layer was dried on Na<sub>2</sub>SO<sub>4</sub> and the solvent removed under vacuum. The product was precipitated from EtOAc/EP and characterized by Mass and <sup>1</sup>H-NMR spectroscopy .

## Amino acid protection

### Fmoc-D-Ala-OH



	H-D-Ala-OH	Fmoc-OSu
mmol	20.10	20.00

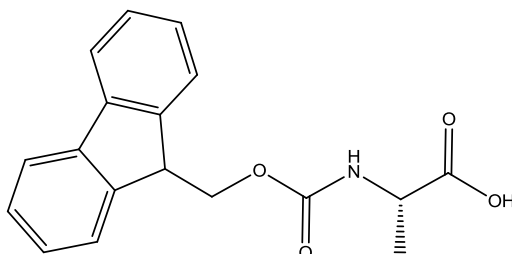
**Yield % = 94%**

**Mass spectrometry (m/z): 312.35 [M+H]<sup>+</sup>**



**<sup>1</sup>H NMR (200 MHz, DMSO):** δ 7.69 (d, 2H, Fmoc), 7.53 (d, 2H, Fmoc), 7.32 (m, 4H, Fmoc), 5.24 (broad, 1H, NH), 4.35 (m, 3H, Cα+CH<sub>2</sub>), 4.14 (t, 1H, Fmoc), 1.43 (d, 3H, Ala α-CH<sub>3</sub>).

### Fmoc-L-Ala-OH



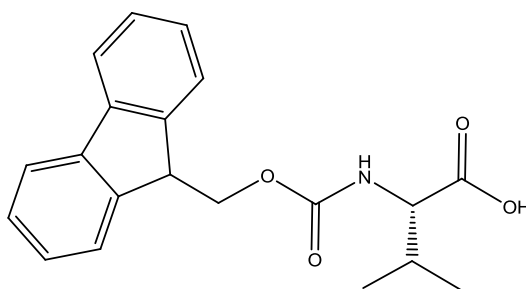
	H-Ala-OH	Fmoc-OSu
mmol	19.9	19.9

**Yield % = 92%**

**Mass spectrometry: m/z:** 312.32 [M+H]<sup>+</sup>

**<sup>1</sup>H NMR (200 MHz, DMSO):** δ 7.69 (d, 2H, Fmoc), 7.53 (d, 2H, Fmoc), 7.29 (m, 4H, Fmoc), 5.26 (broad, 1H, NH), 4.35 (m, 3H, Cα+CH<sub>2</sub>), 4.16 (t, 1H, Fmoc), 1.41 (d, 3H, Ala α-CH<sub>3</sub>).

### Fmoc-Val-OH



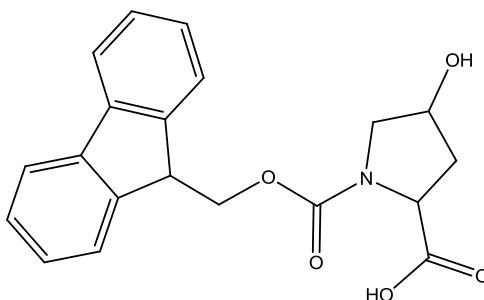
	H-Val-OH	Fmoc-OSu
mmol	19.9	19.9

**Yield % = 75%**

**Mass spectrometry: m/z:** 340.36 [M+H]<sup>+</sup>

<sup>1</sup>H NMR (200 MHz, CDCl<sub>3</sub>): δ 7.78 (d, 2H, Fmoc), 7.61 (d, 2H, Fmoc), 7.42 (t, 2H, Fmoc), 7.33 (t, 2H, Fmoc), 5.25 (d, 1H, NH), , 4.45 (d, 2H, CH<sub>2</sub>), 4.38 (m, 1H, C $\alpha$ ), 4.26 (t, 1H, CH Fmoc), 2.26 (m, 1H, Val  $\alpha$ -CH), 1.04 (d, 6H, Val  $\alpha$ -CH<sub>3</sub>).

### Fmoc-Hyp-OH



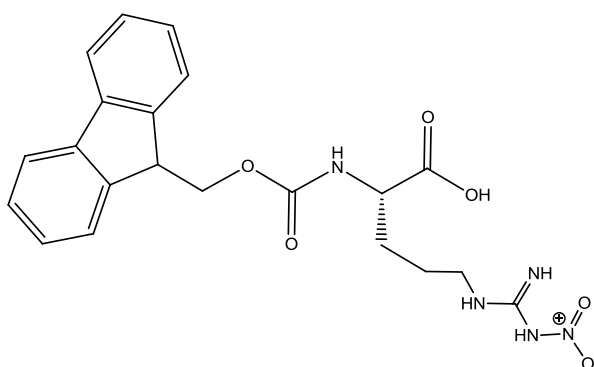
	H-Hyp-OH	Fmoc-OSu
mmol	12.50	12.00

Yield % = 80%

Mass spectrometry: m/z:

<sup>1</sup>H NMR (200 MHz, DMSO): δ 7.82 (d, 2H, Fmoc), 7.58 (d, 2H, Fmoc), 7.31 (m, 4H, Fmoc), 5.09 (t, 1H,  $\alpha$ -C), 2.07 (m, 1H,  $\beta$ -CH<sub>2</sub>-a), 4.31 (t, 1H, -CH- Fmoc), 4.18 (m, 2H, -CH<sub>2</sub>- Fmoc), 4.08 (t, 1H,  $\beta$ -CH-), 3.35 (m, 2H,  $\phi$ -CH<sub>2</sub>-), 2.75 (m, 1H,  $\beta$ -CH<sub>2</sub>-b),.

### Fmoc-Arg(NO<sub>2</sub>)-OH



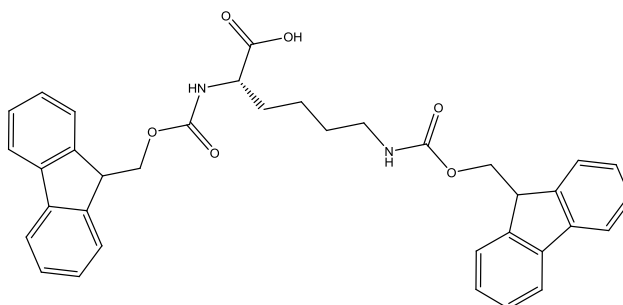
	H-Arg(NO <sub>2</sub> )-OH	Fmoc-OSu
mmol	20.02	20.00

Yield % = 67%

Mass spectrometry: m/z: 221.96 [M+2H]<sup>2+</sup>; 442.44 [M+H]<sup>+</sup>

**<sup>1</sup>H NMR (200 MHz, DMSO):**  $\delta$  7.78 (d, 2H, Fmoc), 7.61 (d, 2H, Fmoc), 7.42 (t, 2H, Fmoc), 7.33 (t, 2H, Fmoc), 5.25 (d, 1H, NH), 4.70 (d, 2H, -CH<sub>2</sub>- Fmoc), 4.55 (t, 1H, C $\alpha$ ), 4.46 (t, 1H, CH Fmoc), 1.78 (m, 1H, Arg  $\beta$ -CH), 1.55 (m, 2H, Arg  $\gamma$ -CH<sub>2</sub>-).

### Fmoc-Lys(Fmoc)-OH



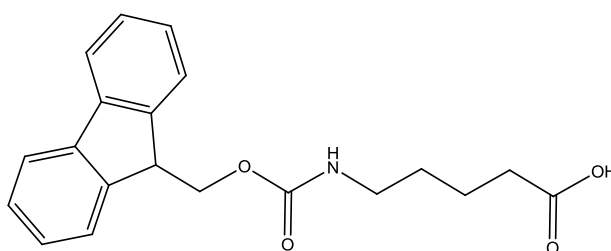
	H-Lys-OH	Fmoc-OSu
mmol	15.6	30.0

Yield % = 63%

Mass spectrometry: m/z: 591.68 [M+H]<sup>+</sup>

**<sup>1</sup>H NMR (200 MHz, DMSO):**  $\delta$  7.73 (d, 4H, Fmoc), 7.58 (d, 4H, Fmoc), 7.45 (t, 4H, Fmoc), 7.33 (t, 4H, Fmoc), 5.36 (d, 1H, NH), 4.36 (t, 2H, CH Fmoc), 3.56 (m, 1H, C $\alpha$ ), 2.75 (t, 2H, Lys  $\epsilon$ -CH<sub>2</sub>-), 1.78 (m, 2H, Lys  $\beta$ -CH<sub>2</sub>-), 1.55 (m, 2H, Lys  $\phi$ -CH<sub>2</sub>-), 1.24 (m, 2H, Lys  $\gamma$ -CH<sub>2</sub>-).

### Fmoc-5-N-valeric acid



	5-N-amino valeric acid	Fmoc-OSu
mmol	10.2	10.2

Yield % = 76%

Mass spectrometry: m/z: 340.15 [M+H]<sup>+</sup>

**<sup>1</sup>H NMR (200 MHz, DMSO):**  $\delta$  7.78 (d, 2H, Fmoc), 7.61 (d, 2H, Fmoc), 7.42 (t, 2H, Fmoc), 7.33 (t, 2H, Fmoc), 5.25 (d, 1H, NH), 4.45 (d, 2H, CH<sub>2</sub>), 4.38 (m, 1H, C $\alpha$ ), 4.26 (t, 1H, CH Fmoc), 3.18 (m, 2H,  $\epsilon$ -CH<sub>2</sub>-), 2.31 (t, 2H,  $\alpha$ -CH-), 1.52 (m, 4H,  $\beta$  and  $\phi$ -CH<sub>2</sub>-).

## Experimental SPPS

Peptides were synthesized step by step by manual solid phase method. 2-Chlorotrityl chloride resin was used. The loading of the resin is 1,6 mmol/g. Amino acids were protected with Fmoc group at the N-terminus; side chain of arginine was protected with Pbf group, whereas the protection used for the imidazole ring of histidine residues was the trityl group.

The following protocol was used:

1. Swelling of the resin with dry DMF, bubbling  $N_2$  for 20 minutes
2. Ethylenediamine in dry DMF was added to the resin in large excess; the coupling goes in 2 hours, bubbling  $N_2$
3. The surplus of reagents were removed and the resin was washed with 3x5 mL dry DMF and 2x3 mL dry DCM
4. HOAt/HATU were used as activating coupling agents; DIPEA was used as the base.



**Figure 94.** Solid phase peptide synthesis reactor

Coupling reaction: a solution of Fmoc-AA-OH (3 equivalents), HOAt (3 equivalents), HATU (3 equivalents), in dry DMF, is kept in an ice bath for 15 minutes. The solution is added to the resin-bound peptide; then DIPEA (5 equivalents) is thrown in. The reaction goes on for 2-4 hours, bubbling  $N_2$ .

5. The surplus of reagents were removed and the resin was washed with 3x5 mL dry DMF and 2x3 mL dry DCM.

6. The removal of Fmoc group was made by means of a solution of 20% piperidine in dry DMF, bubbling N<sub>2</sub> (2 series for 15 minutes).
7. The surplus of reagents were removed and the resin was washed with 3x5 mL dry DMF and 2x3 mL dry DCM.
8. The lipophilic acids were attached to the peptides, still bound to the resin, using the same conditions of amino acids coupling.
9. The cleavage from the resin was made with a solution of 10% TFA in dry DCM (two series for 10 minutes).

Every coupling was verified with the Kaiser test.

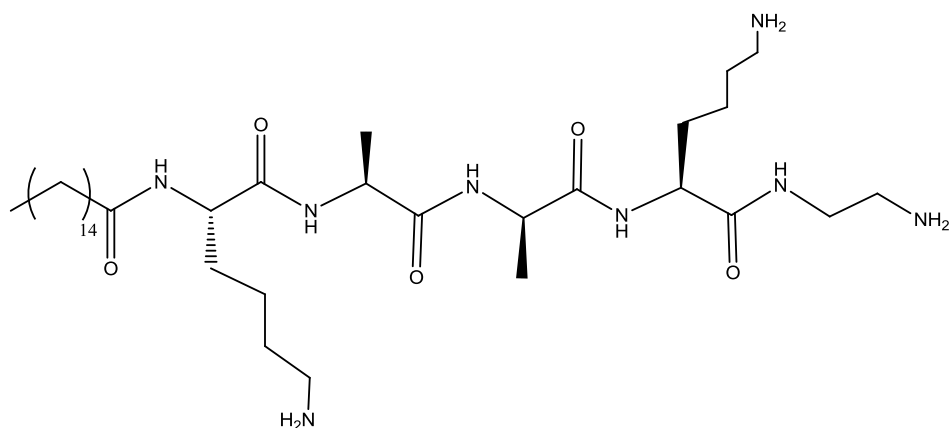
More drastic conditions are necessary to remove Pbf group. The following protocol has been used:

1. A solution of TFA/H<sub>2</sub>O (95-5 %) is prepared.
2. The reaction goes on for 2 hours, at 37°C.
3. Peptides were washed with dry MeCN, dried out, and freeze-dried, to remove TFA.
4. Sep-pak C18 *cartridges* were used in order to separate peptides from Pbf group. Mixtures of H<sub>2</sub>O/MeCN with different ratios (100:0; 70:30; 50:50; 30:70; 0:100) were used as eluent.
5. Fractions were concentrated in vacuo, freeze-dried and characterized.
6. Fractions containing products were joined.

The molecular weight was confirmed with ESI/TOF mass spectroscopy.

<sup>1</sup>H-NMR and HPLC analysis were used to verify the purity of synthesized products

**AP-1: Pal-Lys-Ala-D-Ala-Lys-NH-(CH<sub>2</sub>)<sub>2</sub>-NH<sub>2</sub>**



<b>Fmoc-Aminoacid</b>	<b>mmol</b>	<b>HOAt (mmol)</b>	<b>HATU (mmol)</b>
Fmoc-Lys(Boc)-OH	3.6	3.6	5.5
Fmoc-deprotection			
Fmoc-D-Ala-OH	3.6	3.6	5.5
Fmoc-deprotection			
Fmoc-Ala-OH	3.6	3.6	5.5
Fmoc-deprotection			
Fmoc-Lys(Boc)-OH	3.6	3.6	5.5
Fmoc-deprotection			
Palmitic acid	3.6	3.6	5.5

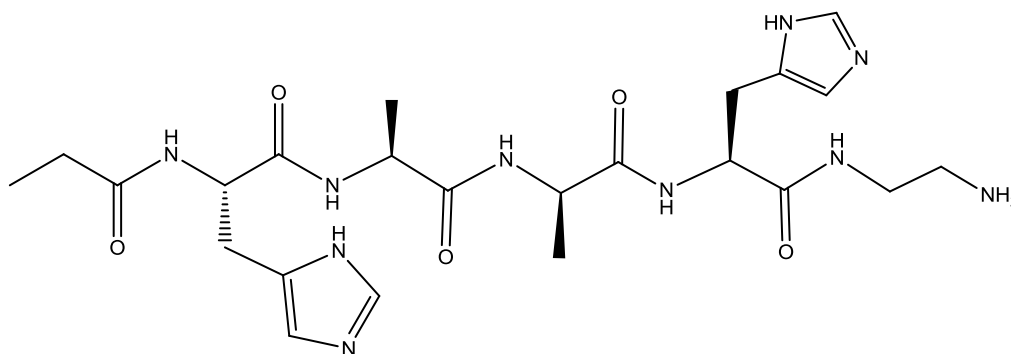
**Yield:** 63.45 %

**<sup>1</sup>H-NMR (DMSO-D<sub>6</sub>) 400 MHz: δ (ppm):** 8,00 (broad, 2,05, *NH* Ala2-3); 7,88 (broad, 1,86, *NH* Lys); 4,29 (broad, 1,74,  $\alpha$  *H* Lys1-Lys4 ); 4,19 (broad, 2,3,  $\alpha$  *H* Ala2-dAla3); 3,35 (broad, *NH-CH*<sub>2</sub>-*CH*<sub>2</sub>-*NH*<sub>2</sub>); 2,84 (broad, *NH-CH*<sub>2</sub>-*CH*<sub>2</sub>-*NH*<sub>2</sub>); 2,73 (t, 4,02,  $\epsilon$ -Lys -*CH*<sub>2</sub>-); 2,08 (broad, 1,93, *CH*<sub>2</sub> Pal); 1,78 (m, 3,86,  $\beta$ -Lys -*CH*<sub>2</sub>-); 1,36 (s, 17,21, *CH*<sub>3</sub>- Boc); 1,23 (broad, *CH*<sub>2</sub> Pal); 1,18 (broad,  $\beta$ -*H* Ala2); 1,10 (broad,  $\beta$  *H* dAla3); 0,85 (broad, 2,71, *H*<sub>3</sub>C-Pal)

**Mass spectrometry: m/z:** 349.28 [*M*+2*H*]<sup>2+</sup>; 233.19 [*M*+3*H*]<sup>3+</sup>

**HPLC (50–100, %B, 20 minutes, 1 mL/min, C18): Rt (minutes):** 14,660

**AP-2: Pal-His-Ala-D-Ala-His-NH-(CH<sub>2</sub>)<sub>2</sub>-NH<sub>2</sub>**



0.7 g of 2-chlorotrityl chloride resin (loading 1,6 mmol) were used.

H<sub>2</sub>N-(CH<sub>2</sub>)<sub>2</sub>-NH<sub>2</sub>: 2 mL of ethylenediamine were used.

Fmoc-Aminoacid	mmol	HOAt (mmol)	HATU (mmol)
Fmoc-His(Trt)-OH	3.6	3.6	5.5
Fmoc-deprotection			
Fmoc-D-Ala-OH	3.6	3.6	5.5
Fmoc-deprotection			
Fmoc-Ala-OH	3.6	3.6	5.5
Fmoc-deprotection			
Fmoc-His(Trt)-OH	3.6	3.6	5.5
Fmoc-deprotection			
Palmitic acid	3.6	3.6	5.5

**Yield:** 56,82 %

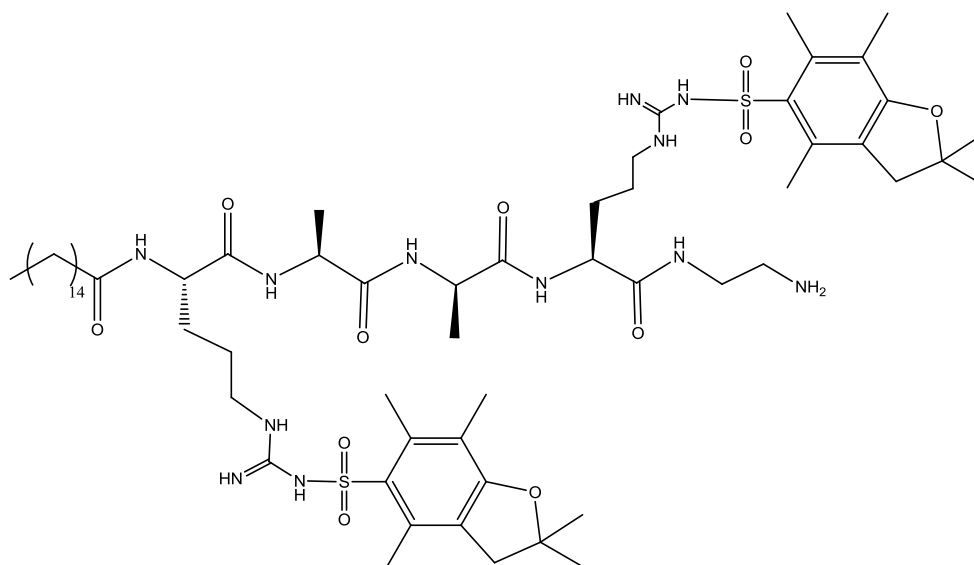
**<sup>1</sup>H-NMR (DMSO-D<sub>6</sub>) 400 MHz:** δ (ppm): 8,95 (b, 1,39, *NH* imidazole); 8,29 (broad, 1,83, *NH* dAla3-His4); 8,19 (broad, 2,30, *NH*-(CH<sub>2</sub>)<sub>2</sub>- dAla3-His1); 8,06 (broad, 1,71, *NH* Ala2); 7,88 (broad, 1,76, *CH* imidazole); 7,72 (broad, 0,55, *CH* imidazole); 7,56 (broad, 0,74, *CH* imidazole); 4,54 (broad, 1,95, α-*H* His1-His4); 4,23 (broad, 2, α-*H* Ala2-dAla3); 3,32 (broad, *NH*-CH<sub>2</sub>-CH<sub>2</sub>-NH<sub>2</sub>); 2,86 (broad, *NH*-CH<sub>2</sub>-CH<sub>2</sub>-NH<sub>2</sub>); 2,85 (broad, β-*H* His1); 2,91 (broad, β-*H* His4); 2,08 (broad, 1,41, CH<sub>2</sub> PAL); 1,25-1,40 (broad, CH<sub>2</sub> Pal); 1,18 (broad, β-*H* Ala2); 1,10 (broad, β-*H* dAla3); 0,85 (broad, 2,71, H<sub>3</sub>C-Pal)

**Mass spectrometry: m/z:** 715,50 (M+H); 358,25 (M+2H)

**HPLC (50–100, %B, 20 minutes, 1 mL/min, C18): Rt (minutes):** 16,820



**AP-3: Pal-Arg(Pbf)-Ala-D-Ala-Arg(Pbf)-NH-(CH<sub>2</sub>)<sub>2</sub>-NH<sub>2</sub>**



0.5 g of 2-chlorotrityl chloride resin (loading 1,6 mmol) was used.

About 2 mL of ethylenediamine in DMF was added.

<b>Fmoc-Amino acid</b>	<b>mmol</b>	<b>HOAt (mmol)</b>	<b>HATU (mmol)</b>
Fmoc-Arg(Pbf)-OH	2.4	2.4	5
Fmoc-deprotection			
Fmoc-D-Ala-OH	2.4	2.4	5
Fmoc-deprotection			
Fmoc-Ala-OH	2.4	2.4	5
Fmoc-deprotection			
Fmoc-Arg(Pbf)-OH	2.4	2.4	5
Fmoc-deprotection			
Palmitic acid	2.4	2.4	5

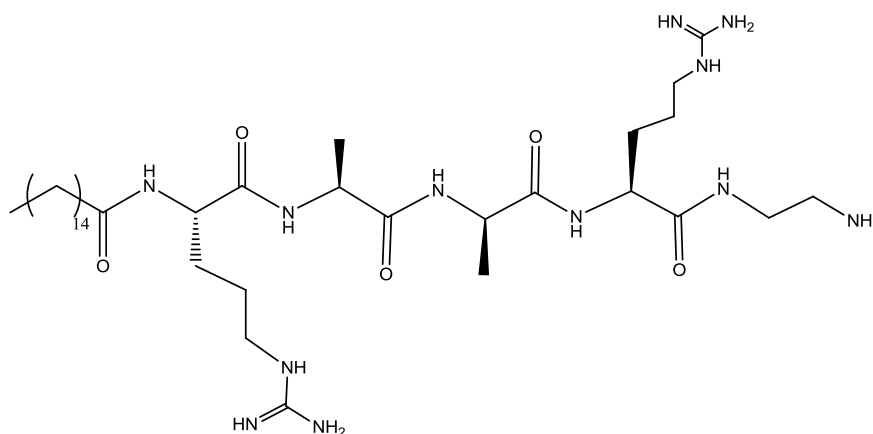
**Yield:** 60,45 % ( 153,19 mg).

**<sup>1</sup>H-NMR (CDCl<sub>3</sub>) 200 MHz:** 8,65 (d, 0,80, *NH*); 8,42 (d, 0,82, *NH*); 7,79 /s, 0,97, *NH*); 7,46 (q, 0,63, *NH*); 4,43 (broad,  $\alpha$ *CH*); 3,97 (s, 0,95,  $\alpha$ *CH*); 3,72 (s, 1,09,  $\alpha$ *CH*); 3,50 (m, *H* Pbf + *NH-CH*<sub>2</sub>-*CH*<sub>2</sub>-*NH*<sub>2</sub>); 2,56 (s, broad, *H* Pbf); 2,49 (s, broad, *H* Pbf); 1,48 (m, *H* Pbf +  $\beta$ -*CH*-Ala); 1,25 (m, 17,38, Pal); 0,86 (t, 9,76, *CH*<sub>3</sub>-Pal)

**Mass spectrometry: m/z:** 1258,70 (M+H); 629,36 (M+2H); 420,24 (M+3H)

**HPLC (50–100, %B, 20 minutes, 1 mL/min, C4): Rt (minutes):** 14,596

## Pbf deprotection of AP-3



The standard protocol to remove Pbf group was used. 54,9 mg ( $4,36 \times 10^{-5}$  mol) of Pal-Arg(Pbf)-Ala-dAla-Arg(Pbf)-NH-(CH<sub>2</sub>)<sub>2</sub>-NH<sub>2</sub> and 10 mL of solution TFA/H<sub>2</sub>O were used.

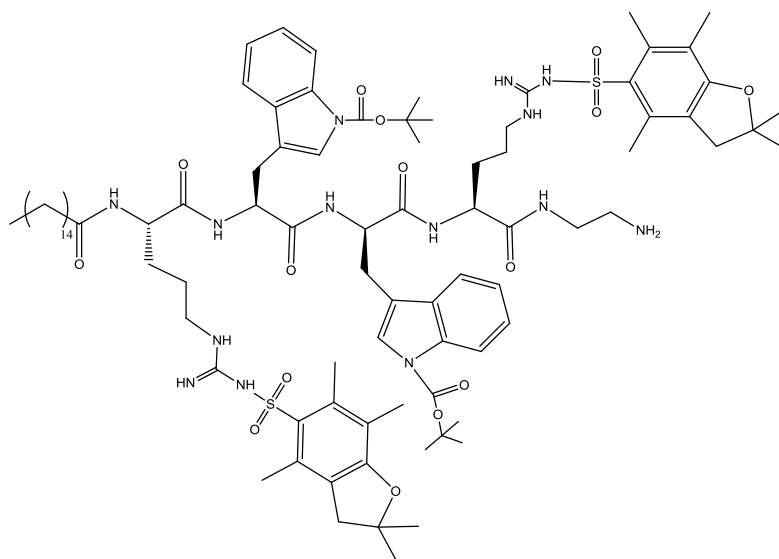
The fraction obtained with eluents H<sub>2</sub>O/MeCN 100:0; 70:30 were collected.

**Yield:** 92,18 % (32,9 mg)

**<sup>1</sup>H-NMR (CDCl<sub>3</sub>) 300 MHz:  $\delta$  (ppm):** 8,65 (broad, 0,85, *NH*); 8,38 (d, 1,00, *NH*); 7,76 (broad, 1,95, 2 *NH*); 7,42 (broad, 1,55, *NH*); 4,77 (broad, 4,39,  $\alpha$ -*CH*); 3,49 (s, 0,43); 2,39 (d, 0,55); 1,48 (s, 4,31,  $\beta$ -*CH*); 1,39 (m, 0,83); 1,25 (s, 3,14); 0,84 (broad, 1,31).

**Mass spectrometry: m/z:** 159,1; 401,7; 608,7

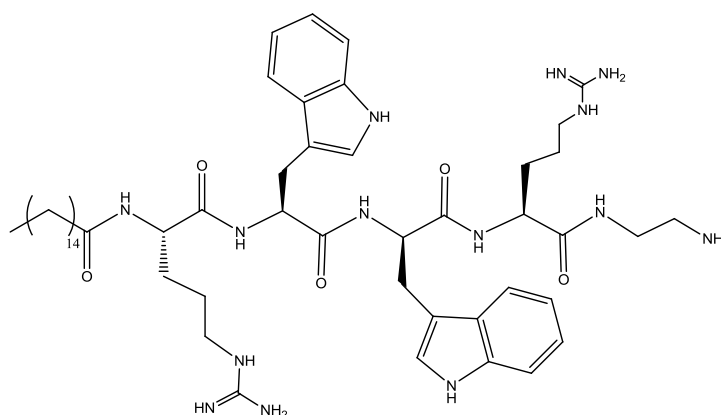
## AP-4: Pal Arg(Pbf)-Trp(Boc)-Trp(Boc)-Arg(Pbf)-NH-(CH<sub>2</sub>)<sub>2</sub>-NH<sub>2</sub>



Fmoc-Amino acid	mmol	HOAt (mmol)	HATU (mmol)
Fmoc-Arg(Pbf)-OH	2.4	2.4	5
Fmoc-deprotection			
Fmoc-Trp(Boc)-OH	2.4	2.4	5

Fmoc-deprotection			
Fmoc-Trp(Boc)-OH	2.4	2.4	5
Fmoc-deprotection			
Fmoc-Arg(Pbf)-OH	2.4	2.4	5
Fmoc-deprotection			
Palmitic acid	2.4	2.4	5

### Pbf deprotection of AP-4



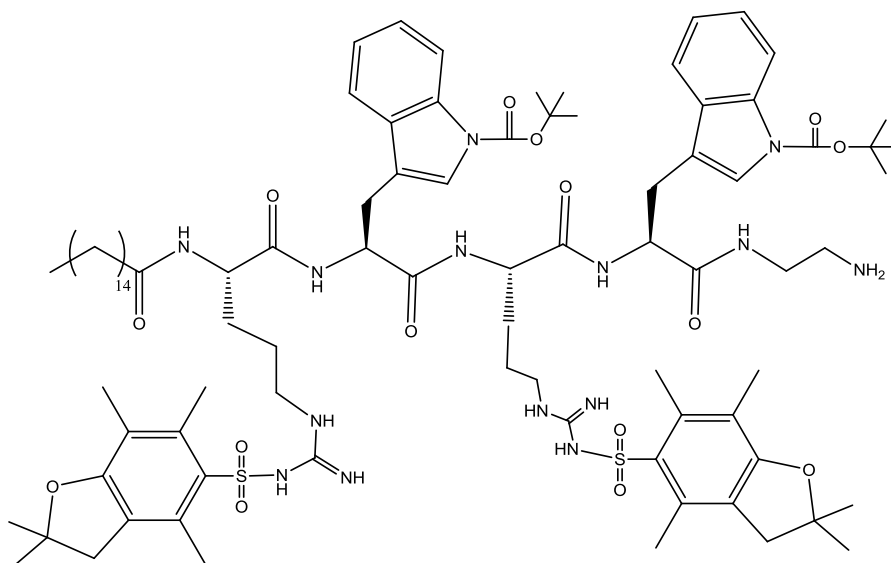
The standard protocol to remove Pbf group was used. 95.3 mg ( $5,65 \times 10^{-5}$  mol) of **Pal-Arg(Pbf)-Trp(Boc)-Trp(Boc)-Arg(Pbf)-NH-(CH<sub>2</sub>)<sub>2</sub>-NH<sub>2</sub>** and 10 mL of solution TFA/H<sub>2</sub>O were used. The fraction obtained with eluents H<sub>2</sub>O/MeCN 100:0; 70:30 were collected. In the same condition Boc-group is easily remove from Trp lateral chain.

**Yield:** 82,18 %

**<sup>1</sup>H-NMR (CDCl<sub>3</sub>) 300 MHz: δ (ppm):** 8.27 (broad, 3.80, ε-**NH** Arg) 8,13 (broad, 0,95, **NH-linker**); 7,67 (broad, 1,95, 2 **NH**-Arg); 7,54 (d, 1,55, α**NH**-**Trp**); 7,38 (d, 1.72, α**NH**-Arg); 7.20 (m, 12.93, Aromatics Trp); 6.78 (broad, 1,45, **NH** aromatic); 5.32 (broad, 0.78, **NH-linker**); 4.45 (m, 1.69, α**CH** Trp); 3,98 (m, 2.12, α**CH**-Arg); 2,98 (m, 4,31, β-**CH**-Trp); 2.15 (t, 1,95, -**CH**<sub>2</sub>-CO Pal), 1.98 (m, 2.12, **CH**<sub>2</sub>- linker) 1,79 (m, 3,83, γ-**CH** Arg); 1,25 (m, 27.35, -**CH**<sub>2</sub>- Pal); 0,84 (t, 3,01 – **CH**<sub>3</sub> Pal)

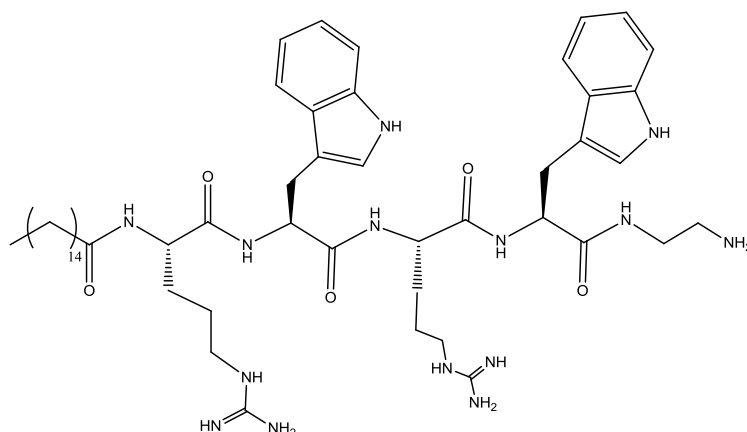
**Mass spectrometry: m/z:** 492.33 [M+H]<sup>2+</sup>, 328.55 [M+2H]<sup>3+</sup>

**AP-5: Pal-Trp(boc)-Arg(Pbf)-Trp(Boc)-Arg(Pbf)-NH-(CH<sub>2</sub>)<sub>2</sub>-NH<sub>2</sub>**



<b>Fmoc-Amino acid</b>	<b>mmol</b>	<b>HOAt (mmol)</b>	<b>HATU (mmol)</b>
Fmoc-Trp(Boc)-OH	2.4	2.4	5
Fmoc-deprotection			
Fmoc-Arg(Pbf)-OH	2.4	2.4	5
Fmoc-deprotection			
Fmoc-Trp(Boc)-OH	2.4	2.4	5
Fmoc-deprotection			
Fmoc-Arg(Pbf)-OH	2.4	2.4	5
Fmoc-deprotection			
Palmitic acid	2.4	2.4	5

## Pbf deprotection of AP-5



The standard protocol to remove Pbf group was used. This condition, also, allow the cleavage of the Boc- group.

**Pal-Trp(boc)-Arg(Pbf)-Trp(Boc)-Arg(Pbf)-NH-(CH<sub>2</sub>)<sub>2</sub>-NH<sub>2</sub>** (72,9 mg, 4,32x10<sup>-5</sup> mol) of and 10 mL of solution TFA/H<sub>2</sub>O were used. In the same condition Boc- group is easily remove from Trp lateral chain.

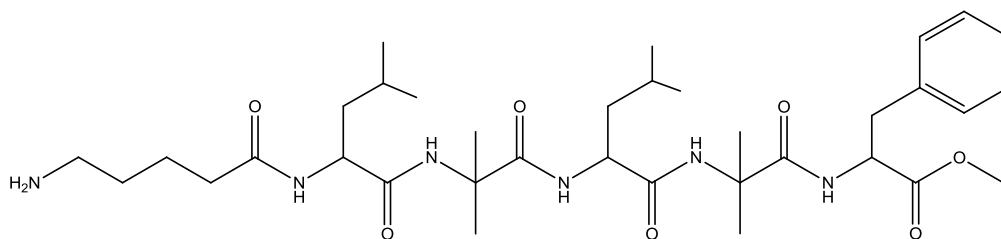
The fraction obtained with eluents H<sub>2</sub>O/MeCN 100:0; 70:30 were collected.

**Yield:** 84,17 %

**<sup>1</sup>H-NMR (CDCl<sub>3</sub>) 300 MHz: δ (ppm):** 8.30 (broad, 3.92, ε-**NH** Arg) 8,15 (broad, 1.02, **NH-linker**); 7,62 (broad, 1,85, 2 **NH**-Arg); 7,56 (d, 1,68, α**NH**-**Trp**); 7,45 (d, 1.75, α**NH**-Arg); 7.20 (m, 12.93, Aromatics Trp); 6.82 (broad, 1,75, **NH** aromatic); 5.27 (broad, 0.96, **NH-linker**); 4.45 (m, 1.69, α**CH** Trp); 3,98 (m, 2.05, α**CH**-Arg); 3.02 (m, 4,43, β-**CH**-Trp); 2.23 (t, 1,75, -**CH**<sub>2</sub>-CO Pal), 1.87 (m, 1.93, **CH**<sub>2</sub>- linker); 1,72 (m, 3,69, γ-**CH** Arg); 1,28 (m, 28.56, -**CH**<sub>2</sub>- Pal); 0,85 (t, 3,01 – **CH**<sub>3</sub> Pal)

**Mass spectrometry: m/z:** 983.66 [M+H]<sup>+</sup>; 492,33 [M+2H]<sup>2+</sup>

**OPP-1 : 5-amino-valeroyl-Leu-Aib-Leu-Aib-Phe-OMe**



**Yield:** 73%

**<sup>1</sup>H-NMR (DMSO-D<sub>6</sub>) 400 MHz: δ (ppm):** δ 7.38-7.18 (7H, Phe NH, Aib<sub>4</sub> NH, 5 Phe CH aromatics), 7.13 (d, 1H, Leu<sub>3</sub> NH), 6.59 (s, 1H, Aib<sub>2</sub> NH), 5.48 (d, 1H, Leu<sub>1</sub> NH), 4.81 (m, 1H, Phe α-CH), 4.24 (m, 1H, Leu<sub>3</sub> α-CH), 3.98 (m, 1H, Leu<sub>1</sub> α-CH), 3.65 (s, 3H, OMe CH<sub>3</sub>), 3.11 (m, 2H, Phe β-CH<sub>2</sub>), 1.76-1.60 (6H, Leu<sub>1</sub> β-CH<sub>2</sub> e γ-CH, Leu<sub>3</sub> β-CH<sub>2</sub> e γ-CH), 1.58, 1.55, 1.52, 1.44 (4s, 12H, Aib<sub>2</sub> β-CH<sub>3</sub> e Aib<sub>4</sub> β-CH<sub>3</sub>), 1.00-0.88 (12H, Leu<sub>1</sub> δ-CH<sub>3</sub> e Leu<sub>3</sub> δ-CH<sub>3</sub>).

**Mass spectrometry: m/z:** 675.44 [M+H]<sup>+</sup>

**HPLC:** gradiente: da 30 a 100% CH<sub>3</sub>CN/H<sub>2</sub>O 9:1 + 0,05% TFA in 20 minuti di flusso: 1ml/min; colonna a fase inversa C<sub>18</sub> Jupiter 300A); λ<sub>ass</sub>: 215nm: t<sub>r</sub> = 8,52 min.

## Experimental part synthesis using *step-by step* (M-1) approach.

Peptides were built on modified cotton fibers by *step-by-step* manual solid phase method.

Modified cotton fiber with bromide moiety on the surface reacts firstly with a 20% ethylenediamine in DMF solution for 12h. Cotton was washed with DMF, MeOH and water and then air dried. The presence of the amino group was confirmed by Kaiser test. The “amino-cotton” obtained was used as a resin for SPPS. Estimated loading was of about 0.8 mmol/gr. Amino acids were protected with Fmoc group.

Side chain protections were opportunely protected: His(Trt), Arg(NO<sub>2</sub>), Arg(Pbf), Fmoc-Lys(Boc), and Fmoc-Lys(Fmoc), Trp(Boc) were used in the different peptides.

Coupling reaction: a solution of Fmoc-AA-OH/fatty acid (3 equivalents), HOAt (3 equivalents), HATU (3 equivalents), in dry DMF, is kept in an ice bath for 15 minutes. The solution is added to the cotton-bound peptide; then DIPEA (5 equivalents) is added. The reaction goes on for 2-4 hours, bubbling N<sub>2</sub>. The surplus of reagents were removed and the cotton was washed with 3x5 mL dry DMF and 2x3 mL dry MeOH, so air dried.

The removal of Fmoc group was made by means of a 20% piperidine solution in dry DMF, bubbling N<sub>2</sub> (2 series for 15 minutes). The surplus of reagents were removed and the cotton was washed with 3x5 mL dry DMF and 2x3 mL dry MeOH, then air dried.

Every coupling and deprotection step was verified with the Kaiser test.

Prepared samples:

Sample code	Peptide linked
AO1	Palmitoyl-Lys-Ala-D-Ala-Lys-linker-cotton
AO2	Palmitoyl-His-Ala-D-Ala-His-linker-cotton
AO3	Palmitoyl-Arg-Ala-D-Ala-Arg-linker-cotton
AO4	Palmitoyl-Arg(NO <sub>2</sub> )-Ala-D-Ala-Arg(NO <sub>2</sub> )-linker-cotton
RW-A	Palmitoyl-Trp-Arg-Trp-Arg-linker-cotton
RW-B	Palmitoyl-Arg-Trp-Trp-Arg-linker-cotton
AO5	Palmitoil-Aib-Gly-Leu-Aib-Gly-Gly-Leu-Aib-Gly-Ile-Leu-linker-cotton
AB1	Palmitoyl-Aib-Hyp-Leu-Val-Gln-Leu-linker-cotton
DC1	Palmitoil-Leu-Aib-Leu-Aib-Phe-linker-cotton
DC2	Palmitoil-Lys-Aib-Lys-Aib-Phe-linker-cotton
D1	[(Palmitoyl-Lys-Ala-D-Ala-Lys) <sub>4</sub> Lys <sub>2</sub> ]Lys-linker-cotton
D2	[(Palmitoyl-His-Ala-D-Ala-His) <sub>4</sub> Lys <sub>2</sub> ]Lys-linker-cotton
D3	[(Palmitoyl-Arg-Ala-Aib-Arg) <sub>4</sub> Lys <sub>2</sub> ]Lys-linker-cotton
D4	[(Palmitoyl-Arg(NO <sub>2</sub> )-Ala-Aib-Arg(NO <sub>2</sub> )) <sub>4</sub> Lys <sub>2</sub> ]Lys-linker-cotton
D5	[(N-5-Valeroyl-His-Arg) <sub>4</sub> Lys <sub>2</sub> ]Lys-linker-cotton

<b>D6</b>	[(N-5-Valeroyl-Trp-Arg) <sub>4</sub> Lys <sub>2</sub> ]Lys- linker-cotton
-----------	---

<b>A</b>	TEMPO-O-succinoyl-Lys-Ala-D-Ala-Lys-linker-cotton
<b>B</b>	(TEMPO-O-succinoyl-Lys-Ala-D-Ala-Lys) <sub>2</sub> -Lys-linker-cotton
<b>C</b>	[(TEMPO-O-succinoyl-Lys-Ala-D-Ala-Lys) <sub>4</sub> -Lys <sub>2</sub> ]-Lys-linker-cotton

### Synthesis of sample AO1

Cotton weight: 0.33 g.

<b>Fmoc-Amino Acid</b>	<b>mmol</b>	<b>HOAt (mmol)</b>	<b>HATU (mmol)</b>	<b>DIPEA</b>
Fmoc-Lys(Boc)-OH	0.79	0.79	0.79	1.32
Fmoc Deprotection				
Fmoc-D-Ala-OH	0.79	0.79	0.79	1.32
Fmoc Deprotection				
Fmoc-Ala-OH	0.79	0.79	0.79	1.32
Fmoc Deprotection				
Fmoc-Lys(Boc)-OH	0.79	0.79	0.79	1.32
Fmoc Deprotection				
Palmitic acid	0.79	0.79	0.79	1.32

**Side chain deprotection:** Boc- protecting group was removed from the Lys ε-NH<sub>2</sub> in boiling water overnight.

**Loading:** 0.72 mmol/g.

**IR:** 1531 cm<sup>-1</sup>, 1649 cm<sup>-1</sup>, 1729 cm<sup>-1</sup>.

**XPS:** C 77.3%, N 4.3% , O 18.4%.

### Synthesis of sample AO2

Cotton weight: 0.36 g, 0.27g, 0.32g.

<b>Fmoc-Amino Acid</b>	<b>mmol</b>	<b>HOAt (mmol)</b>	<b>HATU (mmol)</b>	<b>DIPEA</b>
Fmoc-His(Trt)-OH	0.86	0.86	0.86	1.44
Fmoc Deprotection				
Fmoc-D-Ala-OH	0.86	0.86	0.86	1.44
Fmoc Deprotection				
Fmoc-Ala-OH	0.86	0.86	0.86	1.44
Fmoc Deprotection				
Fmoc-His(Trt)-OH	0.86	0.86	0.86	1.44
Fmoc Deprotection				



Palmitic acid	0.86	0.86	0.86	1.44
---------------	------	------	------	------

**Side chain deprotection:** Trityl protecting group was removed from imidazole using 10% TFA in DCM solution, adding two drops of water as scavenger.

**Loading:** 0.52 mmol/g.

**IR:** 1535 cm<sup>-1</sup>, 1652 cm<sup>-1</sup>, 1736 cm<sup>-1</sup>.

**XPS:** C 77.5%, N 6.5%, O 16.0%.

### Synthesis of sample AO3-AO4

Cotton weight: 0.33 g.

Fmoc-Amino Acid	mmol	HOAt (mmol)	HATU (mmol)	DIPEA
Fmoc-Arg(NO <sub>2</sub> )-OH	0.79	0.79	0.79	1.32
Fmoc Deprotection				
Fmoc-D-Ala-OH	0.79	0.79	0.79	1.32
Fmoc Deprotection				
Fmoc-Ala-OH	0.79	0.79	0.79	1.32
Fmoc Deprotection				
Fmoc-Arg(NO <sub>2</sub> )-OH	0.79	0.79	0.79	1.32
Fmoc Deprotection				
Palmitic acid	0.79	0.79	0.79	1.32

**Side chain deprotection:** Half of sample AO-3 was deprotected from NO<sub>2</sub>, located to the guanidinium moiety, by catalytic hydrogenation using 10% Pd/C as catalyst, 2h in MeOH. The product of deprotection correspond to sample AO-4.

**Loading:** 0.44 mmol/g.

**XPS AO-3:** C 68.7%, N 6.4%, O 24.8%.

**XPS AO-4:** C 72.6%, N 6.3%, O 21.1%

### Synthesis of sample RW-A

Cotton weight: 0.28 g.

Fmoc-Amino Acid	mmol	HOAt (mmol)	HATU (mmol)	DIPEA
Fmoc-Arg(NO <sub>2</sub> )-OH	0.67	0.67	0.67	1.12
Fmoc Deprotection				
Fmoc-Trp(Boc)-OH	0.67	0.67	0.67	1.12
Fmoc Deprotection				

Fmoc-Arg(NO <sub>2</sub> )-OH	0.67	0.67	0.67	1.12
Fmoc Deprotection				
Fmoc-Trp(Boc)-OH	0.67	0.67	0.67	1.12
Fmoc Deprotection				
Palmitic acid	0.67	0.67	0.67	1.12

**Side chain deprotection:**

- Boc protecting group was removed from the indole of Tryptophan in boiling water overnight.
- NO<sub>2</sub> protecting group, located to the guanidinium moiety, was removed by catalytic hydrogenation using 10% Pd/C as catalyst, 2h in MeOH.

**Loading:** 0.71 mmol/g.

**IR:** 1538 cm<sup>-1</sup>, 1654 cm<sup>-1</sup>, 1736 cm<sup>-1</sup>.

**XPS:** C 71.6%, N 7.3%, O 21.1%

**Synthesis of sample RW-B**

Cotton weight: 0.26 g.

Fmoc-Amino Acid	mmol	HOAt (mmol)	HATU (mmol)	DIPEA
Fmoc-Arg(NO <sub>2</sub> )-OH	0.62	0.62	0.62	1.04
Fmoc Deprotection				
Fmoc-Trp(Boc)-OH	0.62	0.62	0.62	1.04
Fmoc Deprotection				
Fmoc-Trp(Boc)-OH	0.62	0.62	0.62	1.04
Fmoc Deprotection				
Fmoc-Arg(NO <sub>2</sub> )-OH	0.62	0.62	0.62	1.04
Fmoc Deprotection				
Palmitic acid	0.62	0.62	0.62	1.04

**Side chain deprotection:**

- Boc protecting group was removed from the indole of Tryptophan in boiling water overnight

- NO<sub>2</sub> protecting group, located to the guanidinium moiety, was removed by catalytic hydrogenation using 10% Pd/C as catalyst, 2h in MeOH.

**Loading:** 0.61 mmol/g.

**IR:** 1531 cm<sup>-1</sup>, 1652 cm<sup>-1</sup>, 1735cm<sup>-1</sup>.

**XPS:** C 72.9%, N 6.3%, O 21.8%.

### Synthesis of sample AO5

Cotton weight: 0.32 g.

Fmoc-Amino Acid	mmol	HOAt (mmol)	HATU (mmol)	DIPEA	N° coupling step
Fmoc-Leu-OH	0.77	0.77	0.77	1.28	
Fmoc Deprotection					
Fmoc-Ile-OH	0.77	0.77	0.77	1.28	
Fmoc Deprotection					
Fmoc-Gly-OH	0.77	0.77	0.77	1.28	
Fmoc Deprotection					
Fmoc-Aib-OH	0.77	0.77	0.77	1.28	2
Fmoc Deprotection					
Fmoc-Leu-OH	0.77	0.77	0.77	1.28	2
Fmoc Deprotection					
Fmoc-Gly-OH	0.77	0.77	0.77	1.28	
Fmoc Deprotection					
Fmoc-Gly-OH	0.77	0.77	0.77	1.28	
Fmoc Deprotection					
Fmoc-Aib-OH	0.77	0.77	0.77	1.28	2
Fmoc Deprotection					
Fmoc-Leu-OH	0.77	0.77	0.77	1.28	2
Fmoc Deprotection					
Fmoc-Gly-OH	0.77	0.77	0.77	1.28	
Fmoc Deprotection					
Fmoc-Aib-OH	0.77	0.77	0.77	1.28	2
Fmoc Deprotection					
Palmitic acid	0.77	0.77	0.77	1.28	2

**Loading:** 0.78 mmol/g.

**IR:** 1532 cm<sup>-1</sup>, 1654 cm<sup>-1</sup>, 1740 cm<sup>-1</sup>.

**XPS:** C 64.3%, N 3.6%, O 32.1%.

### Synthesis of sample AB1

Cotton weight: 0.31 g.

<b>Fmoc-Amino Acid</b>	<b>mmol</b>	<b>HOAt (mmol)</b>	<b>HATU (mmol)</b>	<b>DIPEA</b>
Fmoc-Leu-OH	0.58	0.58	0.58	1.01
Fmoc Deprotection				
Fmoc-Gln-OH	0.58	0.58	0.58	1.01
Fmoc Deprotection				
Fmoc-Val-OH	0.58	0.58	0.58	1.01
Fmoc Deprotection				
Fmoc-Leu-OH	0.58	0.58	0.58	1.01
Fmoc Deprotection				
Fmoc-Hyp-OH	0.58	0.58	0.58	1.01
Fmoc Deprotection				
Fmoc-Aib-OH	0.58	0.58	0.58	1.01
Fmoc Deprotection				
Myristic acid	0.58	0.58	0.58	1.01

**Loading:** 0.20 mmol/g.

**IR:** 1537 cm<sup>-1</sup>, 1649 cm<sup>-1</sup>, 1732 cm<sup>-1</sup>.

**XPS:** C 74.7%, N 5.2%, O 20.1%.

### Synthesis of sample DC1

Cotton weight: 0.32 g

<b>Fmoc-Amino Acid</b>	<b>mmol</b>	<b>HOAt (mmol)</b>	<b>HATU (mmol)</b>	<b>DIPEA</b>
Fmoc-Phe-OH	0.77	0.77	0.77	1.28
Fmoc Deprotection				
Fmoc-Aib-OH	0.77	0.77	0.77	1.28
Fmoc Deprotection				
Fmoc-Leu-OH	0.77	0.77	0.77	1.28
Fmoc Deprotection				
Fmoc-Aib-OH	0.77	0.77	0.77	1.28
Fmoc Deprotection				
Fmoc-Leu-OH	0.77	0.77	0.77	1.28
Fmoc Deprotection				

Palmitic acid	0.77	0.77	0.77	1.28
---------------	------	------	------	------

**Loading:** 0.35 mmol/g.

**IR:** 1535 cm<sup>-1</sup>, 1650 cm<sup>-1</sup>, 1733 cm<sup>-1</sup>.

**XPS:** C 79.1%, N 5.2%, O 15.7%.

### Synthesis of sample DC2

Cotton weight: 0.28 g

Fmoc-Amino Acid	mmol	HOAt (mmol)	HATU (mmol)	DIPEA
Fmoc-Phe-OH	0.67	0.67	0.67	1.12
Fmoc Deprotection				
Fmoc-Aib-OH	0.67	0.67	0.67	1.12
Fmoc Deprotection				
Fmoc-Lys(Boc)-OH	0.67	0.67	0.67	1.12
Fmoc Deprotection				
Fmoc-Aib-OH	0.67	0.67	0.67	1.12
Fmoc Deprotection				
Fmoc-Lys(Boc)-OH	0.67	0.67	0.67	1.12
Fmoc Deprotection				
Palmitic acid	0.67	0.67	0.67	1.12

**Side chain deprotection:** Boc protecting group was removed from the Lys ε-NH<sub>2</sub> in boiling water overnight.

**Loading:** 0.43 mmol/g.

**IR:** 1533 cm<sup>-1</sup>, 1651 cm<sup>-1</sup>, 1736 cm<sup>-1</sup>.

**XPS:** C 78.2%, N 5.4%, O 16.4%.

### Synthesis of sample D1

Cotton weight: 0.25 g

Fmoc-Amino Acid	mmol	HOAt (mmol)	HATU (mmol)	DIPEA
Fmoc-Lys(Fmoc)-OH	0.63	0.63	0.63	1.04
Fmoc Deprotection				
Fmoc-Lys(Fmoc)-OH	1.26	1.26	1.26	2.01
Fmoc Deprotection				
Fmoc-Lys(Boc)-OH	2.52	2.52	2.52	4.12
Fmoc Deprotection				

Fmoc-D-Ala-OH	2.52	2.52	2.52	4.12
Fmoc Deprotection				
Fmoc-Ala-OH	2.52	2.52	2.52	4.12
Fmoc Deprotection				
Fmoc-Lys(Boc)-OH	2.52	2.52	2.52	4.12
Fmoc Deprotection				
Palmitic acid	2.52	2.52	2.52	4.12

**Side chain deprotection:** Boc protecting group was removed from the Lys  $\epsilon$ -NH<sub>2</sub> in boiling water overnight.

**Loading:** 2.79 mmol/g.

**IR:** 1532cm<sup>-1</sup>, 1654 cm<sup>-1</sup>, 1734 cm<sup>-1</sup>.

**XPS:** C 70.3%, N 8.9%, O 20.8%.

### Synthesis of sample D2

Cotton weight: 0.27 g

Fmoc-Amino Acid	mmol	HOAt (mmol)	HATU (mmol)	DIPEA
Fmoc-Lys(Fmoc)-OH	0.65	0.65	0.65	1.08
Fmoc Deprotection				
Fmoc-Lys(Fmoc)-OH	1.3	1.3	1.3	2.16
Fmoc Deprotection				
Fmoc-His(Trt)-OH	2.6	2.6	2.6	4.32
Fmoc Deprotection				
Fmoc-D-Ala-OH	2.6	2.6	2.6	4.32
Fmoc Deprotection				
Fmoc-Ala-OH	2.6	2.6	2.6	4.32
Fmoc Deprotection				
Fmoc-His(Trt)-OH	2.6	2.6	2.6	4.32
Fmoc Deprotection				
Palmitic acid	2.6	2.6	2.6	4.32

**Side chain deprotection:** Trityl protecting group was removed from imidazole using a 10% TFA in DCM solution, adding two drops of water as scavenger.

**Loading:** 1.56 mmol/g.

**IR:** 1531 cm<sup>-1</sup>, 1648 cm<sup>-1</sup>, 1737 cm<sup>-1</sup>.

**XPS:** C 71.2%, N 7.3%, O 22.5%.

### Synthesis of sample D3-4

Cotton weight: 0.43 g

<b>Fmoc-Amino Acid</b>	<b>mmol</b>	<b>HOAt (mmol)</b>	<b>HATU (mmol)</b>	<b>DIPEA</b>
Fmoc-Lys(Fmoc)-OH	1.03	1.03	1.03	1.72
Fmoc Deprotection				
Fmoc-Lys(Fmoc)-OH	2.06	2.06	2.06	3.44
Fmoc Deprotection				
Fmoc-Arg(NO <sub>2</sub> )-OH	4.12	4.12	4.12	6.88
Fmoc Deprotection				
Fmoc-D-Ala-OH	4.12	4.12	4.12	6.88
Fmoc Deprotection				
Fmoc-Ala-OH	4.12	4.12	4.12	6.88
Fmoc Deprotection				
Fmoc-Arg(NO <sub>2</sub> )-OH	4.12	4.12	4.12	6.88
Fmoc Deprotection				
Palmitic acid	4.12	4.12	4.12	6.88

**Side chain deprotection:** Half of sample **D3** was deprotected from NO<sub>2</sub> protecting group, located to the guanidinium moiety, by catalytic hydrogenation using 10% Pd/C as catalyst, 2h in MeOH. The product of deprotection correspond to sample **D4**.

**Loading:** 1.63 mmol/g.

**IR:** 1534 cm<sup>-1</sup>, 1651 cm<sup>-1</sup>, 1733 cm<sup>-1</sup>.

**XPS:** C 70.0%, N 8.1%, O 21.9%.

### Synthesis of sample D5

Cotton weight: 0.32 g

<b>Fmoc-Amino Acid</b>	<b>mmol</b>	<b>HOAt (mmol)</b>	<b>HATU (mmol)</b>	<b>DIPEA</b>
Fmoc-Lys(Fmoc)-OH	0.77	0.77	0.77	1.28
Fmoc Deprotection				
Fmoc-Lys(Fmoc)-OH	1.54	1.54	1.54	2.56
Fmoc Deprotection				

Fmoc-Arg(NO <sub>2</sub> )-OH	3.08	3.08	3.08	5.12
Fmoc Deprotection				
Fmoc-His(Trt)-OH	3.08	3.08	3.08	5.12
Fmoc Deprotection				
Fmoc-N-5-Valeric acid	3.08	3.08	3.08	5.12
Fmoc Deprotection				

#### Lateral chain deprotection:

- Boc protecting group was removed from the indole of Tryptophan in boiling water overnight
- Trityl protecting group, located to the imidazole moiety, was removed by a 10% TFA in DCM solution, adding two drops of water as scavenger.

**Loading:** 2.36 mmol/g.

**IR:** 1528 cm<sup>-1</sup>, 1648 cm<sup>-1</sup>, 1736 cm<sup>-1</sup>.

**XPS:** C 77.6%, N 6.3%, O 16.1%.

#### Synthesis of sample D6

Cotton weight: 0.29 g

Fmoc-Amino Acid	mmol	HOAt (mmol)	HATU (mmol)	DIPEA
Fmoc-Lys(Fmoc)-OH	0.70	0.70	0.70	1.05
Fmoc Deprotection				
Fmoc-Lys(Fmoc)-OH	1.40	1.40	1.40	2.10
Fmoc Deprotection				
Fmoc-Arg(NO <sub>2</sub> )-OH	2.80	2.80	2.80	4.20
Fmoc Deprotection				
Fmoc-Trp(Boc)-OH	2.80	2.80	2.80	4.20
Fmoc Deprotection				
Fmoc-N-5-Valeric acid	2.80	2.80	2.80	4.20
Fmoc Deprotection				

#### Side chain deprotection:

- Boc protecting group was removed from the indole of Tryptophan in boiling water overnight
- NO<sub>2</sub> protecting group, located to the guanidinium moiety, was removed by catalytic hydrogenation using 10% Pd/C as catalyst, 2h in MeOH.

**Loading:** 2.48 mmol/g.

**IR:** 1530 cm<sup>-1</sup>, 1652 cm<sup>-1</sup>, 1734 cm<sup>-1</sup>.

**XPS:** C 73.9%, N 6.7%, O 19.4%.



## Preparation of sample for EPR analysis

A

<b>Fmoc-Amino Acid</b>	<b>mmol</b>	<b>HOAt (mmol)</b>	<b>HATU (mmol)</b>	<b>DIPEA</b>
Fmoc-Lys(Boc)-OH	1.5	1.5	1.5	4.5
Fmoc deprotection				
Fmoc-D-Ala-OH	1.5	1.5	1.5	4.5
Fmoc deprotection				
Fmoc-Ala-OH	1.5	1.5	1.5	4.5
Fmoc deprotection				
Fmoc-Lys(Boc)-OH	1.5	1.5	1.5	4.5
Fmoc deprotection				
Succinic acid	1.5	1.5	1.5	4.5
4-Hydroxy-TEMPO	1.5	1.5	1.5	4.5

**Loading:** 0.86 mmol/g

B

<b>Fmoc-Amino Acid</b>	<b>mmol</b>	<b>HOAt (mmol)</b>	<b>HATU (mmol)</b>	<b>DIPEA</b>
Fmoc-Lys(Fmoc)-OH	1.5	1.5	1.5	4.5
Fmoc deprotection				
Fmoc-Lys(Boc)-OH	3	3	3	9
Fmoc deprotection				
Fmoc-D-Ala-OH	3	3	3	9
Fmoc deprotection				
Fmoc-Ala-OH	3	3	3	9
Fmoc deprotection				
Fmoc-Lys(Boc)-OH	3	3	3	9
Succinic acid	3	3	3	9
4-Hydroxy-TEMPO	3	3	3	9

**Loading:** 1.47 mmol/g

C

<b>Fmoc-Amino Acid</b>	<b>mmol</b>	<b>HOAt (mmol)</b>	<b>HATU (mmol)</b>	<b>DIPEA</b>
------------------------	-------------	--------------------	--------------------	--------------

Fmoc-Lys(Fmoc)-OH	1.5	1.5	1.5	4.5
Fmoc deprotection				
Fmoc-Lys(Fmoc)-OH	3	3	3	9
Fmoc deprotection				
Fmoc-Lys(Boc)-OH	6	6	6	18
Fmoc deprotection				
Fmoc-D-Ala-OH	6	6	6	18
Fmoc deprotection				
Fmoc-Ala-OH	6	6	6	18
Fmoc deprotection				
Fmoc-Lys(Boc)-OH	6	6	6	18
Succinic acid	6	6	6	18
4-Hydroxy-TEMPO	6	6	6	18

**Loading:** 2.85 mmol/g

## Synthesis via *one-pot* approach (M-2).

Peptides were linked on modified cotton fibers by *one-pot* manual method.

Free peptides **OPP-1** and **OPP-2** were prepared by Dr. Daniele Canaglia during his thesis stage.

Modified cotton fiber with bromide moiety on the surface reacts with an amino-peptide (being the amino moiety at C- or N-terminus) in DMF solution (3 eq.) and DIPEA (5 eq.) overnight. Cotton was washed with DMF, MeOH and water and then air dried.

Prepared samples:

Sample code	Peptide linked
<b>OP1</b>	Palmitoyl-Leu-Aib-Leu-Aib-Phe- <i>linker</i> -cotton
<b>OP2</b>	MeO-Phe-Aib-Leu-Aib-Leu-5-N-amino-valeroyl-cotton

### Synthesis of sample OP1

Cotton weight: 0.12 g

A DMF solution (10 ml; 0.5 mM; 5 eq.) of Fmoc-Leu-Aib-Leu-Aib-Phe-NH-(CH<sub>2</sub>)<sub>2</sub>-NH<sub>2</sub> was added to a piece of the “brominated cotton fiber” (0.12 g.; estimated loading 0.8 mmol/g.) with 8 eq. of DIPEA. Reaction occurred overnight. The next day cotton sample was washed with DMF (3 cycles of 15 ml) and the N-terminus deprotected by a 20% piperidine in DMF solution.

Palmitic acid was dissolved in DMF with HOAt/HATU as activating agent, with 8 eq. of DIPEA and then added to the Fmoc-deprotected cotton sample. Reaction occurred in 2 h.

At the end the sample was washed with DMF, MeOH and water and then air dried.

**Loading:** 0.63 mmol/g

**IR:** 1649 cm<sup>-1</sup>, 1534 cm<sup>-1</sup>

### Synthesis of sample OP2

Cotton weight: 0.14 g

A DMF solution (10 ml; 0.5 mM; 5 eq.) of 5-N-valeroyl-Leu-Aib-Leu-Aib-Phe-OMe was added to a piece of the “brominated cotton fiber” (0.14 g.; estimated loading 0.8 mmol/g.) with 8 eq. of DIPEA. Reaction occurred overnight. The next day cotton sample was washed with DMF (3 cycles of 15 ml), MeOH (3 cycles of 15 ml) and water and then air dried.

**IR:** 1748 cm<sup>-1</sup>, 1654cm<sup>-1</sup>, 1533 cm<sup>-1</sup>